Renormalization-group approach to the Anderson model of dilute magnetic alloys. I. Static properties for the symmetric case

H. R. Krishna-murthy,* J. W. Wilkins, and K. G. Wilson
Physics Department, Cornell University, Ithaca, New York 14853
(Received 10 September 1979)

The temperature-dependent impurity susceptibility for the symmetric Anderson model is calculated for all physically relevant values of its parameters U (the Coulomb correlation energy) and Γ (the impurity-level width). It is shown that, when $U > \pi\Gamma$, for temperatures $T < U/(10k_B)$ the symmetric Anderson model exhibits a local moment and that its susceptibility maps neatly onto that of the spin-$\frac{1}{2}$ Kondo model with an effective coupling given by $\rho J_{\text{eff}} = -8\Gamma/\pi U$. Furthermore, this mapping is shown for remarkably large values of $|\rho J_{\text{eff}}|$. At very low temperatures (much smaller than the Kondo temperature) the local moment is frozen out, just as for the Kondo model, leading to a strong-coupling regime of constant susceptibility at zero termperature. The results also depict the formation of a local moment from the free orbital as T drops below U, a feature not present in the Kondo model. Finally, when $U << \pi\Gamma$ there is a direct transition from free-orbital regime for $T >> \Gamma$ to the strong-coupling regime for $T << \Gamma$. The calculations were performed using the numerical renormalization group originally developed by Wilson for the Kondo problem. In addition to the actual numerical calculations, analytic results are presented. In particular, the effective Hamiltonians, i.e., fixed-point Hamiltonian plus relevant and marginal operators, are constructed for the free-orbital, local-moment, and strong-coupling regimes. Analytic formulas for the impurity susceptibility and free energy in all three regimes are developed. The impurity specfic heat in the strong-coupling regime is calculated.

I. INTRODUCTION

The paper and the one following it are devoted to a detailed discussion of the application of renormalization-group techniques to the Anderson model[1] of dilute magnetic alloys and, in particular, to a calculation of the susceptibility. Previously we have published summaries of our calculations for the symmetric case[2]—the subject of this paper (I)—and the asymmetric case[3]—which is covered in the following paper (II). Accordingly we defer any summary of our results until the introduction of the following paper, where we compare and contrast the underlying physics of the symmetric and asymmetric Anderson models. The experimentalist or casual theoretically-inclined reader is directed to that introduction. At the same time we do not have space for a discussion of most of the previous theoretical effort in this area but instead refer the reader to available review articles[4] and the first published susceptibility calculation[5] for the Anderson model.

This work is an extension of the application[6] of the numerical renormalization-group techniques to the Kondo model. That the application is far from trivial can be judged by the length of these papers. Nonetheless, in an attempt to conserve space, we have not repeated in detail arguments from that work[6] which can be used here with essentially no change.

There is one aspect of the papers that may be initially confusing. Although there is extensive numerical work associated with this approach, we would stress that once the underlying fixed points[6] have been identified, many of the calculations can be done *analytically,* albeit in some cases using parameters deduced from the numerical calculations. In these two papers we have stressed the analytic underpinning of the work in the hope that it will offer insight to future research workers attempting to compute other properties such as the electrical resistivity.

The rest of the paper is organized as follows. In Sec. II, we summarize the techniques and transformations that convert the Anderson model into a (numerically and analytically) soluble proble. Section III contains a preliminary presentation of the numerical results, whereas in Sec. IV the analytic machinery is used to derive the effective Hamiltonian about each fixed point. Detailed quantitative results appear in Sec. V, followed by a very brief summary in Sec. VI which serves as a sendoff for the introduction in Paper II. Finally, there is a set of Appendices devoted to various technical details.

II. SUMMARY OF THE BASIC TECHNIQUES

A. Model Hamiltonian

The Anderson Hamiltonian[1] for a single magnetic impurity in a nonmagnetic metal is

$$\mathcal{H}_A \equiv \sum_{\vec{k}} \epsilon_{\vec{k}} c^\dagger_{\vec{k}\mu} c_{\vec{k}\mu} + \epsilon_d c^\dagger_{d\mu} c_{d\mu} + \sum_{\vec{k}} (V_{\vec{k}d} c^\dagger_{\vec{k}\mu} c_{d\mu} + V^*_{\vec{k}d} c^\dagger_{d\mu} c_{\vec{k}\mu}) + U(c^\dagger_{d\uparrow} c_{d\uparrow})(c^\dagger_{d\downarrow} c_{d\downarrow}) \quad . \tag{2.1}$$

$\epsilon_{\vec{k}}$ and ϵ_d are to be measured from the Fermi level. *Repeated spin indices are assumed to be summed over.*

We will prefer to write Eq. (2.1) in another equivalent form

$$\mathcal{H}_A = -\tfrac{1}{2}U + \sum_{\vec{k}} \epsilon_{\vec{k}} c^\dagger_{\vec{k}\mu} c_{\vec{k}\mu} + (\epsilon_d + \tfrac{1}{2}U) c^\dagger_{d\mu} c_{d\mu} + \sum_{\vec{k}} (V_{\vec{k}d} c^\dagger_{\vec{k}\mu} c_{d\mu} + V^*_{\vec{k}d} c^\dagger_{d\mu} c_{\vec{k}\mu}) + \tfrac{1}{2}U(c^\dagger_{d\mu} c_{d\mu} - 1)^2 \quad . \tag{2.2}$$

The equivalence of the two forms can be verified by expanding out the last term in Eq. (2.2) and making use of relations such as $(c^\dagger_{d\uparrow} c_{d\uparrow})^2 = c^\dagger_{d\uparrow} c_{d\uparrow}$.

In this paper a simplified version of Eq. (2.2) will be treated. The simplification is achieved by assuming that the Fermi surface is wholly contained in a single, isotropic ($\epsilon_{\vec{k}}$ depends only on $|\vec{k}|$) conduction band extending in energy from $-D$ to D, and that $V_{\vec{k}d}$ depends only on $|\vec{k}|$. This means that if one uses a set of spherical waves about the impurity site (taken to be at the origin) as the basis states for the conduction electrons, the impurity couples only to the s-wave states. For calculating the changes in various properties of the system due to the presence of the impurity the higher angular momentum states can hence be ignored. It is convenient to let the s-wave states be labeled by energy rather than by momentum. Dropping the constant term in Eq. (2.2), the simplified version of the Hamiltonian $\mathcal{H}_A$ that results when one goes through all the steps indicated above is given by

$$\mathcal{H}_A = \int_{-D}^{D} \epsilon a^\dagger_{\epsilon\mu} a_{\epsilon\mu}\, d\epsilon + (\epsilon_d + \tfrac{1}{2}U) c^\dagger_{d\mu} c_{d\mu} + \frac{1}{2}\frac{U}{D}(c^\dagger_{d\mu} c_{d\mu} - 1)^2 + \int_{-D}^{D} d\epsilon\, [\rho(\epsilon)]^{1/2} [V_d(\epsilon) a^\dagger_{\epsilon\mu} c_{d\mu} + V^*_d(\epsilon) c^\dagger_{d\mu} a_{\epsilon\mu}] \quad , \tag{2.3}$$

where $\rho(\epsilon)$ is the one-electron density of states per spin, and $V_d(\epsilon)$ is V_{kd} expressed as a function of the energy ϵ_k. $a^\dagger_{\epsilon\uparrow}$ creates an electron in an s-wave state (about the origin) of energy ϵ, and is supposed to be normalized as $\{a_{\epsilon\mu}, a^\dagger_{\epsilon'\nu}\} = \delta(\epsilon - \epsilon')\delta_{\mu\nu}$. Note that the Fermi level corresponds to $\epsilon = 0$.

We now further simplify Eq. (2.3) by ignoring the energy dependence of ρ and of V_d and replacing them by their values at the Fermi level. This is *not* a crucial approximation, and the effects of relaxing this assumption will be commented upon in a later section. It is also convenient to measure energies relative to the band edge D by working in terms of the variable $k \equiv \epsilon/D$, and operators $a_{k\mu} \equiv \sqrt{D}\, a_{\epsilon\mu}$ [this makes $\{a_{k\mu}, a_{k'\nu}\} = \delta_{\mu\nu}\delta(k - k')$]. The final version of the model Hamiltonian that results is

$$\mathcal{H}_A = D\left(\int_{-1}^{1} k a^\dagger_{k\mu} a_{k\mu}\, dk + \frac{1}{D}(\epsilon_d + \tfrac{1}{2}U) c^\dagger_{d\mu} c_{d\mu} + \frac{1}{2}\frac{U}{D}(c^\dagger_{d\mu} c_{d\mu} - 1)^2 + \left(\frac{\Gamma}{\pi D}\right)^{1/2} \int_{-1}^{1} dk\, (a^\dagger_{k\mu} c_{d\mu} + c^\dagger_{d\mu} a_{k\mu}) \right) \quad , \tag{2.4}$$

where

$$\Gamma \equiv \pi \rho V_d^2 \quad . \tag{2.5}$$

In this form the Hamiltonian retains only the barest essential structure; only the dimensionless parameters (ϵ_d/D), (U/D), and (Γ/D) enter the theory, and the temperature-dependent properties of the Hamiltonian will be functions only of the ratio $(k_B T/D)$. Appendix A contains more details about the various transformations of the Hamiltonian discussed above.

The *results* to be presented in this paper will be confined to the *symmetric case,* which corresponds to choosing $\epsilon_d = -\frac{1}{2}U$ so that the second term in Eq. (2.4) is absent. (The asymmetric case will be considered in the next paper.) In this case $\mathcal{H}_A$ exhibits particle-hole symmetry; i.e., it remains invariant under the transformation $(a_{k\mu} \leftrightarrow a^\dagger_{-k\mu},\ c_{d\mu} \leftrightarrow -c^\dagger_{d\mu})$. Since the basic techniques to be summarized in the rest of this section are as applicable to the asymmetric case as to the symmetric case, the full Hamiltonian will be considered until we come to Sec. III.

B. Logarithmic discretization

The problem is to calculate the "impurity contribution" to the various properties of the system described by Eq. (2.4). The key to its solution lies in a logarithmic discretization of k space. One introduces a parameter $\Lambda(>1)$ and divides up the k domain $[-1, 1]$ into a sequence of intervals as shown in Fig. 1. The nth interval (for positive k) extends from $\Lambda^{-(n+1)}$ to Λ^{-n}. One can now define a complete set of orthonormal functions spanning the k space by

setting up Fourier series in each of these intervals

$$\psi_{np}^{\pm}(k) \equiv \begin{cases} \dfrac{\Lambda^{n/2}}{(1-\Lambda^{-1})^{1/2}} e^{\pm i\omega_n pk} & \text{if } \Lambda^{-(n+1)} < \pm k < \Lambda^{-n} \ , \\ 0 & \text{if } k \text{ is outside the above interval} \ . \end{cases} \tag{2.6}$$

Here n, the interval index, takes values $0, 1, 2, \ldots$; p, the Fourier harmonic index, takes on all integral values from $-\infty$ to $+\infty$; the superscript $+$ $(-)$ denotes a basis function defined for positive (negative) k. ω_n, the *fundamental* Fourier frequency in the nth interval, is clearly

$$\omega_n \equiv \frac{2\pi}{\Lambda^{-n} - \Lambda^{-(n+1)}} = \frac{2\pi\Lambda^n}{1-\Lambda^{-1}} \ . \tag{2.7}$$

The operators $a_{k\mu}$ can be expanded in this basis

$$a_{k\mu} = \sum_{np} [\, a_{np\mu}\psi_{np}^{+}(k) + b_{np\mu}\psi_{np}^{-}(k)] \ ; \tag{2.8}$$

$$a_{np\mu} \equiv \int_{-1}^{1} dk\, [\psi_{np}^{+}(k)]^* a_{k\mu}; \quad b_{np\mu} \equiv \int_{-1}^{1} dk\, [\psi_{np}^{-}(k)]^* a_{k\mu} \ . \tag{2.9}$$

The operators $a_{np\mu}$ and $b_{np\mu}$ form a complete set of independent, discrete, electron operators obeying standard anticommutation rules

$$\{a_{np\mu}, a_{n'p'\mu'}^{\dagger}\} = \delta_{nn'}\delta_{pp'}\delta_{\mu\mu'} \ , \ldots \ .$$

The Hamiltonian Eq. (2.4) can now be expressed in terms of the discrete operators $a_{np\mu}$ instead of the operators $a_{k\mu}$. It is straightforward to verify the following two results:

$$\int_{-1}^{1} k a_{k\mu}^{\dagger} a_{k\mu}\, dk = \tfrac{1}{2}(1+\Lambda^{-1}) \sum_{np} \Lambda^{-n}(a_{np\mu}^{\dagger} a_{np\mu} - b_{np\mu}^{\dagger} b_{np\mu}) + \frac{1-\Lambda^{-1}}{2\pi i} \sum_{n} \sum_{p \neq p'} \frac{\Lambda^{-n}}{p'-p} (a_{np\mu}^{\dagger} a_{np'\mu} - b_{np\mu}^{\dagger} b_{np'\mu}) \exp\frac{2\pi i(p'-p)}{1-\Lambda^{-1}} \ , \tag{2.10}$$

$$\int_{-1}^{1} a_{k\mu}\, dk = (1-\Lambda^{-1})^{1/2} \sum_{n} \Lambda^{-n/2}(a_{n0\mu} + b_{n0\mu}) \ . \tag{2.11}$$

From Eqs. (2.11) and (2.4) it is clear that the impurity couples directly only to the operators a_{n0} and b_{n0}. The operators a_{np} and b_{np} with $p \neq 0$ have to be considered only because the second term in Eq. (2.10) couples them to the operators a_{n0} and b_{n0}. Because of the factor $(1-\Lambda^{-1})/2\pi$, this coupling will be small if Λ is close to 1.

As a first approximation, one now neglects the terms in Eq. (2.10) containing a_{np} and b_{np} for $p \neq 0$. Calculations for the Kondo problem[6] have shown that this is actually a surprisingly good approximation even for Λ as large as 3. The resulting approximation to $\mathcal{H}_A$ is

$$\frac{\mathcal{H}_A}{D} \cong \tfrac{1}{2}(1+\Lambda^{-1}) \sum_{n=0}^{\infty} \Lambda^{-n}(a_{n\mu}^{\dagger} a_{n\mu} - b_{n\mu}^{\dagger} b_{n\mu}) + \frac{1}{D}(\epsilon_d + \tfrac{1}{2}U) c_{d\mu}^{\dagger} c_{d\mu} + \left[\frac{2\Gamma}{\pi D}\right]^{1/2} (f_{0\mu}^{\dagger} c_{d\mu} + c_{d\mu}^{\dagger} f_{0\mu}) + \frac{1}{2}\frac{U}{D}(c_{d\mu}^{\dagger} c_{d\mu} - 1)^2 \ , \tag{2.12}$$

where we have defined a new operator $f_{0\mu}$, using Eq. (2.11),

$$f_{0\mu} = \left[\tfrac{1}{2}(1-\Lambda^{-1})\right]^{1/2} \sum_{n=0}^{\infty} \Lambda^{-n/2}(a_{n\mu} + b_{n\mu}) \equiv \frac{1}{\sqrt{2}} \int_{-1}^{1} dk\, a_{k\mu} \ . \tag{2.13}$$

The subscript "0" for the operators a_{n0} and b_{n0} has been dropped in Eqs. (2.12) and (2.13), and will be omitted

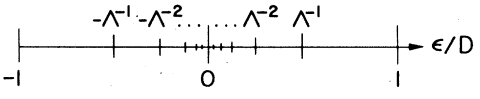

FIG. 1. Logarithmic discretization of the conduction bond. The Fermi energy is at zero and the top and bottom of the conduction bond at $k \equiv \epsilon/D = +1$ and -1, respectively.

hereafter. The factor of $1/\sqrt{2}$ in Eq. (2.13) is to normalize $f_{0\mu}$ so that $\{f_{0\mu}, f_{0\nu}^\dagger\} = \delta_{\mu\nu}$.

In going from the continuum Hamiltonian Eq. (2.4) to the discrete Hamiltonian Eq. (2.12), we have essentially replaced electrons with all possible energies between -1 and $+1$ by electrons with a discrete set of energies $\pm\Lambda^{-n}$. In this process energy values close to the Fermi level, which are the ones that determine the low-temperature ($k_B T \ll D$) properties of the system, *are* being well sampled. The motivation for the *logarithmic* discretization is that electron energies are thereby clearly separated into different "orders of magnitude," each of which contributes equally to logarithmic divergences found in perturbative solutions to the Anderson Hamiltonian.[4,5] See Sec. VII, Ref. 6, for a more detailed discussion regarding the motivation. The limit $\Lambda \to 1$ is the continuum limit in which the discretization ceases to be an approximation.

C. Conversion to a "hopping Hamiltonian"

In Eq. (2.12) the impurity is coupled only to the operator f_0, which is essentially the conduction-electron field operator at the impurity site. It is convenient to make a unitary transformation from the set of operators $(a_{n\mu}, b_{n\mu})$ to a new orthonormal set $(f_{n\mu})$ with $f_{0\mu}$ continuing to be given by Eq. (2.13). There are infinitely many such sets $(f_{n\mu})$. Since the conduction-electron kinetic-energy term in Eq. (2.12) is diagonal in the operators $(a_{n\mu}, b_{n\mu})$, any transformation away from this set of operators will lead to operators $(f_{n\mu})$ that are coupled to one another. The best one can do is choose such a transformation that the operators $(f_{n\mu})$ exhibit only nearest-neighbor coupling; i.e., $f_{n\mu}$ is coupled only to $f_{(n\pm1)\mu}$. Details of the derivation of such a transformation are given in Sec. VII, Ref. 6. The resulting expression for the discrete approximation to $\mathcal{H}_A$ is

$$\frac{\mathcal{H}_A}{D} = \tfrac{1}{2}(1+\Lambda^{-1}) \sum_{n=0}^{\infty} \Lambda^{-n/2} \xi_n [\, f_{n\mu}^\dagger f_{(n+1)\mu} + f_{(n+1)\mu}^\dagger f_{n\mu}] + \frac{1}{D}(\epsilon_d + \tfrac{1}{2}U) c_{d\mu}^\dagger c_{d\mu}$$
$$+ \left(\frac{2\Gamma}{\pi D}\right)^{1/2} (f_{0\mu}^\dagger c_{d\mu} + c_{d\mu}^\dagger f_{0\mu}) + \frac{1}{2}\frac{U}{D}(c_{d\mu}^\dagger c_{d\mu} - 1)^2 \ , \tag{2.14}$$

where the ξ_n's are Λ-dependent coefficients of order 1, given by

$$\xi_n = (1-\Lambda^{-n-1})(1-\Lambda^{-2n-1})^{-1/2}(1-\Lambda^{-2n-3})^{-1/2} \ , \tag{2.15}$$

which can essentially be replaced by 1 for large n.

Note that the transformation from the discrete Hamiltonian (2.12) to the hopping form (2.14) is an exact transformation. For later reference the expressions for the operators f_1 and f_2 will be recorded below. f_0 was defined earlier in Eq. (2.13).

$$f_{1\mu} = [\tfrac{1}{2}(1-\Lambda^{-3})]^{1/2} \sum_{n=0}^{\infty} \Lambda^{-3n/2}(a_{n\mu} - b_{n\mu}) \ , \tag{2.16}$$

$$f_{2\mu} = (\tfrac{1}{2}\Lambda)^{1/2} \frac{(1-\Lambda^{-5})^{1/2}}{(1-\Lambda^{-2})} \sum_{n=0}^{\infty} [(1-\Lambda^{-3})\Lambda^{-5n/2} - (1-\Lambda^{-1})\Lambda^{-n/2}](a_{n\mu} + b_{n\mu}) \ . \tag{2.17}$$

A general rule is that the expression for f_n involves only the combination $(a_n + b_n)$ if n is even, and only the combination $(a_n - b_n)$ if n is odd.

In order to understand the structure of the hopping Hamiltonian (2.14), it is useful to think of the one-electron *wave functions* (to be denoted by kets) to which the various second quantized operators we have defined correspond. For this purpose assume that energy and momentum are proportional, and that $D \sim \epsilon_F$. In the discussion that follows, energies are measured from the Fermi level in units of D, and distances are measured from the impurity site, in units of $1/k_F$.

The wave functions $(|a_k\rangle)$ that correspond to the set of conduction-electron operators in Eq. (2.4) are all s waves, with energies spacings of order v_F/R, where v_F is the Fermi velocity and R the typical size of the metal. They extend throughout the metal.

(See Fig. 2.) The wave functions $|a_{np}\rangle$ and $|b_{np}\rangle$ that correspond to the operators defining the logarithmic discretization, on the other hand, are wave-packet states confined to their respective phase-space cells as depicted in Fig. 3. $|a_{np}\rangle$ has a mean energy $\sim\Lambda^{-n}$ ($|b_{np}\rangle$ has mean energy $-\Lambda^{-n}$), a spread in energy $\Lambda^{-n}(1-\Lambda^{-1})$, is peaked at a distance of $\Lambda^n p/(1-\Lambda^{-1})$ from the impurity site, and has a radial extent $\Lambda^n/(1-\Lambda^{-1})$. As n gets larger (i.e., as their energies get closer to the Fermi level), these wave-packet states resemble more and more the original s-wave states. The approximation of throwing away the $p \neq 0$ states corresponds to throwing away those states which are peaked away from the impurity site.

The states $(|f_n\rangle)$ contain equal amounts of positive and negative energy electron operators and hence have zero mean energies (i.e., their mean energy is at the Fermi level, or their mean wave number is

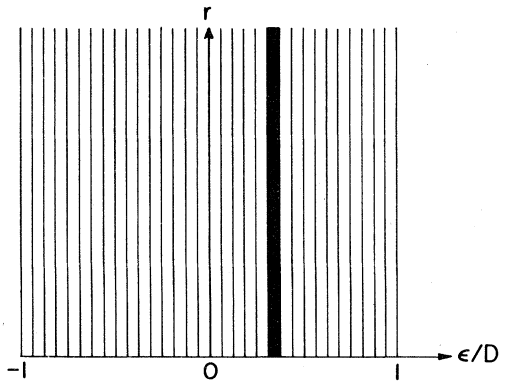

FIG. 2. Phase space for the states $|a_k\rangle$ shown in the $(\epsilon/D,r)$ space. Each state has a well-defined energy and extends throughout the volume of the system, as illustrated by the heavy bar.

$\sim k_F$), which is why there are no diagonal terms in Eq. (2.14). They are all peaked at the impurity site. $|f_n\rangle$ has a spread in energy $\sim\Lambda^{-n/2}$, which is the strength of its off-diagonal coupling in Eq. (2.14), and consequently an extent about the impurity of $\sim\Lambda^{n/2}$. $|f_0\rangle$ has the biggest spread in energy ($\sim$1), and is consequently the most localized (extent $\sim$1 or $1/k_F$ in real units). (See Fig. 4.) The fact that c_d is coupled only to f_0 in Eq. (2.14) is a reflection of the fact that the impurity is localized. [Allowing ρ and V_d in Eq. (2.3) to be weakly energy dependent would couple c_d to some of the *first few* f_n's. See Sec. V D for more discussion.]

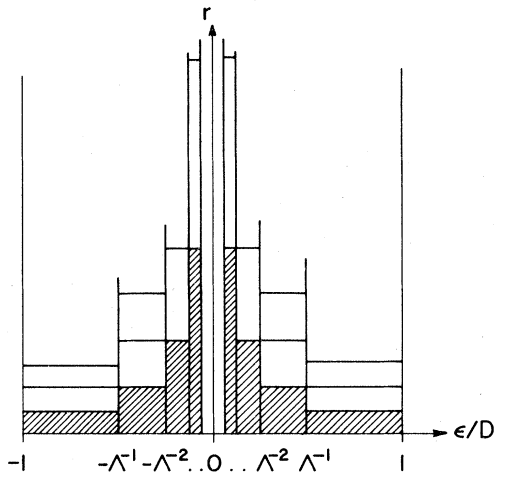

FIG. 3. Phase-space cell analysis for the $|a_{np}\rangle$ and $|b_{np}\rangle$ states [defined in Eq. (2.9)]. Shaded boxes constitute the phase spaces for the states $|a_{n0}\rangle$ and $|b_{n0}\rangle$; the open boxes next to them for $|a_{n1}\rangle$ and $|b_{n1}\rangle$; the next set for $|a_{n2}\rangle$ and $|b_{n2}\rangle$, etc.

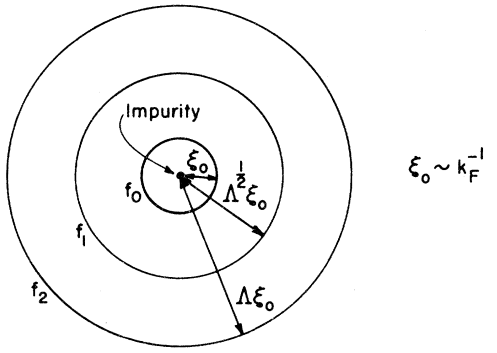

FIG. 4. Spherical shells in r space depicting the extents of the wave functions of f_n. Within their shells, every wave function has oscillations so that they are mutually orthogonal. Alternately one can show that, in the wave-vector space, neglecting a_{np} for $p>0$, $\sqrt{2}f_n = g_n(\Lambda)\int_{-1}^{1} dk\, P_n(k)a_k$, where $P_n(k)$ is the n-order Legendre polynomial and $g_n(\Lambda)$ a function of Λ which goes to $(2n+1)^{1/2}$ as $\Lambda\to 1$.

D. Iterative diagonalization

In order to solve the hopping Hamiltonian, one defines a sequence of Hamiltonians H_N as follows:

$$H_N \equiv \Lambda^{(N-1)/2}\left[\sum_{n=0}^{N-1}\Lambda^{-n/2}\xi_n(f_{n\mu}^{\dagger}f_{n+1\mu}+f_{n+1\mu}^{\dagger}f_{n\mu}) + \tilde{\delta}_d c_{d\mu}^{\dagger}c_{d\mu} + \tilde{\Gamma}^{1/2}(f_{0\mu}^{\dagger}c_{d\mu}+c_{d\mu}^{\dagger}f_{0\mu}) + \tilde{U}(c_{d\mu}^{\dagger}c_{d\mu}-1)^2\right], \tag{2.18}$$

where we have defined, for convenience,

$$\tilde{\delta}_d \equiv \left(\frac{2}{1+\Lambda^{-1}}\right)\frac{1}{D}(\epsilon_d+\tfrac{1}{2}U) \equiv \tilde{\epsilon}_d+\tilde{U}\ , \tag{2.19}$$

$$\tilde{U} \equiv \left(\frac{2}{1+\Lambda^{-1}}\right)\frac{U}{2D}\ , \tag{2.20a}$$

$$\tilde{\Gamma} \equiv \left(\frac{2}{1+\Lambda^{-1}}\right)^2\frac{2\Gamma}{\pi D} = \left(\frac{2}{1+\Lambda^{-1}}\right)^2\frac{2\rho|V_d|^2}{D}\ . \tag{2.20b}$$

The full discrete approximation to $\mathcal{H}_A$ can now be recovered as the limit

$$\mathcal{H}_A = \lim_{N\to\infty}\tfrac{1}{2}(1+\Lambda^{-1})D\Lambda^{-(N-1)/2}H_N\ . \tag{2.21}$$

The scale factor $\Lambda^{(N-1)/2}$ in Eq. (2.18) has been introduced so as to make the lowest energy scale in H_N, which is coefficient of $(f_{N-1\mu}^{\dagger}f_{N\mu}+f_{N\mu}^{\dagger}f_{N-1\mu})$,

be of order 1. Roughly speaking, information about the many-electron energy-level structure of $\mathcal{H}_A$ at energies $\sim\Lambda^{-(N-1)/2}D$ is contained in the energy-level structure of H_N at energies ~ 1. (Energy levels of Hamiltonain are assumed to be measured relative to their ground-state energies throughout both papers.)

It is easy to see from Eq. (2.18) that the Hamiltonians (H_N) satisfy the following *recursion relation:*

$$H_{N+1}=\Lambda^{1/2}H_N+\xi_N(f^\dagger_{N\mu}f_{N+1\,\mu}+f^\dagger_{N+1\,\mu}f_{N\mu}) \quad . \tag{2.22}$$

This recursion relation is the central aspect of the formalism being discussed. The point of defining the sequence (H_N) is in fact that one can use Eq. (2.22) to set up *recursive* procedure (to be described below) for obtaining the many-particle eigenstates and energy levels of H_{N+1} given the same for H_N. The initial Hamiltonian H_0 (H_N for $N=0$) involves only the operators f_0 and $c_{d\mu}$.

$$H_0=\Lambda^{-1/2}[\tilde{\delta}_d c^\dagger_{d\mu}c_{d\mu}+\tilde{\Gamma}^{1/2}(f^\dagger_{0\mu}c_{d\mu}+c^\dagger_{d\mu}f_{0\mu}) + \tilde{U}(c^\dagger_{d\mu}c_{d\mu}-1)^2] \quad . \tag{2.23}$$

It is straightforward to compute the eigenstates and energy levels of this Hamiltonian. Repeated use of the recursive procedure then enables one to solve the whole sequence of Hamiltonians (H_N).

The basic scheme of te recursive procedure, briefly, is as follows. Let $|l,N\rangle\,(l=0,1,2,\ldots,L_N)$ denote the eigenstates of H_N, with $l=0$ corresponding to the ground state. H_N has $2(N+2)$ fermion operators: $c_{d\mu},f_{0\mu},\ldots,f_{N\mu}$. Since each fermion operator has a space of two states (empty and full), L_N will be given by $(2^{2(N+2)}-1)$. Suppose that one knows all the energy levels $E(l,N)$ and all the matrix elements $\langle l,N|f^\dagger_{n\mu}|l',N\rangle$. One now constructs from each of the states $|l,N\rangle$ the following four states:

$$\begin{aligned}
&|1,l,N\rangle \equiv |l,N\rangle \quad ,\\
&|2,l,N\rangle \equiv f^\dagger_{N+1\uparrow}|l,N\rangle \quad ,\\
&|3,l,N\rangle \equiv f^\dagger_{N+1\downarrow}|l,N\rangle \quad ,\\
&|4,l,N\rangle \equiv f^\dagger_{N+1\uparrow}f^\dagger_{N+1\downarrow}|l,N\rangle \quad .
\end{aligned} \tag{2.24}$$

It is clear that the $4(1+L_N)$ states that result provide an orthonormal basis that spans the space of H_{N+1}. One can now calculate the matrix elements of H_{N+1} in this basis by sandwiching Eq. (2.22) between $\langle i',l',N|$ and $|i,l,N\rangle$. All four states in Eq. (2.24) are eigenstates of H_N belonging to the eigenvalue $E(l,N)$. $f_{N+1\,\mu}$ or $f^\dagger_{N+1\,\mu}$ will connect only states with the same index l, and matrix elements such as $\langle i',l,N|f^\dagger_{N+1\,\mu}|i,l,N\rangle$ do not depend on what the index l is, and can be abbreviated as $\langle i'|f^\dagger_{N+1\,\mu}|i\rangle$ (for example, $\langle 2,l,N|f^\dagger_{N+1\uparrow}|1,l,N\rangle \equiv \langle 2|f^\dagger_{N+1\uparrow}|1\rangle = 1$). $f_{N\mu}$ or $f^\dagger_{N\mu}$ does not connect states with different values of i and i', and $\langle i,l',N|f_{N\mu}|i,l,N\rangle = \langle l',N|f_{N\mu}|l,N\rangle$. Therefore we have

$$\begin{aligned}
\langle i',l',N|H_{N+1}|i,l,N\rangle &= \Lambda^{1/2}E(l,N)\delta_{ii'}\delta_{ll'}\\
&\quad+\xi_N(\langle l',N|f^\dagger_{N\mu}|l,N\rangle\langle i'|f_{N+1\,\mu}|i\rangle\\
&\quad+\langle i'|f^\dagger_{N+1\,\mu}|i\rangle\langle l',N|f^\dagger_{N\mu}|l,N\rangle) \quad .
\end{aligned} \tag{2.25}$$

Knowledge of $E(l,N)$ and $\langle l',N|f^\dagger_{N\mu}|l,N\rangle$ is thus sufficient to evaluate the matrix for H_{N+1}. Diagonalizing this matrix yields the new eigenstates $|l,N+1\rangle\,(l=0,1,\ldots,L_{N+1})$ of H_{N+1} and the energies $E(l,N+1)$ and also allows one to calculate $\langle l,N+1|f^\dagger_{N+1\,\mu}|l',N+1\rangle$. One can then use this knowledge and the above procedure to solve H_{N+2}, and so on.

As is well known the symmetries of a Hamiltonian, leading to conserved quantum numbers, considerably reduce the labor involved in diagonalizing that Hamiltonian. All the Hamiltonians we have been considering conserve spin and electron number. The spin operator appropriate to H_N is

$$\vec{S}_N \equiv \tfrac{1}{2}\sum_{n=0}^{N} f^\dagger_{n\mu}\vec{\sigma}_{\mu\nu}f_{n\nu}+\tfrac{1}{2}c^\dagger_{d\mu}\vec{\sigma}_{\mu\nu}c_{d\nu} \quad , \tag{2.26}$$

where $\vec{\sigma}(\sigma_x,\sigma_y,\sigma_z)$ are the Pauli matrices. Instead of the electron-number operator, it is more convenient to define a "charge" operator appropriate to H_N:

$$Q_N \equiv \sum_{n=0}^{N}(f^\dagger_{n\mu}f_{n\mu}-1)+(c^\dagger_{d\mu}c_{d\mu}-1) \quad . \tag{2.27}$$

It is easy to verify that both operators commute with H_N. The eigenstates of H_N can hence be chosen to be also the eigenstates of Q_N, $(\vec{S}_N)^2$, and S_{Nz}, and can be labeled by the corresponding quantum numbers Q, S, and m_S. The point is that when the states in Eq. (2.24) are constructed, they can be classified according to their values of Q, S, and m_S. H_{N+1} will not have matrix elements between states that have different (Q,S,m_S) values, and its diagonalization can be carried out independently in each (Q,S,m_S) subspace. In fact, energy eigenvalues will be independent of m_S, and one can avoid having to keep track of m_S by using Clebsh-Gordon coefficients and working entirely in terms of the *reduced matrix elements* $\langle Q,S\|f^\dagger_N\|Q',S'\rangle$ instead of using $\langle Q,S,m_S|f^\dagger_{N\mu}|Q',S',m_S'\rangle$. All this results in a considerable reduction in the size of matrices that have to be diagonalized. For details see Appendix B.

For the symmetric case $(\epsilon_d=-\frac{1}{2}U)$ it was remarked earlier that $\mathcal{H}_A$ had particle-hole symmetry. In terms of the operators $(f_{n\mu})$ and $(c_{d\mu})$, the symmetry operation is: $f_{n\mu}\leftrightarrow(-1)^n f^\dagger_{n\mu}$ and $c_{d\mu}\leftrightarrow -c^\dagger_{d\mu}$. It is easy to verify that this leaves every H_N invari-

ant, since $\tilde{\delta}_d$ is zero when $\epsilon_d = -\frac{1}{2}U$ [cf. Eqs. (2.18) and (2.19)]. This symmetry operation takes Q_N to $-Q_N$ (which, in fact, is the reason for calling Q_N the charge), which means that the state (Q,S) has the same energy as the state $(-Q,S)$. For the symmetric case, it is hence necessary to carry out the diagonalization only for states with $Q \geq 0$.

As a practical matter, however, calculating *all* the states of H_N for large N is completely out of the question because the number of states of H_N grows exponentially with $N(\sim 2^{2(N+2)})$, and the numerical diagonalization of the large-sized matrices that result becomes prohibitively expensive. We will see in Sec. II E that for calculating low-temperature properties of $\mathcal{H}_A$, one is mainly interested in the low-lying states of H_N. So in practice one selects and keeps only a small number of low-lying states after each step in the iterative process described earlier. In order that the discretized approximation be fairly representatiave of the continuum limit, one would like Λ to be close to 1. But, for a given number of selected states, the accumulation (with increasing N) of errors due to the truncation gets worse as $\Lambda \to 1$. One's choice of Λ and of the number of states one keeps is therefore determined by a trade-off between the accuracy one desires and the consideration of computing costs. The separation and the sequential consideration of the different energy scales is the crucial reason that permits the truncation of states to be a good approximation. For a more detailed discussion, see Sec. VIII, Ref. 6.

E. Calculation of impurity properties and the connection between N and the temperature

The calculation of the temperature-dependent properties of $\mathcal{H}_A$ involves the operator $\exp(-\beta\mathcal{H}_A)$ where $\beta \equiv 1/(k_B T)$ as usual. In view of Eq. (2.21), it seems reasonable to assume that, in the thermodynamic limit, it is correct first to calculate *an equivalent property* for H_M using the operator

$$\exp -\beta[\tfrac{1}{2}(1+\Lambda^{-1})]D\Lambda^{-(M-1)/2}H_M = \exp -\bar{\beta}_M H_M \ , \tag{2.28}$$

where we have written

$$\bar{\beta}_M \equiv \beta[\tfrac{1}{2}(1+\Lambda^{-1})]D\Lambda^{-(M-1)/2} = \tfrac{1}{2}(1+\Lambda^{-1})\Lambda^{-(M-1)/2}\left(\frac{k_B T}{D}\right)^{-1} \ , \tag{2.29}$$

and *then* take the limit $M \to \infty$. M rather than N is used as the index here in order to avoid confusion in the discussion to follow. It is important to note that every property must be calculated as an impurity contribution, i.e., one must always subtract out the value of the property when no impurity is present. In this paper only the initial (zero-field) magnetic susceptibility and the specified heat will be discussed. The definitions are, using Eq. (2.28)

$$\chi_{\rm imp}(T) = \frac{(g\mu_B)^2}{k_B T}\lim_{M\to\infty}\left[\frac{\mathrm{Tr}S_{Mz}^2 \exp -\bar{\beta}_M H_M}{\mathrm{Tr}\exp -\bar{\beta}_M H_M} - \frac{\mathrm{Tr}S_{Mz}^{0^2}\exp -\bar{\beta}_M H_M^0}{\mathrm{Tr}\exp -\bar{\beta}_M H_M^0}\right] \ , \tag{2.30}$$

$$F_{\rm imp}(T) \equiv -k_B T \lim_{M\to\infty}\left[\ln \mathrm{Tr}\exp -\bar{\beta}_M H_M - \ln \mathrm{Tr}\exp -\bar{\beta}_M H_M^0\right] \ , \tag{2.31}$$

$$C_{\rm imp}(T) = -T\frac{\partial^2}{\partial T^2}F_{\rm imp}(T) \ . \tag{2.32}$$

μ_B is the Bohr magneton; g, the electronic g factor, $(=2)$ has been assumed to be the same for both the impurity and the conduction electrons. $\vec{S}_M$ was defined earlier in Eq. (2.26). $F_{\rm imp}$ is essentially the impurity contribution to the free energy (except for contributions due to ground-state energies, which do not affect $C_{\rm imp}$ anyway). The superscript "0" refers to the situation when no impurity is present:

$$H_M^0 \equiv \Lambda^{(M-1)/2}\left[\sum_{n=0}^{M-1}\Lambda^{-n/2}\xi_n(f_{n\mu}^\dagger f_{n+1\mu} + f_{n+1\mu}^\dagger f_{n\mu})\right] \ , \tag{2.33}$$

$$\vec{S}_M^0 \equiv \tfrac{1}{2}\sum_{n=0}^{M} f_{n\mu}^\dagger \vec{\sigma}_{\mu\nu} f_{n\nu} \ . \tag{2.34}$$

For notational convenience, the label "imp" and the factor $(g\mu_B)^2$ will often be omitted hereafter.

Since the lowest-energy scale in H_M is ~ 1, the $M \to \infty$ limit above basically means that one must consider values of M large enough to make $\bar{\beta}_M \ll 1$. A more precise statement of this idea is that the error one makes by evaluating Eqs. (2.30) and (2.31) at a finite value "N" of M instead of taking the limit $M \to \infty$ is only $0(\bar{\beta}_N/\Lambda)$. The proof of this result for the case of the susceptibility proceeds as follows. Consider some large $M > N$, and split H_M and H_M^0 by separating the operators $(c_d, f_0, \ldots, f_N)$ from $(f_{N+1}, \ldots, f_M)$. Starting from the definitions of H_M and H_M^0, it is easy to verify that one can write

$$\bar{\beta}_M H_M = \bar{\beta}_N H_N + \bar{\beta}_N H_I + \bar{\beta}_M R_{M,N+1} \ , \tag{2.35}$$

$$\bar{\beta}_M H_M^0 = \bar{\beta}_N H_N^0 + \bar{\beta}_N H_I + \bar{\beta}_M R_{M,N+1} \ ; \tag{2.36}$$

where $R_{M,N+1}$ contains only the operators $(f_{N+1}, \ldots, f_M)$, and H_I is a term coupling f_N to f_{N+1}:

$$R_{M,N+1} \equiv \Lambda^{(M-1)/2}\left[\sum_{n=N+1}^{M-1} \Lambda^{-n/2}\xi_n(f^\dagger_{n\mu} f_{n+1\mu} + f^\dagger_{n+1\mu} f_{n\mu})\right] , \quad (2.37)$$

$$H_I \equiv \Lambda^{-1/2}(f^\dagger_{N\mu} f_{N+1\mu} + f^\dagger_{N+1\mu} f_{N\mu}) . \quad (2.38)$$

One can similarly split $\vec{S}_M$ and $\vec{S}^0_M$

$$\vec{S}_M = \vec{S}_N + \vec{S}_{M,N+1};\ \vec{S}^0_M = \vec{S}^0_N + \vec{S}_{M,N+1} , \quad (2.39)$$

$$\vec{S}_{M,N+1} \equiv \tfrac{1}{2}\sum_{n=N+1}^{M} f^\dagger_{n\mu}\,\vec{\sigma}_{\mu\nu} f_{n\nu} . \quad (2.40)$$

The point is that, if H_I, which couples f_N to f_{N+1}, is ignored, the separated parts are *completely independent* of each other, and substitution into Eq. (2.30) results in a complete cancellation of the terms involving the operators $(f_{N+1}, \ldots, f_M)$. For details see Sec. IX, Ref. 6. Therefore, if one makes the separation as above for an arbitrarily large $M(>N)$ and evaluates Eq. (2.30) treating H_I as a perturbation the zero-order term will just be Eq. (2.30) evaluated for $M=N$. The contribution due to treating H_I to first order can be shown to vanish; and the contribution due to treating H_I to second order can be shown to be $O(\bar{\beta}_N/\Lambda)$. See Appendix F.

The result cited in the preceding paragraph is the key to the following important connection between the sequence of Hamiltonians $\{H_N\}$ and the physics of the original Hamiltonian $\mathcal{H}_A$. Suppose that one is interested in evaluating $\chi(T)$ and $F(T)$ at some low temperature T, to some preassigned degree of accuracy. All that one has to do is to pick an appropriately small, fixed number $\bar{\beta}$, then choose an N such that $\bar{\beta}_N = \bar{\beta}$, and finally evaluate Eqs. (2.30) and (2.31) at the finite value N of M. In other words, the Hamiltonians H_N enable one to compute χ and F, to an accuracy $O(\bar{\beta}/\Lambda)$, at a whole sequence of temperatures T_N determined by the condition that $\bar{\beta}_N = \bar{\beta}$, i.e.,

$$T_N = \frac{D}{k_B}\tfrac{1}{2}(1+\Lambda^{-1})\Lambda^{-(N-1)/2}/\bar{\beta} . \quad (2.41)$$

The expressions that one uses for this purpose are

$$k_B T_N \chi(T_N) \cong \frac{\mathrm{Tr} S^2_{Nz}\exp-\bar{\beta}H_N}{\mathrm{Tr}\exp-\bar{\beta}H_N} - \frac{\mathrm{Tr} S^{0\,2}_{Nz}\exp-\bar{\beta}H^0_N}{\mathrm{Tr}\exp-\bar{\beta}H^0_N} , \quad (2.42)$$

$$F(T_N) \cong -k_B T_N\{\ln \mathrm{Tr}\exp-\bar{\beta}H_N - \ln \mathrm{Tr}\exp-\bar{\beta}H^0_N\} . \quad (2.43)$$

The index N thus defines a logarithmic temperature scale T_N as given by Eq. (2.41). Large values of N clearly correspond to temperatures T_N that are small compared to the bandwidth.

The evaluation of Eqs. (2.42) and (2.43) can in principle be done if all the energy levels of H_N are known. In accordance with the discussion of Sec. II D, let the states of H_N be denoted $|k,S,m_S,N\rangle$, where k takes care of all labels (charge, etc.) other than the spin labels S and m_S. The energies do not depend on m_S and can be denoted $E_N(k,S)$. One now has the results

$$\mathrm{Tr}\exp-\bar{\beta}H_N = \sum_{k,S}(2S+1)\exp-\bar{\beta}E_N(k,S) , \quad (2.44)$$

$$\mathrm{Tr} S^2_{Nz}\exp-\bar{\beta}H_N = \sum_{k,S}\tfrac{1}{12}(2S+1)[(2S+1)^2-1] \times \exp-\bar{\beta}E_N(k,S) , \quad (2.45)$$

where the spin factors result from summing over m_S. One can write down similar expressions for H^0_N in terms of its energies E^0_N. In fact H^0_N, being a quadratic Hamiltonian, can be diagonalized exactly into a set of single-particle levels whence the evaluation of the above traces becomes rather trivial, as we will see later.

Now consider the *practical* aspects of evaluating the sums (2.44) and (2.45) using the numerical results for the energy levels of H_N. It is at once obvious that one cannot really choose $\bar{\beta}$ to be very small because an accurate evaluation of the above sum requires energy levels up to an energy somewhat bigger than $1/\bar{\beta}$ and highly excited states of H_N are *not* calculated numerically. In other words, there is a trade-off between the small $\bar{\beta}$ one needs in order to make the calculation at a finite value N of M representative of the $M\to\infty$ limit and the large number of states whose energies one needs to know to compute Eqs. (2.44) and (2.45) accurately. The compromise adopted in practice is to choose $\bar{\beta}$ to be only slightly smaller than 1 so that the high-energy states ($E_N > 10$ say) of H_N that are ignored do not contribute appreciably to Eqs. (2.44) and (2.45); and to correct for the effects of $\bar{\beta}$ not being very small by actually calculating the $O(\bar{\beta}/\Lambda)$ correction alluded to earlier. (See Appendix F.)

However, we will see later that there are *ranges of N* where the energy levels of H_N can be obtained analytically by doing perturbation theory using various *effective Hamiltonians.* Then one can indeed use values of $\bar{\beta}$ small enough that one can neglect the $O(\bar{\beta}/\Lambda)$ corrections. For corresponding ranges of temperature [related to the ranges of N by Eq. (2.41)] one can obtain analytical expressions for $\chi_{\mathrm{imp}}(T)$ and $C_{\mathrm{imp}}(T)$. These calculations are presented in Sec. V.

This completes our brief discussion of the basic

TABLE I. States and energies of the initial Hamiltonian H_0 Eq. (2.23) for the symmetric ($\tilde{\delta}_d=0$) Anderson model.

Charge Q	Spin S	Index r	Energy/$\Lambda^{1/2}$	State
-2	0	1	$\frac{1}{2}(\tilde{U}^2+16\tilde{\Gamma})^{1/2}+\frac{1}{2}\tilde{U}$	$\|\Omega\rangle$
-1	$\frac{1}{2}$	1	$\frac{1}{2}(\tilde{U}^2+16\tilde{\Gamma})^{1/2}-\frac{1}{2}(\tilde{U}^2+4\tilde{\Gamma})^{1/2}$	Different linear combinations of $f_0^\dagger\|\Omega\rangle$ and $c_d^\dagger\|\Omega\rangle$
		2	$\frac{1}{2}(\tilde{U}^2+16\tilde{\Gamma})^{1/2}+\frac{1}{2}(\tilde{U}^2+4\tilde{\Gamma})^{1/2}$	
0	0	1	0	Different linear combinations of $f_{0\uparrow}^\dagger f_{0\downarrow}^\dagger\|\Omega\rangle$, $c_{d\uparrow}^\dagger c_{d\downarrow}^\dagger\|\Omega\rangle$ and $(f_0^\dagger c_d^\dagger)_s\|\Omega\rangle$
		2	$\frac{1}{2}(\tilde{U}^2+16\tilde{\Gamma})^{1/2}+\frac{1}{2}\tilde{U}$	
		3	$\frac{1}{2}(\tilde{U}^2+16\tilde{\Gamma})^{1/2}$	
	1	1	$\frac{1}{2}(\tilde{U}^2+16\tilde{\Gamma})^{1/2}-\frac{1}{2}\tilde{U}$	$(f_0^\dagger c_d^\dagger)_t\|\Omega\rangle$
1	$\frac{1}{2}$	1	$\frac{1}{2}(\tilde{U}^2+16\tilde{\Gamma})^{1/2}-\frac{1}{2}(\tilde{U}^2+4\tilde{\Gamma})^{1/2}$	Different linear combinations of $f_0^\dagger(c_{d\uparrow}^\dagger c_{d\downarrow}^\dagger\|\Omega\rangle$ and $c_d^\dagger(f_{0\uparrow}^\dagger f_{0\downarrow}^\dagger)\|\Omega\rangle$
		2	$\frac{1}{2}(\tilde{U}^2+16\tilde{\Gamma})^{1/2}+\frac{1}{2}(\tilde{U}^2+4\tilde{\Gamma})^{1/2}$	
2	0	1	$\frac{1}{2}(\tilde{U}^2+16\tilde{\Gamma})^{1/2}+\frac{1}{2}\tilde{U}$	$f_{0\uparrow}^\dagger f_{0\downarrow}^\dagger c_{d\uparrow}^\dagger c_{d\downarrow}^\dagger\|\Omega\rangle$

techniques. The rest of this paper will consist of a detailed discussion of the results obtained by the application of these techniques to the symmetric case defined by the condition $\epsilon_d=-\frac{1}{2}U$. In this case the parameters that have to be specified are the two dimensionless numbers Γ/D and U/D. One then computes the energy levels and the invariant matrix elements of f_0 between the eigenstates of the initial Hamiltonian H_0 [cf. Eq. (2.23)] with $\tilde{\delta}_d=0$. The energy levels are listed in Table I. Use of the iterative diagonalization procedure discussed in Sec. II D then enables one to solve the whole sequence of Hamiltonians H_N. From the energy levels of H_N one can calculate the susceptibility at temperature T_N determined by Eq. (2.39) using the procedure discussed in Sec. II E.

The numerical calculations that will be presented in this paper were performed on a CDC 7600 computer, Λ was chosen to be 2.5, and a maximum of 611 states was kept. Susceptibility calculations were carried out using $\bar{\beta}$ values 0.460, 0.578, and 0.727. Note that the values of $\bar{\beta}$ were chosen so that T_N for $\bar{\beta}=0.727$ is equal to T_{N+1} for $\bar{\beta}=0.46$. [This follows from Eq. (2.39), and the result that $0.727=(0.460)(2.5)^{1/2}$.] The difference between the susceptibility calculated from H_N for $\bar{\beta}=0.727$ and that calculated from H_{N+1} for $\bar{\beta}=0.460$, which is a *rough* measure of the accuracy of the numerical results for the susceptibility, indicated an absolute error of around 0.004 in $k_BT\chi/(g\mu_B)^2$.

III. PRELIMINARY LOOK AT THE NUMERICAL RESULTS

In this section numerical results for the energy levels of $\{H_N\}$ and for $\chi_{\rm imp}(T)$ for the symmetric Anderson model will be presented for several typical values of Γ/D and U/D. The important characteristic of these results will be that they can be understood in terms of H_N crossing over (as N increases) between various fixed points of the transformation (2.22) which is an example of a renormalization-group transformation. Therefore, prior to the actual presentation of the results, the stage will be set for their interpretation by discussing these fixed points.

A. Renormalization group and fixed points; the free-electron Hamiltonian

Consider the transformation (2.22) relating H_N to H_{N+1} for large N. Since ξ_N is 1 for large N [cf. Eq. (2.15)] and since the Hamiltonians H_N are supposed to be defined with their ground-state energies sub-

tracted, the transformation for large N can be written more precisely as

$$H_{N+1} = \Lambda^{1/2} H_N + (f^\dagger_{N\mu} f_{N+1\,\mu} + f^\dagger_{N+1\,\mu} f_{N\mu}) - E_{G,N+1} \ , \tag{3.1}$$

where $E_{G,N+1}$ is chosen so as to make the ground-state energy of H_{N+1} zero. Equation (3.1) is an example of a renormalization-group transformation.[6,7] One can write this symbolically as $H_{N+1} = \mathcal{T}[H_N]$, and think of the transformation $\mathcal{T}$ as producing, from an input list of the eigenvalues and the matrix elements of f_N between the eigenstates of H_N, an output list of the eigenvalues and the matrix elements of f_{N+1} between the eigenstates of H_{N+1} according to the prescription for iterative diagonalization outlined in Sec. II D.

A fixed point H^* of the transformation $\mathcal{T}$ is a Hamiltonian that remains invariant under $\mathcal{T}$: $\mathcal{T}[H^*] = H^*$. Actually $\mathcal{T}$ itself does not have any fixed points; but $\mathcal{T}^2$ ($\mathcal{T}$ operating twice), which takes H_N to H_{N+2} and is also a renormaliztion-group transformation, does have fixed points. The numerical characterization of a fixed point of $\mathcal{T}^2$ is a set of (many-particle) energy levels and matrix elements (of f_N) that repeat themselves when one performs the iterative diagonalization twice. The point is that a Hamiltonian changes very little under a renormalization-group transformation if it is close to a fixed point of that transformation: if H_N is close to H^* where $\mathcal{T}^2[H^*] = H^*$, by continuity $\mathcal{T}^2[H_N]$ is close to H^* and is therefore close to H_N. This is indeed the way one recognizes fixed points from the numerical results: one sees a set of energy levels that change very little from iteration N to iteration $(N+2)$.

The fixed points of $\mathcal{T}^2$ that are of interest in case of the symmetric Anderson model can all be written down easily once one understands the structure of the free-electron Hamiltonian H_N^0 defined in Eq. (2.31)

$$H_N^0 = \sum_{n=0}^{N-1} \Lambda^{(N-1-n)/2} \xi_n (f^\dagger_{n\mu} f_{n+1\,\mu} + f^\dagger_{n+1\,\mu} f_{n\mu}) \ . \tag{3.2}$$

For large N, H_N^0 clearly satisfies the recursion relation (3.1) (assuming that one subtracts its ground-state energy). What is more, being a quadratic form it can be diagonalized *exactly* into $(N+1)$ *single-particle levels* by making a unitary transformation on the set of operators $(f_0, f_1, \ldots, f_N)$. The single-particle energies are just the eigenvalues of the $(N+1)\times(N+1)$ matrix $\mathcal{K}_N^0$ whose *only* nonvanishing matrix elements are

$$(\mathcal{K}_N^0)_{n,n+1} = (\mathcal{K}_N^0)_{n+1,n} = \Lambda^{(N-1-n)/2} \xi_n \ ; \quad n = 0, 1, 2, \ldots, N-1 \ . \tag{3.3}$$

This follows from the fact that H_N^0 can be written as the scalar product $f^\dagger \mathcal{K}_N^0 f$ where f stands for the "vector" $(f_0, f_1, \ldots, f_N)$; so that if the real orthogonal matrix $\mathfrak{M}$ diagonalizes $\mathcal{K}_N^0$, the operators forming the vector $\mathfrak{M}\tilde{f}$ are just the single-particle operators that diagonalize H_N^0. For details, see Sec. VIII, Ref. 6.

The eigenvalues of the matrix $\mathcal{K}_N^0$ can be obtained by diagonalizing it numerically. The particle-hole symmetry of H_N^0 leads to the result that if η is an eigenvalue of $\mathcal{K}_N^0$, so is $-\eta$ [this can also be deduced directly from Eq. (3.3)]. This has the consequence that when $(N+1)$ is even there are $\frac{1}{2}(N+1)$ *positive* eigenvalues which will be denoted $\eta_j(N)$, $j = 1, 2, \ldots, \frac{1}{2}(N+1)$, and the other $\frac{1}{2}(N+1)$ eigenvalues are just their negatives; when $(N+1)$ is odd, there is one *zero* eigenvalue denoted $\hat{\eta}_0$, there are $(\frac{1}{2}N)$ positive eigenvalues which will be denoted $\hat{\eta}_j(N)$, $j = 1, 2, \ldots, \frac{1}{2}N$, and the other $\frac{1}{2}N$ eigenvalues are just their negatives.

The negative-energy single-particle levels will all be fully occupied (with two electrons each) in the ground state of H_N^0. [For odd $(N+1)$ the ground state of H_N^0 is quadruply degenerate because of the zero-energy single-particle level $\hat{\eta}_0$.] The subtraction of the ground-state energy from H_N^0 can be accomplished by the standard trick of introducing hole operators conjugate to the negative-energy electron operators into H_N^0 and normal ordering them. Electrons and holes then have the same set of positive single-particle energies. [For odd $(N+1)$ there is a lone zero-energy electron level.] Further, holes have a negative charge relative to the electrons and a hole-creation operator with an "up"-spin index actually creates a spin-down hole. All this is summarized in Table II, where we have denoted the electron and hole operators that diagonalize H_N^0 by $g_{j\mu}$ and $h_{j\mu}$, respectively. For $(N+1)$ odd there is an extra electron operator $g_{0\mu}$ (associated with $\hat{\eta}_0$).

What one finds on evaluating $\eta_j(N)$ and $\hat{\eta}_j(N)$ numerically for a given Λ is that, as N increases, they rapidly approach a limiting set of values which will be denoted η_j^* and $\hat{\eta}_j^*$, respectively. For $j \gg 1$ these limiting values are: $\eta_j^* = \Lambda^{j-1}$; $\hat{\eta}_j^* = \Lambda^{j-1/2}$; for small j the Λ dependence of η_j^* and $\hat{\eta}_j^*$ is not so simple. For example, at $\Lambda = 2.5$ one has, accurate to six decimal places,

$$\eta_j^*\text{: } 0.746\,856,\ 2.493\,206,\ 6.249\,995,\ (2.5)^3,\ (2.5)^4,\ \ldots,\ (2.5)^{j-1},\ \ldots,\ (N+1) \text{ even} \ ; \tag{3.4}$$

$$\hat{\eta}_j^*\text{: } 1.520\,483,\ 3.952\,550,\ 9.882\,118,\ (2.5)^{7/2},\ (2.5)^{9/2},\ \ldots,\ (2.5)^{j-1/2},\ \ldots,\ (N+1) \text{ odd} \ ; \tag{3.5}$$

TABLE II. Information about free-electron Hamiltonian H_N^0 (cf. Sec. III A). Note in particular the values of α_O and α_1 and, for large j, η_j, $\hat{\eta}_j$, etc.

$(N+1)$ even	$(N+1)$ odd
$H_N^0 = \sum_{j=1}^{(N+1)/2} \eta_j (g_{j\mu}^\dagger g_{j\mu} + h_{j\mu}^\dagger h_{j\mu})$	$H_N^0 = \hat{\eta}_0 g_{0\mu}^\dagger g_{0\mu} + \sum_{j=1}^{N/2} \hat{\eta}_j (g_{j\mu}^\dagger g_{j\mu} + h_{j\mu}^\dagger h_{j\mu})$
$Q_N^0 = \sum_{j=1}^{(N+1)/2} (g_{j\mu}^\dagger g_{j\mu} - h_{j\mu}^\dagger h_{j\mu})$	$Q_N^0 = (g_{0\mu}^\dagger g_{0\mu} - 1) + \sum_{j=1}^{N/2} (g_{j\mu}^\dagger g_{j\mu} - h_{j\mu}^\dagger h_{j\mu})$
$\vec{S}_N^0 = \sum_{j=1}^{(N+1)/2} \frac{1}{2} [g_{j\mu}^\dagger \vec{\sigma}_{\mu\nu} g_{j\nu} + h_{j\mu} \vec{\sigma}_{\mu\nu} h_{j\nu}^\dagger]$	$\vec{S}_N^0 = \frac{1}{2} g_{0\mu}^\dagger \vec{\sigma}_{\mu\nu} g_{0\nu} + \sum_{j=1}^{N/2} \frac{1}{2} [g_{j\mu}^\dagger \vec{\sigma}_{\mu\nu} g_{j\nu} + h_{j\mu} \vec{\sigma}_{\mu\nu} h_{j\nu}^\dagger]$
$f_{0\mu} = \Lambda^{-[(N-1)/4]} \left(\sum_{j=1}^{(N+1)/2} \alpha_{0j} (g_{j\mu} + h_{j\mu}^\dagger) \right)$	$f_{0\mu} = \Lambda^{-[(N-1)/4]} \left(\hat{\alpha}_{00} g_{0\mu} + \sum_{j=1}^{N/2} \hat{\alpha}_{0j} (g_{j\mu} + h_{j\mu}^\dagger) \right)$
$f_{1\mu} = \Lambda^{-3[(N-1)/4]} \left(\sum_{j=1}^{(N+1)/2} \alpha_{1j} (g_{j\mu} - h_{j\mu}^\dagger) \right)$	$f_{1\mu} = \Lambda^{-3[(N-1)/4]} \left(\sum_{j=1}^{N/2} \hat{\alpha}_{1j} (g_{j\mu} - h_{j\mu}^\dagger) \right)$

where, for large N and for $j \gg 1$, we have

$\eta_j = \Lambda^{j-1}$		$\hat{\eta}_j = \Lambda^{(j-1/2)}$
$\alpha_{Oj} = \alpha_O \Lambda^{(j-1)/2}$	$\alpha_O = [\frac{1}{2}(1-\Lambda^{-1})]^{1/2}$	$\hat{\alpha}_{Oj} = \alpha_O \Lambda^{(j-1/2)/2}$
$\alpha_{1j} = \alpha_1 \Lambda^{3[(j-1)/2]}$	$\alpha_1 = [\frac{1}{2}(1-\Lambda^{-3})]^{1/2}$	$\hat{\alpha}_{1j} = \alpha_1 \Lambda^{3[(j-1/2)/2]}$

and one finds that all the eigenvalues $\eta_j(15)$ and $\hat{\eta}_j(16)$ are already indistinguishable from the above values to six decimal places.

The limiting, *infinite,* set of single-particle levels $\{\eta_j^*\}$ and $\{\hat{\eta}_j^*\}$ and their associated electron and hole operators clearly define two distinct fixed-point Hamiltonians of $\mathcal{T}^2$. The fixed point associated with η_j^* will be referred to as the "even" fixed point H^*. The fixed point associates with $\hat{\eta}_j^*$ will be called the "odd" point $\hat{H}^*$. The result one has is that as $N \to \infty$, H_N^0 goes to H^* if $(N+1)$ is even, and to $\hat{H}^*$ if $(N+1)$ is odd.

An important property of the fixed points which will be useful later is *their insensitivity to the specific values assumed by the coefficients ξ_n for small n.* This property is verified numerically as follows. Suppose that one defines a Hamiltonian $H_N^{0\prime}$ by replacing the coefficients ξ_n in Eq. (3.2) by another set of coefficients ξ_n' but making sure that ξ_n' continues to be 1 for large n so that $H_N^{0\prime}$ also satisfies the renormalization-group transformation (3.1) for large N. The single-particle levels of $H_N^{0\prime}$ can be determined numerically by diagonalizing the matrix $H_N^{0\prime}$ obtained by replacing ξ_n in Eq. (3.3) by ξ_n'. One again finds the results that as $N \to \infty$, $H_N^{0\prime}$ goes to H^* if $(N+1)$ is even and to $\hat{H}^*$ if $(N+1)$ is odd. The only difference is that the approach to H^* or to $\hat{H}^*$ of $H_N^{0\prime}$ is slower than that of H_N^0 and is nonuniform: the jth single-particle level of $H_N^{0\prime}$ is close to the jth single-particle level of the fixed point only for $N \gg j$.

For later reference, also recorded in Table II are the expansions for f_0 and f_1 in terms of the electron and hole operators that diagonalize H_N^0. Note should be taken of the N-dependent factors in front and of the values of the N-independent coefficients α_{0j}, α_{1j}, etc., for $j \gg 1$. The expansions for the operators f_2, f_3, etc., have very similar structures. f_2, for instance, has a piece proportional to f_0 and a piece going as $\Lambda^{-5(N-1)/4}$; f_3 has a price proportional to f_1 and a piece going as $\Lambda^{-7(N-1)/4}$; and so on. These expansions will have a crucial role to play when we come to discuss the "stability" of fixed-point Hamiltonians in Sec. IV.

One can also obtain expansions for f_0, f_1, etc., in terms of the electron and hole operators that diagonalize $H_N^{0\prime}$ (defined above). What one finds is that

the new expansions differ from the corresponding expansions for H_N^0 only by overall proportionality factors. The precise values of these factors will depend on the values of ξ_n' for small n. (Recall that $\xi_n'=1$ for large n.)

The following viewpoint makes the various features of H_N^0 appear rather obvious. The point is that H_N^0 was essentially obtained by the truncation and rescaling of an original set of single-particle levels that scaled as Λ^{-n}. If the truncation were inconsequential, the single-particle levels of H_N^0 would be given by $\Lambda^{(N-1)/2}\Lambda^{-n}$, where n takes values 0, 1, 2, etc., up to $\frac{1}{2}(N-1)$ if $(N+1)$ is even, up to $\frac{1}{2}(N-2)$ if $(N+1)$ is odd. On reindexing the levels, one hence expects that $\eta_j=\Lambda^{j-1}$ and $\hat{\eta}_j=\Lambda^{j-1/2}$, as is indeed the case for large N and for $j\gg 1$. In fact, one can claim that, for large N and for $j\gg 1$, *the operators g_j and $h_j^\dagger$ must be essentially the same as the operators a_n and b_n of the same energy:* $g_j=a_n$ and $h_j^\dagger=b_n$ where n equals $[\frac{1}{2}(N-1)-(j-1)]$ for even $(N+1)$ and $[\frac{1}{2}(N-1)-(j-\frac{1}{2})]$ for odd $(N+1)$. This result plus the expressions for f_0, f_1, etc., in terms of the operators (a_n,b_n) immediately give the correct coefficients for expanding f_0, f_1, etc., in terms of the operators $(g_j,h_j^\dagger)$. For example, according to Eq. (2.13) f_0 has an expansion in (a_n+b_n) with a coefficient $[\frac{1}{2}(1-\Lambda^{-1})]^{1/2}\Lambda^{-n/2}$. By the above prescription this translates to an expansion in $(g_j+h_j^\dagger)$ with a coefficient $[\frac{1}{2}(1-\Lambda^{-1})]^{1/2}\Lambda^{-(N-1)/4+(j-1)/2}$ for even $(N+1)$. This is precisely the result quoted in Table II (for large N and for $j\gg 1$). All other expansions can be similarly obtained.

B. Fixed points for the symmetric Anderson model

There are several interesting fixed points for the symmetric Anderson Hamiltonian, which has the following sequence of Hamiltonians H_N [obtained by setting $\tilde{\delta}_d=0$ in Eq. (2.18)]:

$$H_N=\Lambda^{(N-1)/2}\left[\sum_{n=0}^{N-1}\Lambda^{-n/2}\xi_n(f_{n\mu}^\dagger f_{n+1\,\mu}+f_{n+1\,\mu}^\dagger f_{n\mu})+\tilde{\Gamma}^{1/2}(f_{0\mu}^\dagger c_{d\mu}+c_{d\mu}^\dagger f_{0\mu})+\tilde{U}(c_{d\mu}^\dagger c_{d\mu}-1)^2\right] . \tag{3.6}$$

The important point is that all these fixed points can be obtained by choosing special values for $\tilde{\Gamma}$ and $\tilde{U}$, and comparing the resulting H_N (in the limit $N\to\infty$) with the free-electron Hamiltonian discussed earlier.

1. Free-orbital fixed points: H_{FO}^* and $\hat{H}_{FO}^*$

Suppose that $\tilde{\Gamma}$ and $\tilde{U}$ are both set equal to zero in Eq. (3.6). The resulting Hamiltonian, which will be denoted $H_{N,FO}^*$, is clearly just the free-electron Hamiltonian H_N^0 *plus* a free-impurity orbital of zero energy. Since H_N^0 goes rapidly to its fixed points as $N\to\infty$, one gets two new fixed points of $\mathcal{T}^2$, to be denoted H_{FO}^* and $\hat{H}_{FO}^*$. $H_{FO}^*(H_{FO}^*)$ is just $H^*(\hat{H}^*)$ *plus* a free-impurity orbital of zero energy at the origin. Starting from every many-electron state of $H^*(\hat{H}^*)$ one can construct four degenerate states of $H_{FO}^*(\hat{H}_{FO}^*)$ by combining that state with each of the four states of the impurity orbital (empty, with $\uparrow$ electron, with $\downarrow$ electron, and with $\downarrow\uparrow$ electrons). As $N\to\infty$, $H_{N,FO}^*$ goes to H_{FO}^* for even $(N+1)$ and to $\hat{H}_{FO}^*$ for odd $(N+1)$.

2. Local-moment fixed points: H_{LM}^* and $\hat{H}_{LM}^*$

Now suppose that, keeping $\tilde{\Gamma}$ fixed, one lets U become much larger than the energies of interest in Eq. (3.6). Consider how this affects the energy levels and the states of H_0 listed in Table I. Neglecting states which have energies $\tilde{U}$ above the ground state, and calculating the energies of the other states only to $O(\tilde{\Gamma}/\tilde{U})$, one gets the much simpler Table III. Note that only the singly occupied states of the impurity orbital, i.e., the states $c_{d\uparrow}^\dagger|\Omega\rangle$ and $c_{d\downarrow}^\dagger|\Omega\rangle$ where $|\Omega\rangle$ is the "vacuum" state, appear in this table. These two states can clearly be used to define a spin-$\frac{1}{2}$ variable, with an associated Pauli operator $\vec{\tau}$, say. It is straightforward to show that the states and the energies in Table III are precisely the ones that one would construct had H_0 been the Hamiltonian

$$H_0=\Lambda^{-1/2}\left(\frac{\tilde{\Gamma}}{\tilde{U}}\right)(f_{0\mu}\vec{\sigma}_{\mu\nu}f_{0\nu})\cdot\vec{\tau} . \tag{3.7}$$

This means that for any N, if one neglects states that have energies $\sim\tilde{U}\Lambda^{(N-1)/2}$, then to $O(\tilde{\Gamma}/\tilde{U})$ one is

TABLE III. States and energies of the initial Hamiltonian H_0 Eq. (2.23) in the limit $\Gamma\ll U$. Compare with Table I.

Charge Q	Spin S	Index r	Energy/$\Lambda^{1/2}$	State
-1	$\frac{1}{2}$	1	$3\left(\frac{\tilde{\Gamma}}{\tilde{U}}\right)$	$c_d^\dagger\|\Omega\rangle\equiv\|\tau\rangle$
0	0	1	0	$(f_0^\dagger c_d^\dagger)_s\|\Omega\rangle=(f_0^\dagger\|\tau\rangle)_s$
	1	1	$4\left(\frac{\tilde{\Gamma}}{\tilde{U}}\right)$	$(f_0^\dagger c_d^\dagger)_t\|\Omega\rangle=(f_0^\dagger\|\tau\rangle)_t$
+1	$\frac{1}{2}$	1	$3\left(\frac{\tilde{\Gamma}}{\tilde{U}}\right)$	$(f_{0\uparrow}^\dagger f_{0\downarrow}^\dagger)c_d^\dagger\|\Omega\rangle=f_{0\uparrow}^\dagger f_{0\downarrow}^\dagger\|\tau\rangle$

considering, in effect, a Hamiltonian

$$H_N=\Lambda^{(N-1)/2}\left[\sum_{n=0}^{N-1}\Lambda^{-n/2}\xi_n(f_{n\mu}^{\dagger}f_{n+1\mu}+f_{n+1\mu}^{\dagger}f_{n\mu})+\left(\frac{\tilde{\Gamma}}{\tilde{U}}\right)f_{0\mu}^{\dagger}\,\vec{\sigma}_{\mu\nu}f_{0\nu}\cdot\vec{\tau}\right]\ . \tag{3.8}$$

In other words it is as if the impurity has become a "local moment" of spin-$\frac{1}{2}$. If, in addition, one lets $\tilde{\Gamma}=0$, the impurity spin becomes free (decoupled from the conduction electrons).

In order to make this idea of the impurity degree of freedom getting replaced a local moment more transparent, consider the original H_0 for $\tilde{\Gamma}=0$. From Eq. (3.6),

$$H_0\ (\tilde{\Gamma}=0)=\Lambda^{-1/2}\tilde{U}(c_{d\mu}^{\dagger}c_{d\mu}-1)^2\ . \tag{3.9}$$

This means that the subspace in which the impurity orbital is occupied by one electron ($c_{d\mu}^{\dagger}c_{d\mu}=1$) has zero energy; whereas the subspaces for an empty ($c_{d\mu}^{\dagger}c_{d\mu}=0$) and for a fully occupied ($c_{d\mu}^{\dagger}c_{d\mu}=2$) impurity orbital both have energy $\Lambda^{-1/2}\tilde{U}$. As $\tilde{U}\to\infty$ the latter two subspaces can be ignored. Within the subspace in which $c_{d\mu}^{\dagger}c_{d\mu}=1$, the operator $c_{d\mu}^{\dagger}\,\vec{\sigma}_{\mu\nu}c_{d\nu}$ acts exactly like a Pauli spin operator $\vec{\tau}$. The operators $c_{d\mu}^{\dagger}$ and $c_{d\mu}$ themselves are eliminated since they connect to subspaces of energy $\sim\tilde{U}$, and hence the impurity degree of freedom can be considered to be just a spin-$\frac{1}{2}$ variable.

Thus when $\tilde{\Gamma}=0$ and $\tilde{U}=\infty$ in Eq. (3.6) the resulting Hamiltonian, to be denoted $H_{N,\mathrm{LM}}^{*}$, is just H_N^0 plus a free local moment of spin $\frac{1}{2}$. One can now define two more fixed points of $\mathcal{T}^2$, to be denoted H_{LM}^{*} and $\hat{H}_{\mathrm{LM}}^{*}$. $H_{\mathrm{LM}}^{*}(\hat{H}_{\mathrm{LM}}^{*})$ is just $H^{*}(\hat{H}^{*})$ plus a free local moment of spin $\frac{1}{2}$ at the origin. From every state of $H^{*}(\hat{H}^{*})$ one can construct two degenerate states of $H_{\mathrm{LM}}^{*}(\hat{H}_{\mathrm{LM}}^{*})$ by combining that state with the spin-up and the spin-down states of the local moment. Clearly, as $N\to\infty$ $H_{N,\mathrm{LM}}^{*}$ goes to H_{LM}^{*} for even $(N+1)$ and to $\hat{H}_{\mathrm{LM}}^{*}$ for odd $(N+1)$. (It should be noted that the local-moment fixed points are the same as the $J=0$ fixed points of Ref. 6.)

3. *Strong-coupling fixed points: H_{SC}^{*} and $\hat{H}_{\mathrm{SC}}^{*}$*

Finally, consider the case when $\tilde{\Gamma}\to\infty$ at fixed U. From Table I it is clear that all the excited states of H_0 will then have energies $\sim\tilde{\Gamma}^{1/2}$ and can be ignored, and H_0 is reduced to just its ground state. The operators $c_{d\mu}$ and $f_{0\mu}$ are now eliminated since they connect to the excited states of H_0. The resulting Hamiltonian, to be labeled $H_{N,\mathrm{SC}}^{*}$, is effectively

$$H_{N,\mathrm{SC}}^{*}=\Lambda^{(N-1)/2}\left[\sum_{n=1}^{N-1}\Lambda^{-n/2}\xi_n(f_{n\mu}^{\dagger}f_{n+1\mu}+f_{n+1\mu}^{\dagger}f_{n\mu})\right]\ . \tag{3.10}$$

By relabeling the operators in $H_{N,\mathrm{SC}}^{*}$ —calling f_1 the new f_0, f_2 the new f_1, and so on—one can turn it into the Hamiltonian $H_{N-1}^{0\prime}$ discussed in Sec. III A where the coefficients ξ_n' are now given by $\xi_n'=\xi_{n+1}$. It hence follows that as $N\to\infty$, $H_{N,\mathrm{SC}}^{*}$ goes to H^{*} for even N and to $\hat{H}^{*}$ for odd N. In this connection the fixed points H^{*} and $\hat{H}^{*}$ will be denoted H_{SC}^{*} and $\hat{H}_{\mathrm{SC}}^{*}$, respectively. They correspond to the situation in which the impurity is so strongly coupled to the conduction-electron state at the impurity site that both degrees of freedom are "frozen out." (Note that in Ref. 6, these strong-coupling fixed points were referred to as the $J=-\infty$ fixed points.)

C. Numerical results for the energy levels

The fixed points discussed in Sec. III B were all obtained for specially chosen values of $\tilde{\Gamma}$ and $\tilde{U}$. However, as we will see shortly when we look at the numerical results for the energy levels of H_N, these fixed points *are* relevant for describing H_N for general values of $\tilde{U}$ and $\tilde{\Gamma}$. Typically, there will be ranges of N where H_N will be close to one or the other of the fixed points, in the sense that the low-lying many-electron levels of H_N will be close to the corresponding levels that one can construct for the fixed-point Hamiltonian. The development of H_N with increasing N will be simply characterizable as a cross over from one fixed point to another.

Since it is $\mathcal{T}^2$, and not $\mathcal{T}$, that has fixed points, in order to recognize the behavior stated above we must look at H_N purely for odd N, or purely for even N. Results for physical properties will not depend on whether the choice is odd N or even N. In this paper we will confine our attention to odd N. From Sec. III B it follows that the fixed points relevant for this case are H_{FO}^{*}, H_{LM}^{*}, and $\hat{H}_{\mathrm{SC}}^{*}$.

In Fig. 5, the energies of 12 low-lying excited states of H_N for $U/D=10^{-3}$ and $U/\pi\Gamma=12.66$ are plotted against N. The six states corresponding to the solid lines all have charge $Q=1$ and spin $S=0$; the states corresponding to the dashed lines belong to $Q=2$ and $S=\frac{1}{2}$. For comparison, the energies that these states would have in each of the fixed-point Hamiltonians are listed in Table IV; the numerical values (at $\Lambda=2.5$) for the various combinations that occur in Table IV are indicated in Fig. 5. From this comparison it is quite clear that for N between 5 and 15 all 12 states of H_N have energies close to the values they would have for the fixed-point Hamiltonian H_{FO}^{*}. This result is in fact true not just for these 12 states but for all the low-lying states of H_N. Hence one can say, in short, that H_N is close to H_{FO}^{*} for N between 5 and 15. Similarly, for N between 23 and 51, H_N can be said to be close to H_{LM}^{*}, and for N greater than 61 H_N is clearly close to $\hat{H}_{\mathrm{SC}}^{*}$.

Thus when $U/D=10^{-3}$ and $U/(\pi\Gamma)=12.66$, H_N

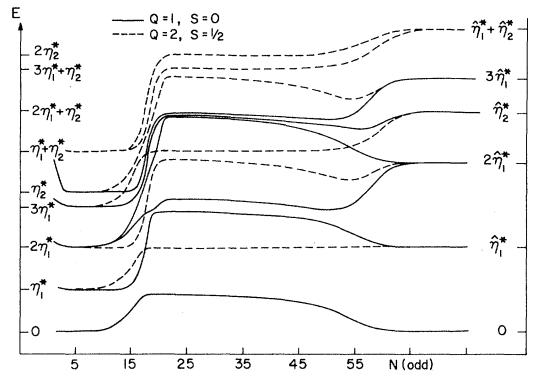

FIG. 5. Low-lying energy levels of H_N as a function of odd N for $U/D=10^{-3}$, $U/\pi\Gamma=12.66$, and $\Lambda=2.5$. On the left-hand vertical scale are the lowest-lying free-electron fixed-point levels for N odd, while on the right-hand side are the equivalent levels for N even. The following fixed-point regimes obtain: free orbital $5<N<15$, local moment $23<N<51$, strong coupling $61<N$.

starts out very close to $H^*_{\rm FO}$ (first several iterations are of no interest); but as N increases its deviations from $H^*_{\rm FO}$ increase rapidly (exponentially with N, to be precise) until, when the deviations get large enough, H_N crosses over to arrive close to (but with small deviations from) $H^*_{\rm LM}$. As N increases further, these deviations of H_N from $H^*_{\rm LM}$ grow slowly (linearly with N at first, as higher powers of N later) until, eventually, it crosses over and stabilizes at $\hat{H}^*_{\rm SC}$. This behavior persists, in essence, for all values of $\tilde{U}$ and $\tilde{\Gamma}$. Only the values of N where the crossovers occur change as $\tilde{U}$ and $\tilde{\Gamma}$ are changed.

TABLE IV. Energies of the states plotted in Figs. 5–7 for odd-N fixed-point Hamiltonians $H^*_{\rm FO}$, $H^*_{\rm LM}$, and $\hat{H}^*_{\rm SC}$.

Charge Q	Spin S	Index r	Energy in $H^*_{\rm FO}$	$H^*_{\rm LM}$	$\hat{H}^*_{\rm SC}$
1	0	1	0	η_1^*	0
		2	η_1^*	$3\eta_1^*$	$\hat{\eta}_1^*$
		3	$2\eta_1^*$	η_2^*	$2\hat{\eta}_1^*$
		4	$2\eta_1^*$	$2\eta_1^*+\eta_2^*$	$2\hat{\eta}_1^*$
		5	$3\eta_1^*$	$2\eta_1^*+\eta_2^*$	$3\hat{\eta}_1^*$
		6	η_2^*	$2\eta_1^*+\eta_2^*$	$\hat{\eta}_2^*$
2	$\frac{1}{2}$	1	η_1^*	$2\eta_1^*$	$\hat{\eta}_1^*$
		2	$2\eta_1^*$	$\eta_1^*+\eta_2^*$	$2\hat{\eta}_1^*$
		3	$3\eta_1^*$	$\eta_1^*+\eta_2^*$	$3\hat{\eta}_1^*$
		4	η_2^*	$3\eta_1^*+\eta_2^*$	$\hat{\eta}_2^*$
		5	$\eta_1^*+\eta_2^*$	$3\eta_1^*+\eta_2^*$	$\hat{\eta}_1^*+\hat{\eta}_2^*$
		6	$\eta_1^*+\eta_2^*$	$2\eta_2^*$	$\hat{\eta}_1^*+\hat{\eta}_2^*$

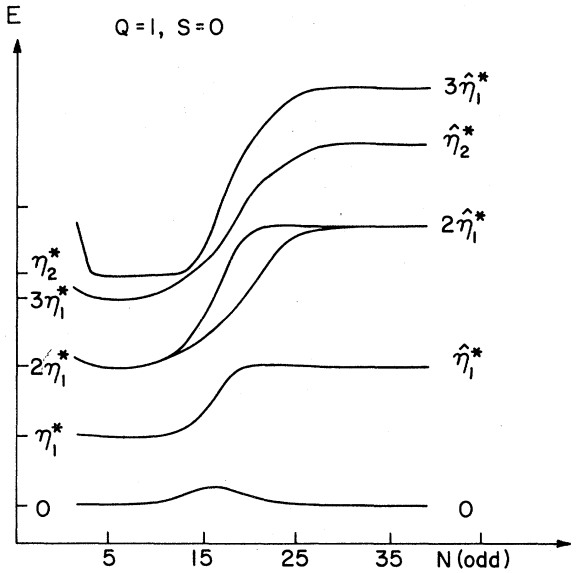

FIG. 6. Low-lying energy levels of H_N as a function of odd N for $U/D=10^{-3}$, $U/\pi\Gamma=1.013$, and $\Lambda=2.5$. There is direct transition between the free-orbital and strong-coupling regimes without passing through the local-moment regime.

The reasons for the crossovers of H_N away from $H^*_{\rm FO}$ and $H^*_{\rm LM}$, the difference in character between the crossover from $H^*_{\rm FO}$ to $H^*_{\rm LM}$ and that from $H^*_{\rm LM}$ to $\hat{H}^*_{\rm SC}$, the dependence of the crossover positions on the values of $\tilde{U}$ and $\tilde{\Gamma}$, etc., will be discussed at length in Sec. V. Here we will just quote some results and illustrate them with some examples. First of all, the condition that H_N start out close to $H^*_{\rm FO}$ is that (U/D) and (Γ/D) both be small. The crossover away from $H^*_{\rm FO}$ begins roughly when either $(U/D)\Lambda^{(N-1)/2}$ or $(\Gamma/D)\Lambda^{(N-1)/2}$ grows to become of order unity, whichever is earlier. If $U/\Gamma \gg 1$, the crossover is to $H^*_{\rm LM}$, but with a deviation from $H^*_{\rm LM}$ or order (Γ/U). This deviation then grows roughly

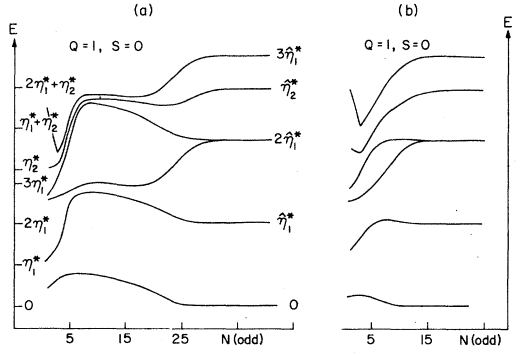

FIG. 7. Low-lying energy levels of H_N as a function of odd N for $U/D=\frac{1}{2}$. (a) $U/\pi\Gamma=5.63$ and (b) $U/\pi\Gamma=1.013$.

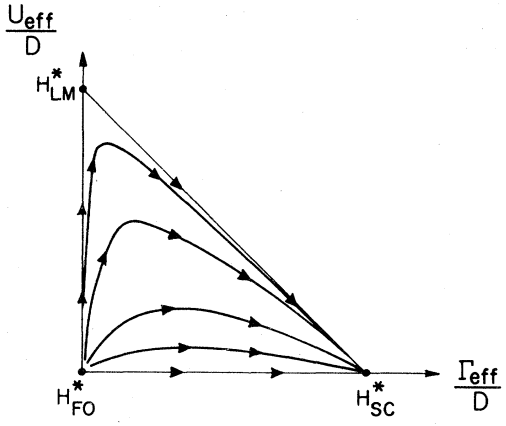

FIG. 8. Schematic renormalization-group flow diagram. Each H_N is thought of as associated with a $U_{\rm eff}$ and $\Gamma_{\rm eff}$. Trajectories depict the flow of H_N with increasing N. Note that only the strong-coupling fixed point is stable.

linearly with N, and the final crossover to $\hat{H}^*_{SC}$ occurs roughly when $(\Gamma/U)(N\ln\Lambda)$ grows to become of order unity. So that, as the ratio U/Γ is decreased, the region where H_N is close to the H^*_{LM} shrinks and eventually when Γ becomes larger than U the crossover is directly to $\hat{H}^*_{SC}$. Figures 6 and 7 where only the $Q=1$, $S=0$ energy levels are plotted against N, serve to illustrate these results. For Fig. 6, U/D is still 10^{-3} but $U/\pi\Gamma$ has been decreased to 1.013, and the crossover is almost directly from H^*_{FO} to $\hat{H}^*_{SC}$. Figs. 7(a) and 7(b) both correspond to $U/D=\frac{1}{2}$, so that the crossover away from H^*_{FO} happens right away. In Fig. 7(a) $U/\pi\Gamma=5.63$ so that H_N is near H^*_{LM} for some range of N before crossing over to $\hat{H}^*_{SC}$; but in Fig. 7(b) $U/\pi\Gamma=1.013$, so that the crossover to $\hat{H}^*_{SC}$ also occurs for a smallish N. No numerical results are shown for the regime when $U/\pi\Gamma \ll 1$, since this case can be handled analytically (see Sec. V). Figure 8 sums up the various regimes in the form of a schematic, renormalization-group flow diagram. Note that when $\tilde{\Gamma}=0$, H_N crosses over from H^*_{FO} to *stabilize* at H^*_{LM}.

D. Numerical results for the impurity susceptibility

Figures 9 and 10 depict the results for the impurity susceptibility for the same values of U and Γ as considered above. The form in which the results are plotted, namely $k_BT\chi(T)$ vs $\ln(k_BT/D)$, may seem rather unconventional; but is very convenient because one can make a one to one correspondence between such plots and the development of H_N with N discussed in Sec. III C. This connection follows from the expression (2.42) for evaluating $k_BT\chi$ and from the expression (2.41) showing N to be proportional to $\ln(D/k_BT)$.

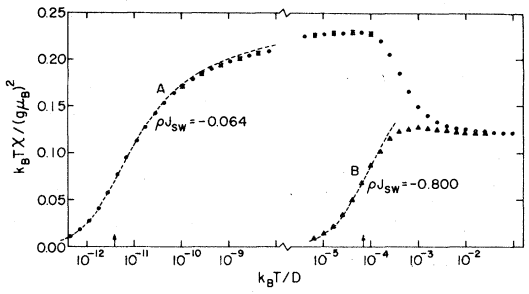

FIG. 9. Plots of $k_BT\chi(T)/(g\mu_B)^2$ vs $\ln(k_BT/D)$ for the symmetric Anderson model for $U/D=10^{-3}$; $U/\pi\Gamma=12.66$(A) and 1.013(B). The dashed curves correspond to the universal susceptibility curve for the Kondo model (see Fig. 11 and Sec. V). The vertical arrows on the abscissa mark the effective Kondo temperature (5.16) for the two plots. Note that the curves mirror the pattern of energy levels in Figs. 5 and 6. For $U \gg \pi\Gamma$, there is a well-developed local-moment regime ($T\chi=\frac{1}{4}$) between the free-orbital regime ($T\chi=\frac{1}{8}$) and the strong-coupling regime ($\chi=$ constant), whereas for $U\sim\pi\Gamma$, there is a direct transition from the free-orbital to strong-coupling regime. The labels ρJ_{SW} are deduced from Eq. (5.14).

Compare Fig. 5 with the plot labeled (A) in Fig. 9, both of which correspond to $U/D=10^{-3}$ and $U/\pi\Gamma=12.66$. For small N, which corresponds to temperatures close to the band edge, the leading contribution to (2.42) is obtained by replacing H_N by $H^*_{N,FO}$ (cf. Sec. III B). Since $H^*_{N,FO}$ is just H^0_N plus the free-impurity orbital, the answer one gets for $k_BT\chi$ is just $\frac{1}{8}$. The increase in the deviation of H_N from $H^*_{N,FO}$ as N increase is reflected in the increase in the deviation of $k_BT\chi$ from $\frac{1}{8}$ as the temperature decreases. If H_N is replaced by the local-moment Ham-

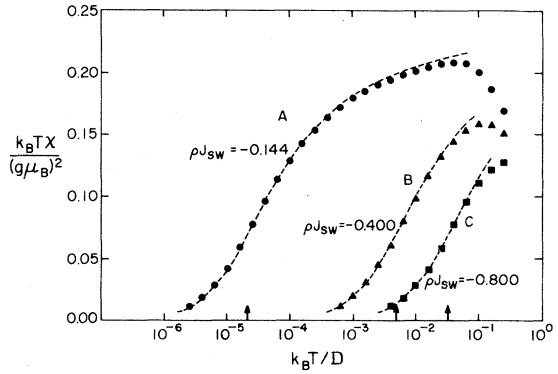

FIG. 10. Plots of $k_BT\chi(T)/(g\mu_B)$ vs $\ln(k_BT/D)$ for $U/D=\frac{1}{2}$; $U/\pi\Gamma=5.629$(A), 2.026(B), and 1.013(C). The dashed curves are the universal Kondo susceptibility curve with the appropriate Kondo temperatures marked with an arrow on the abscissa. The ρJ_{SW} values are calculated from Eq. (5.14). Note that for $U\sim D$, there is no free-orbital regimes, in contrast to Fig. 9.

iltonian $H^*_{N,\mathrm{LM}}$ in Eq. (2.42), the resulting answer for $k_BT\chi$ would be the value $\frac{1}{4}$ characteristic of a free-spin-$\frac{1}{2}$ impurity. The fact that H_N crosses over fairly rapidly (in N) and arrives close to the local-moment fixed point is therefore reflected in the fairly rapid [in $\ln(k_BT/D)$] increases in $k_BT\chi$ to a value close to $\frac{1}{4}$. Finally, the gradual decrease in $k_BT\chi$ as the temperature is reduced further reflects the gradual crossover of H_N from the local-moment regime to the strong-coupling fixed-point because, as we will see in Sec. V, the replacement of H_N by $\hat{H}^*_{N,\mathrm{SC}}$ in Eq. (2.42) makes $k_BT\chi$ vanish. One can similarly relate the qualitative features of the rest of the susceptibility plots to the qualitative features of the corresponding energy-level plots.

This completes our preliminary survey of the numerical results. The relevance of the renormalization-group aspect of the problem, namely the flow (under repeated application of the renormalization-group transformation $\mathcal{T}^2$) of H_N among the various fixed points of $\mathcal{T}^2$, in understanding the temperature dependence of the impurity properties should by now be clear. The next step is to arrive at a *quantitative* understanding of the numerical results that have been presented so far. The formal machinery needed for this purpose, which enables one to write down effective Hamiltonians that describe H_N when it is in the vicinity of the fixed points of $\mathcal{T}^2$, is set up in Sec. IV. In Sec. V we use this machinery to understand the flow of H_N and the temperature dependence of the impurity susceptibility in quantitative detail.

IV. DEVIATIONS FROM FIXED POINTS AND EFFECTIVE HAMILTONIANS

A. Linearization of $\mathcal{T}^2$, eigenoperators and effective Hamiltonians

Suppose that H_N is close to a fixed point H^* (which may stand for any of the fixed points discussed in Sec. III B) of $\mathcal{T}^2$. Then H_{N+2}, given by $\mathcal{T}^2[H_N]$, will also be close to H^* (by continuity H_{N+2} will be close to $\mathcal{T}^2[H^*]$, which is just H^*). Let δH_N stand for the deviation of H_N from H^*: $\delta H_N \equiv (H_N - H^*)$. Clearly,

$$\delta H_{N+2} \equiv H_{N+2} - H^* = \mathcal{T}^2[H^* + \delta H_N] - H^* \quad . \tag{4.1}$$

Since δH_N is supposed to be small one can expand the right-hand side in powers of δH_N. Retaining only the term linear in δH_N leads to the result

$$\delta H_{N+2} = \mathfrak{L}_{(H^*)}\delta H_N \equiv \mathfrak{L}^*\delta H_N \quad , \tag{4.2}$$

where $\mathfrak{L}^*$ is now a *linear* transformation that depends upon the choice of the fixed point H^*. Recall that, for the purposes of the transformation $\mathcal{T}^2$, H_N can be specified by a list of its energy levels and the matrix elements of f_N between its eigenstates. Therefore δH_N can also be thought of as a correction list of energies and matrix elements. Equation (4.2) is just a formal way of stating that the correction list for $(N+2)$ is linearly related to the correction list for N if the latter is small enough.

Since $\mathfrak{L}^*$ is a linear transformation, there can exist some operators O_l^* that are *eigenoperators* of $\mathfrak{L}^*$ belonging to eigenvalues λ_l^*, say, i.e.,

$$\mathfrak{L}^* O_l^* = \lambda_l^* O_l^* \quad . \tag{4.3}$$

It is important to remember that O_l^* and λ_l^* will both depend upon the particular fixed point one is considering. One can now construct linear combinations such as

$$\delta H_N = \sum_l C_l \lambda_l^{*N/2} O_l^* \quad , \tag{4.4}$$

which clearly satisfy Eq. (4.2) for arbitrary coefficients C_l. As N increases, the contribution to Eq. (4.4) of operators O_l^* whose eigenvalues λ_l^* are greater than 1 increases rapidly. Such operators are termed *relevant.* Similarly, an operator O_l^* for which $\lambda_l^* < 1$ is termed *irrelevant.* Such operators make negligible contributions to Eq. (4.4) for large N. Operators O_l^* belonging to $\lambda_l^* = 1$ are called *marginal* operators. If the set of eigenoperators is complete, Eq. (4.4) represents the most general solution to Eq. (4.2). By allowing the coefficients C_l to depend on N, one can then extend the expansion (4.4) beyond the linearized regime. See Wegner[8] and Sec. V of Ref. 6 for further discussions.

The eigenoperators of a fixed point are also crucial in determining the stability of that fixed point, that is in determining whether a Hamiltonian that starts out close to that fixed point flows toward it or away from it under the action of the renormalization-group transformation. A fixed point H^* that has relevant eigenoperators will be *unstable,* because any Hamiltonian whose deviation from H^* has a component in any of its relevant eigenoperators will flow away from H^* under the action of $\mathcal{T}^2$. Similarly a fixed point H^* that has *only* irrelevant eigenoperators is a *stable* fixed point; once a Hamiltonain comes close to such a fixed point, it will flow to that fixed point under the renormalization-group transformation. The question of the stability of fixed points with marginal operators is more complicated. See Refs. 6–8 for details.

In order to describe the deviations of H_N from a fixed point H^* of $\mathcal{T}^2$, we must therefore identify the eigenoperators and the eigenvalues of the linearized transformation $\mathfrak{L}^*$ for that fixed point. One way to do this is to actually set up and solve Eq. (4.3). An alternative approach more useful for our purposes is as follows. In Sec. III B it was noted that for every fixed point of $\mathcal{T}^2$ there are special choices for Γ and U which make the corresponding H_N go rapidly to

that fixed point as $N \to \infty$. Let H_N^* denote such a special H_N. (H_N^* can be $H_{N,\mathrm{FO}}^*$, $H_{N,\mathrm{LM}}^*$, or $H_{N,\mathrm{SC}}^*$.) Consider a new Hamiltonian defined as

$$H_N' = H_N^* + \Lambda^{(N-1)/2}\delta H \ , \tag{4.5}$$

where δH is small and depends only on the *first few degrees of freedom consistent with the H_N^* under consideration.* (What the emphasized phrase means will become clear by example in Sec. IV B.) Then for large N, H_N' satisfies the same recursion relation as H_N^*, namely: $H_{N+2}' = \mathcal{T}^2[H_N']$. If δH is small enough, the difference $(H_N' - H_N^*)$ will be small. It is easy to prove that $(H_N' - H_N^*)$ will then satisfy the linearized recursion relation (4.2): clearly

$$\begin{aligned}(H_{N+2}' - H_{N+2}^*) &= \mathcal{T}^2[H_N^* + (H_N' - H_N^*)] - \mathcal{T}^2(H_N^*) \\ &\cong \mathfrak{L}_{(H_N^*)}(H_N' - H_N^*) \ ;\end{aligned} \tag{4.6}$$

furthermore, $H_N^* \cong H^*$ for large N so that $\mathfrak{L}_{(H_N^*)} \cong \mathfrak{L}_{(H^*)} \equiv \mathfrak{L}^*$, and the result follows. This means that for large N the difference $(H_N' - H_N^*)$ should be expandable in terms of the eigenoperators of the linearized transformation about H^*:

$$H_N' - H_N^* = \sum_l C_l \lambda_l^{*N/2} O_l^* \ . \tag{4.7}$$

For simple choices of δH, H_N' can be explicitly solved (i.e., its energy levels and the matrix elements of f_N between its eigenstates determined) to first order in δH, and the left-hand side of Eq. (4.7) can hence be computed. From the N dependence of the results for $(H_N' - H_N^*)$, one can verify Eq. (4.7) as well as identify those eigenoperators and eigenvalues for which $C_l \neq 0$. By considering a wide enough choice for δH one can, in principle, identify all the eigenoperators. Usually, one is only interested in Hamiltonians H_N that obey certain symmetries. Then the eigenopertors that need be considered must also obey the same symmetries, and to identify them it is enough to consider $\delta H'$s that themselves display these symmetries.

The basic idea, therefore, is that for every fixed point H^*, one can write down various simple $\delta H'$s that *generate eigenoperators* about that fixed point. One can now imagine arranging these $\delta H'$s in a hierarchy—δH_1, δH_2, δH_3, etc.,—such that the larger the index of a δH, the smaller is the eigenvalue of the eigenoperator it generates. This immediately leads to the idea that when H_N is close to some fixed point, its states and energy levels can be calculated by using an *effective Hamiltonian,* given by the corresponding H_N^* plus correction terms:

$$H_N^{\mathrm{eff}} = H_N^* + \omega_1 \Lambda^{(N-1)/2}\delta H_1 + \omega_2 \Lambda^{(N-1)/2}\delta H_2 + \cdots \ , \tag{4.8}$$

where ω_1, ω_2, etc., are some coefficients. The *form* of the operators δH_1, δH_2, etc., when expressed in terms of the electron and hole operators that diagonalize H_N^*, depends only on the particular fixed point that one is considering and on the symmetries one wants H_N^{eff} to obey. The dependence of H_N^{eff} on the parameters in the problem, such as $\tilde{U}$ and $\tilde{\Gamma}$, is only via the coefficients ω_1, ω_2, etc. It must be emphasized that effective Hamiltonians are to be used only for those values of N where the correction terms in Eq. (4.8) are small enough for them to be treated perturbatively.

B. Eigenoperators and effective Hamiltonians for the symmetric Anderson model

The discussion in Sec. IV A was somewhat general and abstract. In this section we will apply those ideas to the symmetric Anderson model. In this case H_N conserves charge, spin, and particle-hole symmetry. Therefore it is enough for us to consider only those $\delta H'$s that themselves have these symmetries. As in Sec. III C, we will consider only odd N. The fixed points that are of interest are therefore H_{FO}^*, H_{LM}^*, and $\hat{H}_{\mathrm{SC}}^*$.

a. Consider first the free-orbital fixed point H_{FO}^*. H_N^* is then just the Hamiltonian $H_{N,\mathrm{FO}}^*$ (defined in Sec. III B) obtained by putting $\tilde{\Gamma} = \tilde{U} = 0$ in H_N. The first few degrees of freedom consistent with this fixed point are hence the operators $c_{d\mu}$, $f_{0\mu}$, $f_{1\mu}$, etc. Some examples of operators δH that conserve charge, spin, and particle-hole symmetry are

$$\begin{aligned}
\delta H_1 &\equiv (c_{d\mu}^\dagger c_{d\mu} - 1)^2 \ , \\
\delta H_2 &\equiv (c_{d\mu}^\dagger f_{0\mu} + f_{0\mu}^\dagger c_{d\mu}) \ , \\
\delta H_3 &\equiv (c_{d\mu}^\dagger f_{0\mu} + f_{0\mu}^\dagger c_{d\mu})^2 \ , \\
\delta H_4 &\equiv (c_{d\mu}^\dagger c_{d\mu} - 1)(f_{0\mu}^\dagger f_{0\mu} - 1) \ , \\
\delta H_5 &\equiv (c_{d\mu'}^\dagger \vec{\sigma}_{\mu'\nu'} c_{d\nu'})(f_{0\mu}^\dagger \vec{\sigma}_{\mu\nu} f_{0\nu}) \ , \\
\delta H_6 &\equiv (f_{0\mu}^\dagger f_{1\mu} + f_{1\mu}^\dagger f_{0\mu}), \text{ etc.}
\end{aligned} \tag{4.9}$$

The general principles that determine the hierarchy of the various $\delta H'$s in the sense of the degree of relevance of the eigenoperators that they generate, are as follows. In order to generate an eigenoperator of maximum relevance, one must use the minimum possible number of operators, with the lowest possible indices from among (f_n), within the constraints imposed by the symmetry requirements. This is because when one works out the effect of δH on H_N, one finds that the use of f_0 in δH gives rise to a factor $\Lambda^{-N/4}$ [cf. Eq. (4.11) below], use of f_1 in δH, to a factor $\Lambda^{-3N/4}$ [cf. Eq. (4.17)]. Using f_2 is *equivalent to using* f_0 except for a term that carries a factor of $\Lambda^{-5N/4}$, and using f_3 is equivalent to using f_1 but for a term going as $\Lambda^{-7N/4}$.

We will now illustrate these principles by demonstrating (using the methods outlined in Sec. IV A)

that among the operators listed in Eq. (4.9), δH_1 and δH_2 generate relevant operators, δH_3, δH_4, and δH_5 generate marginal operators, and δH_6, etc., generate irrelevant operators about $H^*_{\rm FO}$.

The result for δH_1 is rather trivial. Consider the corresponding H'_N

$$H'_N = H^*_{N,\rm FO} + \omega_1 \Lambda^{(N-1)/2} \delta H_1$$
$$= H^*_{N,\rm FO} + \omega_1 \Lambda^{(N-1)/2} (c^\dagger_{d\mu} c_{d\mu} - 1)^2 \ . \quad (4.10)$$

Clearly, the many-particle states of $H^*_{N,\rm FO}$ continue to be eigenstates of H'_N. All that the δH_1 term does is to lift the quadruple degeneracy in $H^*_{N,\rm FO}$ corresponding to the different occupations of the impurity orbital. States in which the impurity orbital is singly occupied will have the same energies as in $H^*_{N,\rm FO}$, but states in which the impurity orbital is either empty or doubly occupied will have their energies increased by $\omega_1 \Lambda^{(N-1)/2}$. Comparing the N dependence of the changes in the energy levels with Eq. (4.7) makes it clear that δH_1 generates a relevant eigenoperator with eigenvalue Λ.

Next consider δH_2. In order to calculate its effects on the states of $H^*_{N,\rm FO}$, we express it in terms of the electron and hole operators, g_j and h_j, that diagonalize $H^*_{N,\rm FO}$. From Secs. III A and B we know that (cf. Table II)

$$f_{0\mu} = \Lambda^{-(N-1)/4} \sum_j \alpha_{0j} (g_{j\mu} + h^\dagger_{j\mu}) \ . \quad (4.11)$$

So that we have for the corresponding H'_N,

$$H'_N = H^*_{N,\rm FO} + \omega_2 \Lambda^{(N-1)/2} \delta H_2$$
$$= \sum_j \eta^*_j (g^\dagger_{j\mu} g_{j\mu} + h^\dagger_{j\mu} h_{j\mu}) + \omega_2 \Lambda^{(N-1)/4} \times \sum_j \alpha_{0j} (c^\dagger_{d\mu} g_{j\mu} + c^\dagger_{d\mu} h^\dagger_{j\mu} + g^\dagger_{j\mu} c_{d\mu} + h_{j\mu} c_{d\mu}) \ , \quad (4.12)$$

where we have used the result that the single-particle energies $\eta_j(N)$ are essentially equal to their fixed-point values η^*_j. It is hence clear that the effect due to δH_2 on the states of $H^*_{N,\rm FO}$ increases with N as $\Lambda^{N/4}$, so that it generates a relevant operator. Actually, it is easy to see from Eq. (4.12) that energy levels are not affected to first order in δH_2. Since H'_N is a quadratic Hamiltonian, it can be diagonalized exactly, and one finds that to leading order in $\omega_2 \Lambda^{(N-1)/4}$ (which is supposed to be small), the new single-particle energies are given by

$$\eta'_j = \eta^*_j + \frac{\omega_2^2 \alpha_{0j}^2}{\eta^*_j} \Lambda^{(N-1)/2} \ . \quad (4.13)$$

This is proved in Appendix E (in a somewhat different context). Of course, Eq. (4.13) is obtainable quite trivially from (4.12) by using second-order perturbation theory.

The proof that δH_3, δH_4, and δH_5 generate marginal operators about $H^*_{\rm FO}$ is obtained by substituting the expansion (4.11) for $f_{0\mu}$ in the expressions for these operators. It is straightforward to verify that

$$\Lambda^{(N-1)/2} \delta H_3 = \left(\sum_j \alpha_{0j} (c^\dagger_{d\mu} g_{j\mu} + c^\dagger_{d\mu} h^\dagger_{j\mu} + g^\dagger_{j\mu} c_{d\mu} + h_{g\mu} c_{d\mu}) \right)^2 \ , \quad (4.14)$$

$$\Lambda^{(N-1)/2} \delta H_4 = (c^\dagger_{dv} c_{dv} - 1) \sum_{jj'} \alpha_{0j} \alpha_{0j'} (g^\dagger_{j\mu} g_{j'\mu} - h^\dagger_{j\mu} h_{j'\mu} + h_{j\mu} g_{j'\mu} + g^\dagger_{j\mu} h^\dagger_{j'\mu}) \ , \quad (4.15)$$

$$\Lambda^{(N-1)/2} \delta H_5 = (c^\dagger_{d\mu} \vec{\sigma}_{\mu' v'} c_{dv'}) \sum_{jj'} \alpha_{0j} \alpha_{0j'} (g^\dagger_{j\mu} \vec{\sigma}_{\mu\nu} g_{j'v} + h_{j\mu} \vec{\sigma}_{\mu\nu} h^\dagger_{j'v} + g^\dagger_{j\mu} \vec{\sigma}_{\mu\nu} h_{j'v} + h_{j\mu} \vec{\sigma}_{\mu\nu} g_{j'v}) \ . \quad (4.16)$$

[Perhaps the only tricky part of the verification will be in connection with Eq. (4.15), where one will need to use the result that $2(\sum_j \alpha_{0j}^2) = \Lambda^{(N-1)/2}$.] Each of these operators when added to $H^*_{N,\rm FO}$ will clearly produce first-order changes in its energy levels; which changes will be determined by the matrix elements of these operators between different states of $H^*_{N,\rm FO}$. The changes will clearly be independent of N; the corresponding eigenoperators are hence all marginal.

In order to show that δH_6 generates an irrelevant operator about $H^*_{\rm FO}$, we need to know the expansion for f_1 in terms of g_j and h_j as well. From Table II

$$f_{1\mu} = \Lambda^{-3(N-1)/4} \sum_j \alpha_{1j} (g_{j\mu} - h^\dagger_{j\mu}) \ . \quad (4.17)$$

Substituting this equation and Eq. (4.11) into the expression for δH_6, one gets

$$\Lambda^{(N-1)/2} \delta H_6 = \Lambda^{-(N-1)/2} \sum_{jj'} [\alpha_{0j} a_{1j} (g^\dagger_{j\mu} g_{j'\mu} - h_{j\mu} h^\dagger_{j'\mu} - g^\dagger_{j\mu} h^\dagger_{j'\mu} + h_{j\mu} g_{j'\mu}) + \text{H.c.}] \ , \quad (4.18)$$

where H.c. represents the Hermitian conjugate term. The matrix elements of this operator between the states

of $H^*_{N,\mathrm{FO}}$, which determine the effect of δH_6 on their energy levels, clearly decrease as $\Lambda^{-N/2}$. Hence δH_6 generates an irrelevant operator with eigenvalue Λ^{-1}.

It is easy to verify, using arguments similar to those given above, that any *new* eigenoperator that can be generated by using a δH that conserves charge, spin, and particle-hole symmetry and is not in the list (4.9) will have an eigenvalue <1.

b. Next, consider the local-moment fixed point H^*_{LM}. It was seen in Sec. III B that the corresponding H^*_N, denoted $H^*_{N,\mathrm{LM}}$, is obtained by choosing $\tilde{\Gamma}=0$ and $\tilde{U}=\infty$, which choice eliminates the operator $c_{d\mu}$ and replaces it by a Pauli spin operator $\vec{\tau}$. The first few degrees of freedom consistent with $H^*_{N,\mathrm{LM}}$ are therefore the operators $\vec{\tau}$, f_0, f_1, etc. Using the general principles set forth above, it is easy to show that the first three operators in the hierarchy of $\delta H'$s that conserve charge, spin, and particle-hole symmetry are

$$\begin{aligned}\delta H_1&=(f^\dagger_{0\mu}\,\vec{\sigma}_{\mu\nu}f_{0\nu})\cdot\vec{\tau}\ ,\\ \delta H_2&=(f^\dagger_{0\mu}f_{1\mu}+f^\dagger_{1\mu}f_{0\mu})\ ,\\ \delta H_3&=(f^\dagger_{0\mu}f_{0\mu}-1)^2\ .\end{aligned}\tag{4.19}$$

δH_1 generates a marginal operator while δH_2 and δH_3 generate irrelevant eigenoperators belonging to an eigenvalue Λ^{-1}. There are no relevant operators for H^*_{LM}. The proof proceeds exactly as in the case of H^*_{FO}. The expansions for f_0 and f_1 in terms of the electron and hole operators that diagonalize $H^*_{N,\mathrm{LM}}$ are still given by Eqs. (4.11) and (4.18). Substituting this into Eq. (4.19), it is straightforward to verify that

$$\Lambda^{(N-1)/2}\delta H_1=\sum_{jj'}\alpha_{0j}\alpha_{0j'}(g^\dagger_{j\mu}\,\vec{\sigma}_{\mu\nu}g_{j'\nu}+h_{j\mu}\vec{\sigma}_{\mu\nu}h^\dagger_{j'\nu}+g^\dagger_{j\mu}\,\vec{\sigma}_{\mu\nu}h^\dagger_{j'\nu}+h_{j\mu}\sigma_{\mu\nu}g_{j'\nu})\cdot\vec{\tau}\ ,\tag{4.20}$$

$$\Lambda^{(N-1)/2}\delta H_2=\Lambda^{-(N-1)/2}\sum_{jj'}[\alpha_{0j}\alpha_{1j'}(g^\dagger_{j\mu}g_{j'\mu}-h_{j\mu}h^\dagger_{j'\mu}-g^\dagger_{j\mu}h^\dagger_{j'\mu}+h_{j\mu}g_{j'\mu})+\mathrm{H.c.}]\ ,\tag{4.21}$$

$$\Lambda^{(N-1)/2}\delta H_3=\Lambda^{-(N-1)/2}\left[\sum_{jj'}\alpha_{0j}\alpha_{0j'}(g^\dagger_{j\mu}g_{j'\mu}-h^\dagger_{j\mu}h_{j'\mu}+h_{j\mu}g_{j'\mu}+g^\dagger_{j\mu}h^\dagger_{j'\mu})\right]^2\ .\tag{4.22}$$

Considering the H'_N that can be formed by adding each of these terms to $H^*_{N,\mathrm{LM}}$, it is at once obvious that the first-order effects due to δH_1 are independent of N, whereas those due to δH_2 and δH_3 fall off as $\Lambda^{-N/2}$. In order to generate a relevant eigenoperator around H^*_{LM}, one would need a δH that has at the most a single f_0. There are no such operators that conserve charge, spin, and particle-hole symmetry. It is easily verified that the choice of $(f^\dagger_{0\mu}f_{0\mu}-1)$ for δH would generate a marginal eigenoperator, but this operator is *odd* under particle-hole symmetry. One can also verify that any new eigenoperators generated by using $\delta H'$s other than the ones in Eq. (4.19) have eigenvalues $<\Lambda^{-1}$.

c. Finally, consider the strong-coupling fixed point $\hat{H}^*_{\mathrm{SC}}$. Recall (cf. Sec. III B) that the corresponding H^*_N is the Hamiltonian $H^*_{N,\mathrm{SC}}$ obtained by choosing $\tilde{\Gamma}=\infty$ [see Eq. (3.10)]. *The first few degrees of freedom consistent with* $H^*_{N,\mathrm{SC}}$ are hence the operators f_1, f_2, etc. Further, from the discussions in Secs. III A and B it should be clear that the expansions for f_1 and f_2 in terms of the operators g_0, g_j, and h_j that diagonalize $H^*_{N,\mathrm{SC}}$ for odd N are

$$f_{1\mu}\propto\Lambda^{-(N-1)/4}\left(\hat{\alpha}_{00}g_{0\mu}+\sum_j\hat{\alpha}_{0j}(g_{j\mu}+h^\dagger_{j\mu})\right)\ ,\tag{4.23}$$

$$f_{2\mu}\propto\Lambda^{-3(N-1)/4}\sum_j\hat{\alpha}_{1j}(g_{j\mu}-h^\dagger_{j\mu})\ .\tag{4.24}$$

It immediately follows that there can be no relevant or marginal operators around $\hat{H}^*_{\mathrm{SC}}$ that conserve charge, spin, and particle-hole symmetry. The operator $(f^\dagger_{1\mu}f_{1\mu}-1)$, which would generate a marginal eigenoperator, is odd under particle-hole symmetry. It is easy to verify that the first two operators in the hierarchy of $\delta H'$s are

$$\begin{aligned}\delta H_1&=(f^\dagger_{1\mu}f_{2\mu}+f^\dagger_{2\mu}f_{1\mu})\ ,\\ \delta H_2&=(f^\dagger_{1\mu}f_{1\mu}-1)^2\ .\end{aligned}\tag{4.25}$$

Both of these generate irrelevant eigenoperators of eigenvalue Λ^{-1}. The proof is obtained by making use of Eqs. (4.23) and (4.24) in Eq. (4.25). One gets

$$\Lambda^{(N-1)/2}\delta H_1\propto\Lambda^{-(N-1)/2}\left[\sum_{jj'}\hat{\alpha}_{00}\hat{\alpha}_{1j'}(g^\dagger_{0\mu}g_{j'\mu}-g^\dagger_{0\mu}h^\dagger_{j'\mu})+\sum_{jj'}\hat{\alpha}_{0j}\hat{\alpha}_{1j}(g^\dagger_{j\mu}g_{j'\mu}-h_{j\mu}h^\dagger_{j'\mu}-g^\dagger_{j\mu}h^\dagger_{j'\mu}+h_{j\mu}g_{j'\mu})+\mathrm{H.c.}\right]\ ,\tag{4.26}$$

$$\begin{aligned}\Lambda^{(N-1)/2}\delta H_2\propto\Lambda^{-(N-1)/2}\Bigg[&\hat{\alpha}^2_{00}(g^\dagger_{0\mu}g_{0\mu}-1)+\sum_j\hat{\alpha}_{00}\hat{\alpha}_{0j}(g^\dagger_{0\mu}g_{j\mu}+g^\dagger_{0\mu}h^\dagger_{j\mu}+g^\dagger_{j\mu}g_{0\mu}+h_{j\mu}g_{0\mu})\\&+\sum_{jj'}\hat{\alpha}_{0j}\hat{\alpha}_{0j'}(g^\dagger_{j\mu}g_{j'\mu}+g^\dagger_{j\mu}h^\dagger_{j'\mu}-h^\dagger_{j\mu}h_{j'\mu}+h_{j\mu}g_{j'\mu})\Bigg]^2\ .\end{aligned}\tag{4.27}$$

[In order to verify Eq. (4.27), one has to use the result that $\hat{\alpha}_{00}^2 + 2\sum_j \hat{\alpha}_{0j}^2 = \Lambda^{(N-1)/2}$.] The factors of $\Lambda^{-N/2}$ in Eqs. (4.26) and (4.27) prove the required result. Again, the use in δH of f_3, which is proportional to f_1 but for a piece going as $\Lambda^{-5(N-1)/4}$, or of f_4, which is proportional to f_2 but for a term going as $\Lambda^{-7(N-1)/4}$, will generate the same eigenoperators (4.26) and (4.27) and new eigenoperators with eigenvalues $<\Lambda^{-1}$. For example, $\delta H = (f_{2\mu}^\dagger f_{2\mu} - 1)^2$ generates a new eigenoperator with eigenvalue Λ^{-5}.

This completes the machinery needed to analyze the numerical results presented in Sec. III. The next step is to use the effective Hamiltonian around each specific fixed point to calculate the energy levels of H_N for the values of N where it is close to that fixed point. Fitting the results of such calculations to the numerical results for the energy levels will enable one to determine the corresponding coefficients ω_1, ω_2, etc., for general values of the parameters $\tilde{U}$ and $\tilde{\Gamma}$. For limiting cases, one may be able to calculate analytically the dependence of ω_1, ω_2, etc., on $\tilde{U}$ and $\tilde{\Gamma}$; examples will be seen in Sec. V. Once the coefficients ω_1, ω_2, etc., are determined the effective Hamiltonian can be used to calculate the impurity susceptibility for temperatures where $k_B T\chi(T)$ is close to its fixed-point value.

However, it must be obvious from the structure of the effective Hamiltonians that have been written down that calculations keeping many correction terms, while quite feasible, can be very tedious. The calculations to be presented in Sec. V will be made keeping only the most dominant correction terms around each fixed point. This means keeping only the two relevant terms for $H_{\rm FO}^*$, only the marginal term for $H_{\rm LM}^*$, and only the two leading irrelevant terms for $H_{\rm SC}^*$.

V. QUANTITATIVE ANALYSIS OF THE NUMERICAL RESULTS

Now we will present a detailed quantitative analysis of the numerical results presented earlier. The analysis will primarily concentrate on the case when $\tilde{U}$ and $\tilde{\Gamma}$ are both small, i.e., when U and Γ are both smaller than D. As before, we consider only odd N.

A. Free-orbital regime

When $\tilde{\Gamma}$ and $\tilde{U}$ are both small, it follows from the discussion of the free-orbital fixed point in Sec. III B that one can write

$$H_N = H_{N,\rm FO}^* + \tilde{U}\Lambda^{(N-1)/2}(c_{d\mu}^\dagger c_{d\mu} - 1)^2 + \tilde{\Gamma}^{1/2}\Lambda^{(N-1)/4}(c_{d\mu}^\dagger f_{0\mu} + f_{0\mu}^\dagger c_{d\mu}) \quad . \tag{5.1}$$

Since the smallest energy scale in $H_{N,\rm FO}^*$ is ~ 1, for small N the second and the third terms above constitute perturbations about $H_{N,\rm FO}^*$, and therefore H_N will be close to $H_{N,\rm FO}^*$ for small N. In fact, Eq. (5.1) has precisely the form of the effective Hamiltonian about the free-orbital fixed point discussed in Sec. IV. The two operators are precisely the correction terms $\Lambda^{(N-1)/2}\delta H_1$ and $\Lambda^{(N-1)/2}\delta H_2$ [cf. Eq. (4.9)] both of which generate relevant eigenoperators about $H_{\rm FO}^*$. Furthermore, the coefficients of the correction terms are now explicitly known, namely $\tilde{U}$ and $\tilde{\Gamma}^{1/2}$. In terms of the electron and hole operators that diagonalize $H_{N,\rm FO}^*$, we have (cf. Sec. IV B)

$$H_N = \sum_{l=1}^{(N+1)/2} \eta_l^*(g_{l\mu}^\dagger g_{l\mu} + h_{l\mu}^\dagger h_{l\mu}) + \tilde{U}\Lambda^{(N-1)/2}(c_{d\mu}^\dagger c_{d\mu} - 1)^2 + \tilde{\Gamma}^{1/2}\Lambda^{(N-1)/4}\sum_l \alpha_{0l}(c_{d\mu}^\dagger g_{l\mu} + c_{d\mu}^\dagger h_{l\mu}^\dagger + g_{l\mu}^\dagger c_{d\mu} + h_{l\mu} c_{d\mu}) \quad . \tag{5.2}$$

As has been discussed earlier, to leading (first) order, the effect of the $\tilde{U}$ term is to lift the quadruple degeneracy associated with $H_{N,\rm FO}^*$; the states in which the impurity orbital is either empty or doubly occupied have their energies increased by $\tilde{U}\Lambda^{(N-1)/2}$ while the energies of the states in which the impurity orbital is singly occupied remain unaltered. The effect of the $\tilde{\Gamma}^{1/2}$ term to leading (second) order is to increase each single-particle energy η_l^* by an amount $\tilde{\Gamma}\Lambda^{(N-1)/2}(\alpha_{0l}^2/\eta_l^*)$. It is easily verified that these two effects account, in quantitative detail, for the energy levels in Fig. 5 for $N<13$. (Note: for $U/D = 10^{-3}$ and $\Lambda = 2.5$, $\tilde{U}\Lambda^{(N-1)/2} = 0.17$ at $N = 13$.)

One can also substitute Eq. (5.2) into the expressions (2.42) and (2.43) for $k_B T_B \chi(T)_N$ and $F(T_N)$. Treating the $\tilde{U}$ and the $\tilde{\Gamma}^{1/2}$ terms by finite temperature perturbation theory, it is straightforward to obtain the leading contributions:

$$k_B T_N \chi(T_N) \cong \tfrac{1}{8} + \bar{\beta}(\tilde{U}\Lambda^{(N-1)/2})\tfrac{1}{16} - \bar{\beta}(\tilde{\Gamma}^{1/2}\Lambda^{(N-1)/4})^2 \times \sum_{l=1}^{(N+1)/2} \frac{\alpha_{0l}^2}{\eta_l^*}\frac{e^{-\bar{\beta}\eta_l^*}(1-e^{-\bar{\beta}\eta_l^*})}{(1+e^{-\bar{\beta}\eta_l^*})^3} \quad , \tag{5.3}$$

$$F(T_N) \cong -k_B T_N \left[\ln 4 - \bar{\beta}(\tilde{U}\Lambda^{(N-1)/2})\tfrac{1}{2} + \bar{\beta}(\tilde{\Gamma}^{1/2}\Lambda^{(N-1)/4})^2 \times 2\sum_{l=1}^{(N+1)/2} \frac{\alpha_{0l}^2}{\eta_l^*}\frac{1-e^{-\bar{\beta}\eta_l^*}}{1+e^{-\bar{\beta}\eta_l^*}}\right] \quad . \tag{5.4}$$

Note that the zero-order term in each of the above results is entirely due to the free orbital in $H_{N,\rm FO}^*$, since the contribution arising from the H_N^0 part of $H_{N,\rm FO}^*$ is precisely subtracted out in Eq. (2.42) and (2.43). Note also that the leading contribution from

the $\tilde{\Gamma}^{1/2}$ term is in second order. Substituting for $\tilde{U}$ and $\tilde{\Gamma}$ from Eqs. (2.20) and making use of the connection (2.41) between N and T_N, one gets

$$k_B T_N \chi(T_N) \cong \frac{1}{8} + \frac{1}{32}\frac{U}{k_B T_N} - \frac{\Gamma/\pi}{k_B T_N}\frac{4}{1+\Lambda^{-1}} \times \sum_{l=1}^{(N+1)/2} \frac{\alpha_{0l}^2}{\eta_l^*}\frac{e^{-\bar{\beta}\eta_l^*}(1-e^{-\bar{\beta}\eta_l^*})}{(1+e^{-\bar{\beta}\eta_l^*})^3} , \quad (5.5)$$

$$F(T_N) \cong -k_B T_N \left[\ln 4 - \frac{1}{4}\frac{U}{k_B T_N} + \frac{2\Gamma/\pi}{k_B T_N}\frac{4}{1+\Lambda^{-1}} \times \sum_{l=1}^{(N+1)/2} \frac{\alpha_{0l}^2}{\eta_l^*}\frac{1-e^{-\bar{\beta}\eta_l^*}}{1+e^{-\bar{\beta}\eta_l^*}} \right] . \quad (5.6)$$

In order that the above expressions for χ and F be useful, it is clearly necessary for the temperature T_N to be such that $U/(k_B T_N)$ and $\Gamma/(k_B T_N)$ are both small. It is not hard to see how the temperature range crept into the calculation. The point is that the dominant contribution to Eqs. (2.42) and (2.43) comes from energies of order $1/\bar{\beta}$. Therefore, $\bar{\beta}\tilde{U}\Lambda^{(N-1)/2}$ and $\bar{\beta}\tilde{\Gamma}\Lambda^{(N-1)/2}$ (rather than $\tilde{U}\Lambda^{(N-1)/2}$ and $\tilde{\Gamma}\Lambda^{(N-1)/2}$) must be small compared to 1; which in view of Eq. (2.41) is identical to the requirement that $U/(k_B T_N)$ and $\Gamma/(k_B T_N)$ be small compared to one. One may now let $\bar{\beta}\to 0$ and $N\to\infty$ in Eqs. (5.5) and (5.6), keeping the temperature T_N fixed at some value T within the range: $D > k_B T > \max(U, \Gamma)$. Taking this limit is equivalent to evaluating χ and F using Eqs. (2.30) and (2.31). Furthermore, one can also take the $\Lambda\to 1$ limit (after the $\bar{\beta}\to 0$ limit is taken), and show that Eqs. (5.5) and (5.6) reduce to the results one would get by treating the continuum Hamiltonian perturbatively[9]

$$k_B T \chi(T) = \frac{1}{8} + \frac{1}{32}\frac{U}{k_B T} - \frac{\Gamma/\pi}{k_B T}\int_0^D \frac{d\epsilon}{\epsilon}\frac{e^{-\beta\epsilon}(1-e^{-\beta\epsilon})}{(1+e^{-\beta\epsilon})^3} , \quad (5.7)$$

$$F(T) = -k_B T \left[\ln 4 - \frac{1}{4}\frac{U}{k_B T} + \frac{2\Gamma/\pi}{k_B T}\int_0^D \frac{d\epsilon}{\epsilon}\frac{1-e^{-\beta\epsilon}}{1+e^{-\beta\epsilon}} \right] . \quad (5.8)$$

The proof of this assertion is given in Appendix C.

In summary, when U and Γ are much smaller than D, $\chi(T)$ and $F(T)$ can be evaluated, for temperatures well above U and Γ, by doing perturbation theory in U and Γ. However, there is not much point in carrying out such a calculation to high orders because once the temperature gets small enough for the higher-order terms to be important, the perturbation theory breaks down rapidly as the temperature is decreased further. In terms of H_N, once N gets large enough for the deviations of H_N from $H_{\rm FO}^*$ to become of order 1, further increases in N will cause H_N to pull away rapidly from $H_{\rm FO}^*$ as one or the other of the deviations $\tilde{U}\Lambda^{(N-1)/2}$ and $\tilde{\Gamma}\Lambda^{(N-1)/2}$ begins to build up.

It is not hard to guess what happens to H_N next. We have seen in Sec. III B that, roughly speaking, the local-moment fixed point can be thought of as the $\tilde{U}=\infty$ fixed point whereas the the strong-coupling fixed point can be thought of as the $\tilde{\Gamma}=\infty$ fixed point. Therefore, if U is much bigger than Γ, $\tilde{U}\Lambda^{(N-1)/2}$ builds up first and one might expect that H_N crosses over to $H_{\rm LM}^*$; on the other hand, if Γ is much bigger than U, $\tilde{\Gamma}\Lambda^{(N-1)/2}$ builds up first and one might expect H_N to cross over to $H_{\rm SC}^*$. As we have seen earlier, this is indeed the behavior that characterizes the numerical results.

Of course, if either $\tilde{U}$ or $\tilde{\Gamma}$ is of order 1 to start with, there will be no range of N where H_N is close to $H_{\rm FO}^*$. Instead, after very few iterations, H_N will be close to $H_{\rm LM}^*$ if $U >> \Gamma$, or close to $H_{\rm SC}^*$ if $U << \Gamma$. We look at the local-moment case first.

B. Local-moment regime

When $D >> U >> \Gamma$, H_N begins to cross over away from $H_{\rm FO}^*$ and towards $H_{\rm LM}^*$ at a value N_{c1} of N given roughly by the condition that $\tilde{U}\Lambda^{(N_{c1}-1)/2}$ is of order 1. (For example, in Fig. 5, $\tilde{U}\Lambda^{(N-1)/2}\simeq 1$ for $N=17$.) In terms of temperature this corresponds to $k_B T \sim U$. Within the range of N in which the crossover takes place (until $\tilde{U}\Lambda^{(N-1)/2}$ is of order 10, say) the energy levels of H_N have a rather complicated structure, with levels crossing and so on (cf. Fig. 5). Consequently, for temperatures between U and $\frac{1}{5}U$, say, it is difficult to calculate χ except numerically as described earlier. Well past the crossover, H_N is once again simply describable in terms of an effective Hamiltonian constructed around $H_{N,\rm LM}^*$; so that for temperatures well below $\frac{1}{5}U$, one can again calculate the temperature dependence of χ analytically.

If one is only interested in H_N well past the crossover, one is justified in keeping only the dominant, marginal, term in the effective Hamiltonian around $H_{N,\rm LM}^*$; i.e, one can write

$$H_N = H_{N,\rm LM}^* - \tilde{J}\Lambda^{(N-1)/2}(f_{0\mu}^\dagger \vec{\sigma}_{\mu\nu} f_{0\nu})\cdot\vec{\tau} , \quad (5.9)$$

where, for notational convenience, $-\tilde{J}$ has been written for the coefficient ω_1. The justification for this step is that the rest of the corrections consist of irrelevant operators which decay at least as fast as $\Lambda^{-(N-N_{c1})/2}$. [It would not be correct to claim that the irrelevant deviations around $H_{\rm LM}^*$ will be as small as $\Lambda^{-N/2}$, because for $N=N_{c1}$, H_N is *not* close to $H_{\rm LM}^*$, so that these deviations must be of order 1 for

$N = N_{c1}$. In other words, the coefficients ω_2, ω_3, etc., of the irrelevant terms in the effective Hamiltonian will be large, at least as large as $\Lambda^{N_{c1}/2}$ ($\sim 1/\tilde{U}$). Nevertheless, it is still true that for N much larger than N_{c1} the irrelevant deviations can be neglected.] In terms of the electron and hole operators that diagonalize $H^*_{N,\mathrm{LM}}$ [cf. Eq. (4.20)],

$$H_N = \sum_{l=1}^{(N+1)/2} \eta_l^* (g_{l\mu}^\dagger g_{l\mu} + h_{l\mu}^\dagger h_{l\mu}) - \tilde{J} \sum_{ll'} \alpha_{0l}\alpha_{0l'} (g_{l\mu}^\dagger \vec{\sigma}_{\mu\nu} g_{l'\nu} + h_{l\mu} \vec{\sigma}_{\mu\nu} h_{l'\nu}^\dagger + g_{l\mu}^\dagger \vec{\sigma}_{\mu\nu} h_{l'\nu}^\dagger + h_{l\mu} \vec{\sigma}_{\mu\nu} g_{l'\nu}) \cdot \vec{\tau} \quad . \tag{5.10}$$

By fitting the energy levels calculated from this expression (perturbatively in $\tilde{J}$) to the numerical results, one can determine $\tilde{J}$ for different values of the parameters $\tilde{U}$ and $\tilde{\Gamma}$.

The correction to $H^*_{N,\mathrm{LM}}$ in Eq. (5.9) is clearly a spin-spin interaction between the local moment and the conduction-electron spin density at the impurity site. In fact, if follows from the discussion of $H^*_{N,\mathrm{LM}}$ in Sec. III B that Eq. (5.9) can be written

$$H_N = \Lambda^{(N-1)/2} \left[\sum_{n=0}^{N-1} \Lambda^{-n/2} \xi_n (f_{n\mu}^\dagger f_{n+1\,\mu} + f_{n+1\,\mu}^\dagger f_{n\mu}) - \tilde{J} f_{0\mu}^\dagger \vec{\sigma}_{\mu\nu} f_{0\nu} \cdot \vec{\tau} \right] , \tag{5.11}$$

which is precisely the Hamiltonian one uses in the renormalization-group treatment of the spin-$\frac{1}{2}$ Kondo problem.[6] Using the same approximations as in Sec. II A, the spin-$\frac{1}{2}$ Kondo Hamiltonian can be written as [compare Eq. (2.4)],

$$\mathcal{H}_K = D \left[\int_{-1}^{1} k a_{k\mu}^\dagger a_{k\mu}\, dk - \rho J \int_{-1}^{1} dk \int_{-1}^{1} dk' (\tfrac{1}{2} a_{k\mu}^\dagger \vec{\sigma} a_{k'\nu}) \cdot (\tfrac{1}{2}\vec{\tau}) \right] ; \tag{5.12}$$

which, when subject to discretization, etc., as before, leads to precisely the sequence of Hamiltonians (5.11), with the parameter J being related to ρJ as

$$\tilde{J} = \left(\frac{2}{1+\Lambda^{-1}} \right) \tfrac{1}{2} \rho J \quad . \tag{5.13}$$

This confirms the well-known connection between the Anderson Hamiltonian and the Kondon Hamiltonian.[10] *Note that the connection is valid only for temperatures much smaller than U.*

Since $\tilde{J}$ can be determined from the numerical results for the energy levels of H_N, Eq. (5.13) enables one to determine the coupling constant ρJ for different values of $\tilde{U}$ and $\tilde{\Gamma}$. When $U \gg \Gamma$, it is straightforward to show that the discretization preserves the Schrieffer-Wolff formula[10] connecting ρJ to U and Γ, namely, the result

$$\rho J = \rho J_{\mathrm{SW}} \equiv -8\Gamma/(\pi U) \quad . \tag{5.14}$$

For the case that U itself is much larger than D, the above result follows immediately from our earlier discussion of the local-moment fixed point in Sec. III B. There it was shown that for $U \gg D$, the low-lying states of H_N can be described by the Hamiltonian (3.8), which is precisely of the form (5.11) if we identify $\tilde{J} = -\tilde{\Gamma}/\tilde{U}$. Expressing $\tilde{\Gamma}$ and $\tilde{U}$ in terms of Γ and U [cf. Eqs. (2.20)], we get $\tilde{J} = -[2/(1+\Lambda^{-1})](4\Gamma/\pi U)$. Comparing this with Eq. (5.13) immediately yields Eq. (5.14). When U/D is not large, one can again obtain the results $\tilde{J} = -\tilde{\Gamma}/\tilde{U}$ starting from the Hamiltonian (5.10), either by second-order perturbation theory in the $\tilde{\Gamma}^{1/2}$ term, or by means of a Schrieffer-Wolff-type unitary transformation; and this once again leads to Eq. (5.14). The point is that $\tilde{U}$ and $\tilde{\Gamma}$ are both increasing as $\Lambda^{(N-1)/2}$, so that their ratio remains unchanged through the crossover. When $\tilde{U}\Lambda^{(N-1)/2} \gg 1$ (>10, say) one can neglect the subspace where the impurity orbital is empty or doubly occupied, and the states associated with the singly occupied orbital will be described by the Hamiltonian (5.11) with $\tilde{J} = -\tilde{\Gamma}/\tilde{U}$ (neglecting irrelevant operators). Note that J and ρJ_{SW} are antiferromagnetic (negative in sign).

Once H_N arrives close to H^*_{LM}, it continues to remain close to H^*_{LM} for a long range of N because of the marginal nature of the leading deviation around H^*_{LM}. As N gets well past the crosssover from H^*_{FO} to H^*_{LM}, the information about H_N having been close to H^*_{FO} before the crossover (which information is contained in the coefficients of the irrelevant operators about H^*_{LM}) is rapidly lost in H_N. The flow of H_N thereafter will hence be indistinguishable from that for the corresponding spin-$\frac{1}{2}$ Kondo Hamiltonian. Since the calculations of the energy levels and the susceptibility for the Kondo Hamiltonian have been discussed extensively in Ref. 6, there is no need to repeat them here.

Mapping between the susceptibilities of the Anderson and the Kondo Hamiltonian: The mapping between the symmetric Anderson Hamiltonian and the Kondo Hamiltonian will now be illustrated by means of the numerical results for the impurity susceptibility depicted in Figs. 9 and 10. First, we briefly review the results for the Kondo Hamiltonian.

For the spin-$\frac{1}{2}$ Kondo Hamiltonian, it is shown in Sec. IX of Ref. 6 that for temperatures much less than the band edge, and for small anitferromagnetic

ρJ, the functional dependence of χ on the temperature and on ρJ can be expressed in terms of an implicit equation of the form

$$\Phi(4k_B T\chi(T)-1)=\ln[T/T_K(J)] \ , \qquad (5.15)$$

where $\Phi(y)$ is a *universal* function of its argument y (i.e., its functional form is independent of ρJ, band-edge effects, etc.). $T_K(J)$, the Kondo temperature, is defined in terms of the same universal function by

$$k_B T_K(J)=\tilde{D}(J)\exp[-\Phi(\rho J)] \ , \qquad (5.16)$$

where $\tilde{D}(J)$ is an effective band edge of order D, and the ratio $\tilde{D}/D$ has a regular (but nonuniversal) power-series expansion in ρJ. Equation (5.15) implies that $k_B T\chi(T)$ itself is a universal function of $T/T_K(J)$. The single curve in Fig. 11 represents both the universal functions. This curve has been obtained from rather accurate numerical calculations of $\chi(T)$ for the Kondo Hamiltonian.[6] For small values of its argument, Φ can also be obtained using perturbation theory, and is given by[6]

$$\Phi(y)=\frac{1}{y}-\tfrac{1}{2}\ln|y|+1.58y+O(y^2) \ . \qquad (5.17)$$

One can use this expression for Φ in Eq. (5.15) and invert the resulting equation numerically to determine $k_B T\chi$ for $T/T_K \gtrsim 16$. Use of Eq. (5.17) in Eq. (5.16) shows that for small ρJ, $T_K(J)\sim D|\rho J|^{1/2}\exp(-1/|\rho J|)$. For $0.5T_K < T < 16T_K$, the universal curve fits a Curie-Weiss law: $\chi=0.17(g\mu_B)^2/k_B(T+2T_K)$. Note that the universal curve in Fig. 11 describes the susceptibility obtained from the Kondo Hamiltonian only in the temperature range in which the dominant contribution to the susceptibility comes from the logarithmically divergent terms in its perturbation expansion [i.e., when nonuniversal corrections, such as terms of $O(k_B T/D)$, etc., can be ignored]. A set of numerical values for the universal curve are given in Table V.

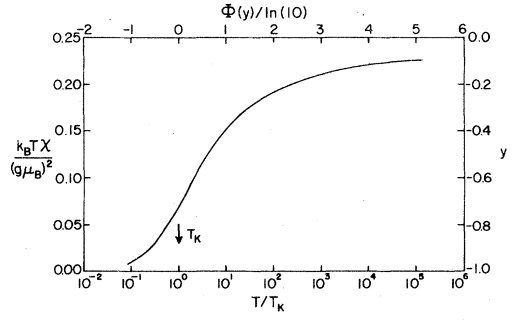

FIG. 11. Universal $k_B T\chi(T)/(g\mu_B)^2$ vs $\ln(T/T_K)$ plot for the spin-$\frac{1}{2}$ Kondo Hamiltonian. At $T=T_K$, $T\chi=0.701$. The same plot also serves as a graph of the universal function $\Phi(y)$, see Eq. (5.15).

TABLE V. Values of the universal Kondo susceptibility versus T/T_K. For a plot see Fig. 11. For $T \gtrsim 20T_K$, $\chi(T)$ is accurately calculable using the Eqs. (5.15) and (5.17).

T/T_K	$\log_{10}(T/T_K)$	$\frac{k_B T\chi}{(g\mu_B)^2}$
28.270	1.451	0.173
18.851	1.275	0.166
12.565	1.099	0.157
8.379	0.923	0.147
5.585	0.7470	0.135
3.723	0.5709	0.122
2.482	0.3958	0.107
1.655	0.2187	0.0910
1.103	0.0426	0.0739
0.735	−0.1335	0.0580
0.490	−0.3098	0.0430
0.327	−0.4859	0.0310
0.218	−0.6620	0.0213
0.145	−0.8388	0.0145
0.0969	−1.014	0.0095

In view of the results stated in the preceding paragraph, the existence of a correspondence between the Anderson and the Kondo Hamiltonians must imply the existence of a Kondo temperature $T_K(\Gamma,U)$ such that the low-temperature part of the curve obtained by plotting $k_B T\chi$ calculated for the Anderson Hamiltonian against $T/T_K(\Gamma,U)$ coincides with the universal curve in Fig. 11 obtained for the Kondo Hamiltonian. Figures 9 and 10 serve to illustrate this assertion. Since temperature is plotted on a logarithmic scale in each of the graphs, scale changes in temperature can be effected by translations along the temperature axis. One can verify that Fig. 11 can be slid on top of Figs. 9 and 10 so as to make the universal curve pass neatly through the low-temperature points for each of the five sets of points plotted, as indicated by the dashed lines in Figs. 9 and 10. For each such correspondence, the point on the temperature axis which lies directly beneath the point $T/T_K=1$ in Fig. 11 immediately gives the Kondo temperature $T_K(\Gamma,U)$ for the relevant U and Γ. These temperatures are indicated by the little arrows (Figs. 9 and 10), and their numerical values are listed in Table VI.

To compare these numbers from the numerical calculations with the analytic formula for T_K Eqs. (5.16) and (5.17) we need to evaluate three items. (i) What is D replaced by in the Anderson model where $U < D$? Haldane[11] has done the lowest nontrivial calculation for the susceptibility and has found that the effective bandwidth for the symmetric Anderson model is

$$D_A=0.182U \ , \qquad (5.18)$$

TABLE VI. Kondo temperatures for symmetric Anderson model for various values of Γ and U. In the next to last column are the values computed using Eq. (5.21) while in the last column are those deduced from Figs. 9 and 10. T_K is the temperature where $k_B T\chi = 0.07$.

U/D	$(U/\pi\Gamma)$	$\lvert\rho J_{\rm SW}\rvert$	$\lvert\rho J_{\rm eff}(\Lambda)$	$T_K(\Gamma,U)/D$ from Eq. (5.21)	$T_K(\Gamma,U)/D$ from Figs. 9 and 10
10^{-3}	12.66	0.064	0.0599	2.50×10^{-12}	$(3.7\pm0.2)\times10^{-12}$
10^{-3}	1.013	0.800	0.748	4.13×10^{-5}	$(6.9\pm0.3)\times10^{-5}$
$\frac{1}{2}$	5.63	0.144	0.1347	2.00×10^{-5}	$(2.1\pm0.2)\times10^{-5}$
$\frac{1}{2}$	2.03	0.400	0.374	3.84×10^{-3}	$(4.9\pm0.3)\times10^{-3}$
$\frac{1}{2}$	1.013	0.800	0.748	2.07×10^{-2}	$(3.3\pm0.2)\times10^{-2}$

where $0.182 = (1/4\pi)\exp(0.25 + C)$, where C is Euler's constant (0.57721). (ii) How is D_A renormalized by finite ρJ? Preliminary work for the Kondo problem[12] suggests a reduction of the form $\tilde{D} = D(1 - 0.1\rho J)$. Nothing is known about this for the Anderson model. The most consistent thing we can do is to neglect this effect and the term $1.58\rho J$ in Φ (see Eq. (5.17)]. (iii) How are results calculated at finite Λ to be connected with the $\Lambda = 1$ limit? The major effect[12] is that ρJ is renormalized to $J_{\rm eff}(\Lambda)$

$$J_{\rm eff}(\Lambda) = \frac{\rho J}{A_\Lambda} \ , \tag{5.19}$$

where

$$A_\Lambda = \tfrac{1}{2}\ln\Lambda\left(\frac{1+\Lambda^{-1}}{1-\Lambda^{-1}}\right) \ . \tag{5.20}$$

Accordingly, our estimation of T_K at finite Λ is

$$T_K = 0.182\,U\lvert\rho J_{\rm eff}(\Lambda)\rvert^{1/2}\exp\left(\frac{1}{\lvert J_{\rm eff}(\Lambda)\rvert}\right) \ . \tag{5.21}$$

The results of using this formula are shown in the last column of Table VI. All of the numbers from Eq. (5.21) are within 40% of those deduced from the numerical calculations. However, in those calculations, originally done in 1975, the maximum on the matrix size was smaller than that we now believe necessary to assure 10% accuracy. If larger matrices had been used, we would expect all of the T_K to drop slightly. In the second paper, appropriately large matrices were used.

The remarkable result that follows from the numerical results in Table VI is that the mapping between the Anderson and Kondo Hamiltonians and the Schrieffer-Wolff result for the effective ρJ [cf. Eq. (5.14)] are meaningful for $\lvert\rho J_{\rm SW}\rvert$ as large as 0.8, and for values of the Kondo temperature, $T_K(\Gamma,U)$, as large as $\frac{1}{30}D$.

Because of the antiferromagnetic character of the coupling constant ρJ, the deviation of $k_B T\chi$ from its value of $\frac{1}{4}$ in the local-moment fixed point increases gradually as the temperature is reduced. This behavior of the susceptibility reflects the gradual increase in the deviation of H_N from $H^*_{\rm LM}$ as N increases. Eventually, when N gets to be N_{c2}, where $\Lambda^{-(N_{c2}-1)/2}$ is of the order of $k_B T_K(\Gamma,U)/D$, H_N begins to cross over to the strong-coupling fixed point $\hat{H}^*_{\rm SC}$. Since the strong-coupling fixed point has only irrelevant eigenoperators, it is a stable fixed point as discussed in Sec. IV A, so that as $N \to \infty$, $H_N \to \hat{H}^*_{\rm SC}$. Consequently, for temperatures much smaller than $T_K(\Gamma,U)$, the temperature dependence of the impurity susceptibility can again be calculated analytically, using an effective Hamiltonian constructed around $H^*_{N,\rm SC}$.

C. Strong-coupling regime

For every set of values for $\tilde{U}$ and $\tilde{\Gamma}$ (as long as $\Gamma \neq 0$), there is a correspondidng N beyond which H_N will be close to the strong-coupling fixed point, $\hat{H}^*_{\rm SC}$. Consequently, for every $(\tilde{U},\tilde{\Gamma})$ there is a threshold temperature well below which the impurity properties can be calculated using an effecitve Hamiltonian constructed around $H^*_{N,\rm SC}$. When $U >> \Gamma$, this threshold temperature is the Kondo temperature, $T_K(\Gamma,U)$; when $\Gamma >> U$, the threshold temperature is essentially of the order of Γ, assuming $\Gamma < D$. In this paper we will keep only the leading irrelevant deviations in the effective Hamiltonian, namely the two operators in Eqs. (4.26) and (4.27). The resulting approxima-

tion to H_N is

$$H_N \cong \sum_{l=1}^{(N-1)/2} \hat{\eta}_l^* (g_{l\mu}^\dagger g_{l\mu} + h_{l\mu}^\dagger h_{l\mu})$$
$$+ \omega_1 \Lambda^{-(N-1)/2} \left(\sum_{ll'} \hat{\alpha}_{0l}\hat{\alpha}_{1l'} (g_{l\mu}^\dagger g_{l'\mu} - h_{l\mu} h_{l'\mu}^\dagger - g_{l\mu}^\dagger h_{l'\mu}^\dagger + h_{l\mu} g_{l'\mu}) + \sum_l \hat{\alpha}_{00}\hat{\alpha}_{1l} (g_{0\mu}^\dagger g_{l\mu} - g_{0\mu}^\dagger h_{l\mu}^\dagger) + \text{H.c.} \right)$$
$$+ \omega_2 \Lambda^{-(N-1)/2} \left(\hat{\alpha}_{00}^2 (g_{0\mu}^\dagger g_{0\mu} - 1) + \sum_l \hat{\alpha}_{00}\hat{\alpha}_{0l} (g_{0\mu}^\dagger g_{l\mu} + g_{0\mu}^\dagger h_{l\mu}^\dagger + g_{l\mu}^\dagger g_{0\mu} + h_{l\mu} g_{0\mu}) \right.$$
$$\left. + \sum_{ll'} \hat{\alpha}_{0l}\hat{\alpha}_{0l'} (g_{l\mu}^\dagger g_{l'\mu} + g_{l\mu}^\dagger h_{l'\mu}^\dagger - h_{l\mu}^\dagger h_{l'\mu} + h_{l\mu} g_{l'\mu}) \right)^2 , \tag{5.22}$$

where the coefficients ω_1 and ω_2 are obtained by fitting the energy levels calculated using Eq. (5.22) (treating the ω_1 and the ω_2 terms as perturbations) to the numerical results.

We will treat the correction terms above only to first order, so that for calculating energy levels only the diagonal part (i.e., only those terms that connect degenerate states of $H_{N,\text{SC}}^*$) of Eq. (5.22) has to be kept. It is easy to see that the diagonal part of the ω_1 term is given by

$$2\omega_1 \Lambda^{-(N-1)/2} \sum_l \hat{\alpha}_{0l}\hat{\alpha}_{1l} (g_{l\mu}^\dagger g_{l\mu} + h_{l\mu}^\dagger h_{l\mu}) ,$$

which just shifts every single-particle (or hole) energy $\hat{\eta}_l^*$ by an amount $2\omega_1 \hat{\alpha}_{0l}\hat{\alpha}_{1l}\Lambda^{-(N-1)/2}$. The diagonal part of the ω_2 term is straightforward to work out but too lengthy to be recorded here. Its essential feature is that it does not affect single-particle (or hole) states, but affects only two- or higher-particle (or hole) states. It is important to appreciate the non-triviality of the statment that *two parameters* are enough to describe the $O(\Lambda^{-(N-1)/2})$ deviations of *all* the low-lying many particle energy levels of H_N from their fixed-point values. One can determine ω_1 and ω_2 just from the numerical results for one single-particle state and one two-particle state. (For example, letting $|\Omega\rangle$ denote the state annihilated by g_0, g_l, and h_l, the single-particle state $g_1^\dagger|\Omega\rangle$ will have an energy $\hat{\eta}_1^* + 2\omega_1 \hat{\alpha}_{01}\hat{\alpha}_{11}\Lambda^{-(N-1)/2}$, while the two-particle state $g_{0\uparrow}^\dagger g_{0\downarrow}^\dagger |\Omega\rangle$ will have an energy $\omega_2 \hat{\alpha}_{00}^4 \Lambda^{-(N-1)/2}$.) The numerical results for all other low-lying energy levels then agree with the calculations made from Eq. (5.22) using the values of ω_1 and ω_2 so determined. The renormalization-group aspects of the formalism are crucial for this simple description of H_N to be possible. The details of the calculation are essentially the same as in Ref. 6.

It is straightforward to calculate $\chi(T_N)$ and $F(T_N)$ using Eq. (5.22) as the Hamiltonian in Eqs. (2.42) and (2.43), and treating the ω_1 and the ω_2 terms to first order. One finds that

$$\chi(T_N) = \frac{(g\mu_B)^2}{k_B T_N} \left[\left(\frac{1}{8} + \sum_{l=1}^{(N-1)/2} \frac{e^{-\bar{\beta}\hat{\eta}_l^*}}{(1+e^{-\bar{\beta}\hat{\eta}_l^*})^2} \right) - \left(\sum_{l=1}^{(N+1)/2} \frac{e^{-\bar{\beta}\eta_l^*}}{(1+e^{-\bar{\beta}\eta_l^*})^2} \right) \right.$$
$$- 2\omega_1 \Lambda^{-(N-1)/2} \bar{\beta} \left(\sum_{l=1}^{(N-1)/2} \hat{\alpha}_{0l}\hat{\alpha}_{1l} \frac{e^{-\bar{\beta}\hat{\eta}_l^*}(1-e^{-\bar{\beta}\hat{\eta}_l^*})}{(1+e^{-\bar{\beta}\hat{\eta}_l^*})^3} \right)$$
$$\left. + 4\omega_2 \Lambda^{-(N-1)/2} \bar{\beta} \left(\frac{1}{8}\hat{\alpha}_{00}^2 + \sum_{l=1}^{(N-1)/2} \hat{\alpha}_{0l}^2 \frac{e^{-\bar{\beta}\hat{\eta}_l^*}}{(1+e^{-\bar{\beta}\hat{\eta}_l^*})^2} \right) \right] , \tag{5.23}$$

$$F(T_N) = -k_B T_N \left[\left(\ln 4 + \sum_{l=1}^{(N-1)/2} 4\ln(1+e^{-\bar{\beta}\hat{\eta}_l^*}) \right) - \left(\sum_{l=1}^{(N+1)/2} 4\ln(1+e^{-\bar{\beta}\eta_l^*}) \right) \right.$$
$$\left. - 8\omega_1 \Lambda^{-(N-1)/2} \bar{\beta} \left(\sum_{l=1}^{(N-1)/2} \hat{\alpha}_{0l}\hat{\alpha}_{1l} \frac{e^{-\bar{\beta}\hat{\eta}_l^*}}{(1+e^{-\bar{\beta}\hat{\eta}_l^*})} \right) \right] . \tag{5.24}$$

The first large parenthesis in both Eqs. (5.23) and (5.24) is due to $H^*_{N,\mathrm{SC}}$, the $\frac{1}{8}$ term in Eq. (5.23) and the $\ln 4$ term in Eq. (5.24) being due to the zero-energy electron level in $H^*_{N,\mathrm{SC}}$ (for odd N). The second large parenthesis in Eq. (5.23) and in Eq. (5.24) is the free-electron contribution that has to be subtracted out. Note that the ω_2 term makes no first-order contribution to the free energy.

As long as T_N is much less than the band edge D, the upper limits in all sums in Eqs. (5.23) and (5.24) can be replaced by ∞. The reason is that the factors $e^{-\bar{\beta}\hat{\eta}_l^*}$ and $e^{-\bar{\beta}\eta_l^*}$ provide adequate damping. [When $l \sim \frac{1}{2}N$, $\hat{\eta}_l^*$ and η_l^* are of the order of $\Lambda^{N/2}$, so that from Eq. (2.4) we see that $e^{-\bar{\beta}\hat{\eta}_l^*}$ and $e^{-\bar{\beta}\eta_l^*}$ are of the order of e^{-D/k_BT_N}.]

It is convenient to define the following quantities

$$\chi_{0,\mathrm{SC}}(\bar{\beta},\Lambda) \equiv \tfrac{1}{8} + \sum_{l=1}^{\infty} \frac{e^{-\bar{\beta}\hat{\eta}_l^*}}{(1+e^{-\bar{\beta}\hat{\eta}_l^*})^2} - \sum_{l=1}^{\infty} \frac{e^{-\bar{\beta}\eta_l^*}}{(1+e^{-\bar{\beta}\eta_l^*})^2} \ , \tag{5.25}$$

$$\chi_{1,\mathrm{SC}}(\bar{\beta},\Lambda) \equiv \bar{\beta}^2 \ln\Lambda \sum_{l=1}^{\infty} \frac{\hat{\alpha}_{0l}\hat{\alpha}_{1l}}{\alpha_0\alpha_1} \frac{e^{-\bar{\beta}\hat{\eta}_l^*}(1-e^{-\bar{\beta}\hat{\eta}_l^*})}{(1+e^{-\bar{\beta}\hat{\eta}_l^*})^3} \ , \tag{5.26}$$

$$\chi_{2,\mathrm{SC}}(\bar{\beta},\Lambda) \equiv \bar{\beta}^2(\ln\Lambda)^2 \times \left[\frac{1}{8}\frac{\hat{\alpha}_{00}^2}{\alpha_0^2} + \sum_{l=1}^{\infty} \frac{\hat{\alpha}_{0l}^2}{\alpha_0^2} \frac{e^{-\bar{\beta}\hat{\eta}_l^*}}{(1+e^{-\bar{\beta}\hat{\eta}_l^*})^2}\right]^2 \ , \tag{5.27}$$

$$F_{0,\mathrm{SC}}(\bar{\beta},\Lambda) \equiv \ln 4 + \sum_{l=1}^{\infty} 4\ln(1+e^{-\bar{\beta}\hat{\eta}_l^*}) - \sum_{l=1}^{\infty} 4\ln(1+e^{-\bar{\beta}\eta_l^*}) \ , \tag{5.28}$$

$$F_{1,\mathrm{SC}}(\bar{\beta},\Lambda) \equiv \bar{\beta}^2 \ln\Lambda \sum_{l=1}^{\infty} \frac{\hat{\alpha}_{0l}\hat{\alpha}_{1l}}{\alpha_0\alpha_1} \frac{e^{-\bar{\beta}\hat{\eta}_l^*}}{(1+e^{-\bar{\beta}\hat{\eta}_l^*})} \ ; \tag{5.29}$$

where we have introduced the quantities (cf. Table II)

$$\alpha_0 \equiv [\tfrac{1}{2}(1-\Lambda^{-1})]^{1/2}, \quad \alpha_1 \equiv [\tfrac{1}{2}(1-\Lambda^{-3})]^{1/2} \ . \tag{5.30}$$

These sums can be evaluated numerically for any given Λ and $\bar{\beta}$. One finds that for $\bar{\beta} \ll 1$, as $\Lambda \to 1$ all five sums are essentially independent of $\bar{\beta}$ and converge very rapidly to the values

$$\chi_{0,\mathrm{SC}} = 0, \quad \chi_{1,\mathrm{SC}} = \tfrac{1}{2},$$

$$\chi_{2,\mathrm{SC}} = \tfrac{1}{4}, \quad F_{0,\mathrm{SC}} = 0,$$

and

$$F_{1,\mathrm{SC}} = \tfrac{1}{12}\pi^2 \ . \tag{5.31}$$

For example, at $\Lambda = 2$ the variation in χ_1 as $\bar{\beta}$ is changed is only 0.03% and its mean value if $\frac{1}{2}$, correct to five decimal places. In the limit of small $\bar{\beta}$, one can actually prove analytically that Eq. (5.31) gives the correct $\Lambda \to 1$ limits for χ_0, χ_1, etc. A brief discussion is given in Appendix D. For details, and for an explanation for the rapid-convergence (as $\Lambda \to 1$) properties of these expressions, see Sec. IX of Ref. 6.

Substituting the definitions (5.25)–(5.30) in Eq. (5.23) and in Eq. (5.24), making use of the connection (2.41) between $\bar{\beta}$ and T_N, keeping T_N fixed at some small temperature T, letting $\bar{\beta} \to 0$, and using (5.31), we find

$$\chi(T) = \frac{(g\mu_B)^2}{D}\left[-\omega_1\left(\frac{2}{1+\Lambda^{-1}}\right)\frac{\alpha_0\alpha_1}{\ln\Lambda} + \omega_2\left(\frac{2}{1+\Lambda^{-1}}\right)\frac{\alpha_0^4}{(\ln\Lambda)^2}\right] \ , \tag{5.32}$$

$$F(T) = +\frac{(k_BT)^2}{D}\omega_1\left(\frac{2}{1+\Lambda^{-1}}\right)\frac{\alpha_0\alpha_1}{\ln\Lambda}\tfrac{2}{3}\pi^2 \ . \tag{5.33}$$

For the specific heat $C(T)$ we get, using Eqs. (5.23) and (2.32),

$$C(T) = \tfrac{4}{3}\pi^2\frac{k_B^2T}{D}\left[-\omega_1\left(\frac{2}{1+\Lambda^{-1}}\right)\frac{\alpha_0\alpha_1}{\ln\Lambda}\right] \ . \tag{5.34}$$

Thus, when the temperature is small enough to be in the strong-coupling regime, the dominant contribution to the impurity susceptibility is a constant, while the dominant contribution to the impurity specific heat is linear in temperature.

The quantities in the large square brackets in Eqs. (5.32) and (5.34) can be evaluated numerically, using the values of ω_1 and ω_2 obtained from the numerical results for the energy levels of H_N in the strong-coupling regime, for any U and Γ. Instead of the specific heat, it is conventional to calculate the quantity

$$R \equiv \tfrac{4}{3}\pi^2\frac{k_B^2}{(g\mu_B)^2}\frac{T\chi}{C} = 1 - \frac{\omega_2}{\omega_1}\frac{\alpha_0^3}{\alpha_1\ln\Lambda} \ . \tag{5.35}$$

Table VII lists the results for $\chi D/(g\mu_B)^2$ and R obtained at $\Lambda = 2.5$ for the same U and Γ values as were considered earlier. An investigation of the convergence of theses numbers as Λ is brought closer to 1 for fixed U and Γ has not been made. The excellent evidence for the existence of such a convergence in connection with the Kondo problem[6] would lead one to expect that the numbers in Table VII are

TABLE VII. Zero-temperature χ and C for the symmetric Anderson model. The first column under the zero-temperature susceptibility is deduced using (5.32), while the second column is based on the value of the Kondo temperature found from the calculated susceptibility (in last column of Table VI). The final column is calculated from Eq. (5.35).

		$\chi(T=0)D/(g\mu_B)^2$		
U/D	$\lvert\rho J_{SW}\rvert$	Calculated using Eq. (5.32)	$0.10\ D/k_BT_K(\Gamma,U)$	$R\equiv\frac{4}{3}\pi^2\frac{k_B^2T\chi}{(g\mu_B)^2C}$
10^{-3}	0.064	2.93×10^{10}	$(2.7\pm0.2)\times10^{10}$	2.00
10^{-3}	0.800	1.62×10^{3}	$(1.4\pm0.1)\times10^{3}$	1.79
$\frac{1}{2}$	0.144	5.18×10^{3}	$(4.8\pm0.3)\times10^{3}$	2.00
$\frac{1}{2}$	0.400	2.26×10^{1}	$(2.0\pm0.1)\times10^{1}$	1.98
$\frac{1}{2}$	0.800	3.36	(3.0 ± 0.2)	1.82

equal to their limiting values as $\Lambda\to1$ to within a few percent.

There are two limiting cases, namely the cases $U>>\Gamma$ and $U<<\Gamma$, in which the functional dependence of $\chi(T)$ and of R on the parameters U and Γ can be worked out explicitly.

(i) First consider the case when $U>>\Gamma$. Then there exists a local-moment regime of temperature: $T_K(\Gamma,U)<T<<\min(U,D)$. In this case, as discussed earlier, $k_BT\chi$ is a universal function of T/T_K. Therefore, $k_BT_K\chi$ should also be a universal function of T/T_K, whence it follows that the constant susceptibility in Eq. (5.32) should be of the form

$$\chi(T)=(g\mu_B)^2\chi_u/[k_BT_K(\Gamma,U)]\ , \tag{5.36}$$

where χ_u is a universal constant. χ_u has been determined to be equal to 0.103 from the results for the Kondo Hamiltonian.[6] Since one knows $T_K(\Gamma,U)$ for all the cases in Table VII one can calculate $\chi D/(g\mu_B)^2$ using the above equation. These are also listed in Table VII, and their agreement with the results for $\chi D/(g\mu_B)^2$ calculated directly from Eq. (5.32) reconfirms the mapping between the susceptibility results of the Anderson and the Kondo Hamiltonians for all the (U,Γ) values considered in Table VII. Furthermore, when $U>>\Gamma$, $|\rho J_{SW}|$ is small, and one may argue exactly as in the case of the Kondo Hamiltonian[4] that the ratio ω_2/ω_1, and therefore the quantity R, is independent of $|\rho J_{SW}|$ except for corrections of the order of $\exp(-1/|\rho J_{SW}|)$. This constant value of R has been determined to be equal to 2 for the Kondo Hamiltonian and Table VII confirms that $R=2$ for the Anderson model also, as long as $|\rho J_{SW}|$ is small.

(ii) Next consider the case when $\Gamma>>U$. If, in addition, $\Gamma<<D$ also, it is clear from the general analysis we have presented so far that the flow of H_N with N will be a crossover from H_{FO}^* directly to $\hat{H}_{SC}^*$ when $\tilde{\Gamma}\Lambda^{(N-1)/2}$ grows to be of order 1. Consequently, the susceptibility will have a free-orbital character [i.e., $\chi\simeq1/(8k_BT)$] for temperatures well above Γ, and strong-coupling character (i.e., $\chi\simeq$ constant) for temperatures much smaller than Γ. The point is that in this case one can do the whole problem analytically—one can first diagonalize the quadratic Hamiltonian

$$H_{N0}\equiv\Lambda^{(N-1)/2}\left[\sum_{n=0}^{N-1}\Lambda^{-n/2}\xi_n(f_{n\mu}^\dagger f_{n+1\mu}+f_{n+1\mu}^\dagger f_{n\mu})+\tilde{\Gamma}^{1/2}(f_{0\mu}^\dagger c_{d\mu}+c_{d\mu}^\dagger f_{0\mu})\right]\ , \tag{5.37}$$

and then include the $\tilde{U}$ term and treat it as a perturbation. This is done in Appendix E. One can thereby verify the above assertion about the flow of H_N as well as obtain explicit formulas for the coefficients ω_1 and ω_2. To leading order in $\tilde{U}$ one finds that,

$$\omega_1=-\tfrac{1}{2}[\tfrac{1}{2}(1+\Lambda^{-1})]^2\frac{(\ln\Lambda)^2}{\alpha_0^3\alpha_1}\frac{D}{2\pi\Gamma}\ , \tag{5.38}$$

$$\omega_2=[\tfrac{1}{2}(1+\Lambda^{-1})]^3\frac{(\ln\Lambda)^4}{\alpha_0^8}\left[\frac{D}{2\pi\Gamma}\right]^2\left[\frac{U}{2D}\right]\ . \tag{5.39}$$

Substituting these results into Eq. (5.32) and into Eq. (5.35), one gets

$$\chi=\frac{(g\mu_B)^2}{2\pi\Gamma}A_\Lambda\left[1+\frac{U}{\pi\Gamma}A_\Lambda+O\left(\frac{U}{\pi\Gamma}\right)^2\right]\ , \tag{5.40}$$

$$R=\left[1+\frac{U}{\pi\Gamma}A_\Lambda+O\left(\frac{U}{\pi\Gamma}\right)^2\right]\ , \tag{5.41}$$

where the Λ dependence is contained entirely in the quantity A_Λ, given by

$$A_\Lambda\equiv\tfrac{1}{2}(1+\Lambda^{-1})\frac{\ln\Lambda}{2\alpha_0^2}=\frac{1+\Lambda^{-1}}{1-\Lambda^{-1}}\frac{1}{2}\ln\Lambda$$
$$=1+[\tfrac{1}{12}(\ln\Lambda)]^2-\tfrac{1}{720}(\ln\Lambda)^4+\cdots\ . \tag{5.42}$$

As $\Lambda \to 1$, $A_\Lambda \to 1$ quite rapidly, and the results (5.40) and (5.41) reduce to the standard results [13] obtained by doing continuum perturbation theory in U. Even for $\Lambda = 2.5$, whence A_Λ is 1.07, the error due to the discretization is only 7%. Note that, for a fixed Γ, as U is increased from the value much less that Γ, R increases from 1 to 2.

In order to verify Eq. (5.40) as well as to get a rough measure of the error due to the truncation of states, a computer run was made letting $U = 0$ and $D/(2\pi\Gamma) = 1.013 \times 10^3$. According to Eqs. (5.40) and (5.41) one expects $\chi D/(g\mu_B)^2 = 1.083 \times 10^3$ and $R = 1$. The numerical results obtained [using Eqs. (5.32) and (5.35)] were 1.04×10^3 and 0.99, respectively. The reason that R is not strictly one is that, because of the truncation of states, ω_2 is not strictly zero. The numerical value for $\chi D/(g\mu_B)^2$ shows that the truncation error amounts to no more than 4%.

This completes our description of the strong-coupling regime. Our analysis has been confined to the dominant terms in the susceptibility and in the specific heat. The less dominant corrections can, in principle, be obtained by treating the ω_1 and the ω_2 terms in Eq. (5.22) to higher orders, and by including irrelevant eigenoperators with eigenvalues smaller than Λ^{-1} in the effective Hamiltonian (5.22). Such calculations will clearly be tedious [higher-order calculations will involve the off-diagonal terms in Eq. (5.22), and there are six distinct irrelevant eigenoperators belonging to the eigenvalue Λ^{-3}], and have not been attempted so far.

D. Universality

A very important aspect of any renormalization-group calculation is *universality,* which is the result that a large class of "initial Hamiltonians," i.e., many different choices for H_N for small N (which involve only the first few degrees of freedom), can lead to essentially a single sequence of Hamiltonians H_N for large N. The reason is that changes in the initial Hamiltonian which will only generate irrelevant operators about the various fixed points of $\mathcal{T}^2$ with coefficients that are not too large will be unimportant for large N.

We now show that allowing ρ and V_d in Eq. (2.3) to depend on energy, for example, corresponds to making just such changes. Since the impurity orbital is supposed to be localized, its interaction with the conduction electrons must have a short range, which requires that $V_d(\epsilon)$ be only weakly dependent of ϵ and hence expandable in powers of ϵ. It is reasonable to assume that $\rho(\epsilon)$ is also so expandable. In Eq. (2.4) we kept only the zero-order term in the expansion of the product $(\rho D)^{1/2} V_d$ in powers of ϵ. The first-order term will lead to an interaction in Eq. (2.4) of the form

$$\delta H = \int_{-1}^{1} k\, dk\, (a_{k\mu}^\dagger c_{d\mu} + c_{d\mu}^\dagger a_{k\mu}) \quad . \tag{5.43}$$

Consider expressing this in terms of the discretized operators $\{a_{np\mu}, b_{np\mu}\}$. It is straightforward to verify that

$$\int_{-1}^{1} dk\, k\, a_{k\mu} = \sum_n \tfrac{1}{2} \Lambda^{-3n/2} \frac{(1-\Lambda^{-2})}{(1-\Lambda^{-1})^{1/2}} (a_{n0\mu} - b_{n0\mu}) + (p \neq 0 \text{ part}) \quad . \tag{5.44}$$

Ignoring the $p \neq 0$ part as before, Eq. (5.44) can be seen to be proportional to the operator f_1 [cf. Eq. (2.16)], so that the inclusion of a term proportional to δH in Eq. (2.4) will result in the addition of a term proportional to $\Lambda^{(N-1)/2} (f_{1\mu}^\dagger c_{d\mu} + c_{d\mu}^\dagger f_{1\mu})$ to H_N. One can now go through exactly the same kind of arguments as used in Sec. IV B and demonstrate that this term only generates an irrelevant eigenoperator about H_{FO}^*: use of the expansion (4.17) for f_1 in terms of the electron and hole operators that diagonalize $H_{N,FO}^*$ shows that

$$\Lambda^{(N-1)/2}(f_{1\mu}^\dagger c_{d\mu} + c_{d\mu}^\dagger f_{1\mu}) = \Lambda^{-(N-1)/4} \sum_l \alpha_{1l} (g_{l\mu}^\dagger c_{d\mu} - h_{l\mu} c_{d\mu} + c_{d\mu}^\dagger g_{l\mu} - c_{d\mu}^\dagger h_{l\mu}^\dagger) \; ; \tag{5.45}$$

and the power of $\Lambda^{-N/4}$ on the right-hand side proves the result stated. The effect of Eq. (5.45) on the energy levels will only be in second order and will therefore fall off as $\Lambda^{-N/2}$. One can similarly show that the interaction terms obtained by considering higher powers of ϵ in the expansion of $(\rho D)^{1/2} V_d$ generate irrelevant eigenoperators about H_{FO}^* belonging to even smaller eigenvalues, so that their effects fall off even faster as N increases. Therefore, even when the coefficients of the interaction terms due to the energy dependence of $(\rho D)^{1/2} V_d$ are as large as the band edge D, their effect will be merely to cause changes of order 1 in the coefficients of the irrelevant operators about the various fixed points involved in the flow of H_N. To the extent that such corrections are unimportant, it is quite unnecessary to worry about the energy dependence of ρ and of V_d.

It should be noted in this connection that terms such as Eq. (5.43) break particle-hole symmetry, so that H_N for small N will no longer have particle-hole symmetry when the energy dependence of ρ and V_d is allowed for. However, since the effects of these terms die off rapidly as N increases, once N gets large enough the particle-hole symmetry of H_N will be recovered. It is only when particle-hole symmetry is broken via the $c_{d\mu}^\dagger c_{d\mu}$ term, as happens when $\epsilon_d \neq \frac{1}{2} U$, that the symmetry breaking has any conse-

quences for the low-temperature properties of the system.

As another illustration of universality, consider the so-called "local-spin-fluctuation" model[14] which is often used to describe dilute magnetic alloys. The Hamiltonian is

$$\mathcal{H}_{sf}=\sum_k \epsilon_k c_{k\mu}^\dagger c_{k\mu}+I n_\uparrow(0)n_\downarrow(0)+V[n_\uparrow(0)+n_\downarrow(0)] \ , \tag{5.46}$$

where $n_\uparrow(0)$ and $n_\downarrow(0)$ are the spin-up and the spin-down electron-density operators at the impurity site. The same approximations as in Sec. II A then lead to

$$\mathcal{H}_{sf}=D\Big[\int_{-1}^{1} k a_{k\mu}^\dagger a_{k\mu}+4\rho^2 ID(f_{0\uparrow}^\dagger f_{0\uparrow})(f_{0\downarrow}^\dagger f_{0\downarrow}) +2\rho V f_{0\mu}^\dagger f_{0\mu}\Big] \ , \tag{5.47}$$

where, as before [cf. Eq. (2.13)], f_0 is the electron creation operator at the impurity site: $f_0 \equiv 2^{-1/2} \times \int_{-1}^{1} dk\, a_{k\mu}$. Going through the discretization, etc., as before, one gets, apart from an unimportant constant,

$$\frac{\mathcal{H}_{sf}}{D} \cong \tfrac{1}{2}(1+\Lambda^{-1})\sum_{n=0}^{\infty}\Lambda^{-n/2}\xi_n(f_{n\mu}^\dagger f_{n+1\mu}+f_{n+1\mu}^\dagger f_{n\mu}) +2\rho^2 ID(f_{0\mu}^\dagger f_{0\mu}-1)^2 +(2\rho V+2\rho^2 ID)f_{0\mu}^\dagger f_{0\mu} \ . \tag{5.48}$$

By a trivial relabeling of the operators $f_0, f_1, \ldots,$ one can now establish a one-to-one correspondence between this Hamiltonian and the discretized version of the asymmetric Anderson Hamiltonian, namely Eq. (2.14). Replacing $f_{0\mu}$ by $\bar{c}_{d\mu}$, $f_{1\mu}$ by $\bar{f}_{0\mu}$, and so on in Eq. (5.48) gives

$$\frac{\mathcal{H}_{sf}}{D\Lambda^{-1/2}} \cong \tfrac{1}{2}(1+\Lambda^{-1})\sum_{n=0}^{\infty}\Lambda^{-n/2}\xi_{n+1}(\bar{f}_{n\mu}^\dagger \bar{f}_{n+1\mu}+\bar{f}_{n+1\mu}^\dagger \bar{f}_{n+1\mu}) +\Lambda^{1/2}(2\rho V+2\rho^2 ID)\bar{c}_{d\mu}^\dagger \bar{c}_{d\mu}+\tfrac{1}{2}(1+\Lambda^{-1})\xi_0\Lambda^{1/2}(\bar{f}_{0\mu}^\dagger \bar{c}_{d\mu}+\bar{c}_{d\mu}^\dagger \bar{f}_{0\mu})+(2\rho^2 ID)\Lambda^{1/2}(\bar{c}_{d\mu}^\dagger \bar{c}_{d\mu}-1)^2 \ , \tag{5.49}$$

which is exactly of the form (2.14) except for the fact that ξ_{n+1} replaced ξ_n, which change is unimportant as far as low-temperature properties are concerned.

Thus, for a given Λ, the results for the (asymmetric) Anderson Hamiltonian can be converted into the corresponding results for the (asymmetric) local-spin-fluctuation Hamiltonian merely by replacing the parameters for the Anderson model by the parameters for the spin-fluctuation model according to the following prescription [compare Eqs. (2.14) and (5.49)]:

$$D\to D\Lambda^{-1/2}, \quad \left(\frac{2\Gamma}{\pi D}\right)^{1/2}\to \tfrac{1}{2}(1+\Lambda^{-1})\xi_0\Lambda^{1/2} \ , \quad \frac{U}{D}\to(4\rho^2 ID)\Lambda^{1/2}, \quad \frac{\epsilon_d}{D}\to(2\rho V)\Lambda^{1/2} \ . \tag{5.50}$$

One can hence make the following statements about the symmetric spin-fluctuation model (defined by the condition $V=-\rho ID$). First of all, since the effective (Γ/D) is already of order 1, there will be no free-orbital regime of temperatures. If $\rho^2 ID \gg 1$, one will have a local-moment regime followed by a strong-coupling regime as one goes down in temperatures. If $\rho^2 ID$ is of order 1 or smaller, one will have a strong-coupling regime for all temperatures of interest.

VI. SUMMARY

We can now summarize the various results that have so far been obtained for the symmetric Anderson model. We will choose to survey the parameter space of U and Γ by fixing attention at a particular value of U/D and then reviewing what happens as Γ is increased from a value much smaller than U to a value much larger than U.

To start with, let $U \ll D$. Then, if $\Gamma \ll U$, as one goes down in temperature from the band edge D, one essentially encounters three distinct regimes. First of all, for $D > k_B T > U$, there is the free-orbital regime where the dominant part of the impurity susceptibility is given by $\frac{1}{8}(g\mu_B)^2/(k_B T)$. As $k_B T$ decreases below U a local moment begins to develop, and for $k_B T$ less than about $\frac{1}{10}U$, the susceptibility is essentially the same as is obtainable from a Kondo Hamiltonian with an effective coupling constant ρJ given by Schrieffer-Wolff value of $-8\Gamma/(\pi U)$ and an effective band edge of order $\frac{1}{10}U$. This implies a local-moment regime which may be considered to extend down to the Kondo temperature $T_K(\Gamma,U)$ which is of order $\frac{1}{10}U(\Gamma/U)^{1/2}\exp(-\pi U/8\Gamma)$, followed by a strong-coupling regime for temperatures much less than T_K (say for $T < \frac{1}{10}T_K$). In the local-moment regime, for $0.5T_K < T < 16T_K$, the

susceptibility has a Curie-Weiss form: $\chi(T)=0.17(g\mu_B)^2/k_B(T+2T_K)$; in the strong-coupling regime the susceptibiltiy is predominantly a constant, which in this case has the value $0.10(g\mu_B)^2/k_BT_K$.

If one now increases Γ keeping U fixed, the effect until $|\rho J|$ gets to be about 0.8 (i.e, until $\pi\Gamma \simeq U$) is essentially that of an increase in T_K. The free-orbtial region is essentially unchanged, the local-moment region shrinks and the strong-coupling region grows. Once $|\rho J|$ gets past about 0.8, T_K begins to become of order U, so that the two transition regions (free orbital to local moment and local moment to strong coupling) begin to merge into one. For larger values of Γ, one therefore has only two regimes; a free-orbital regime for $D < k_BT < \Gamma$, and a strong-coupling regime for temperatures much smaller than Γ. At any fixed value of Γ/U, the effect of increasing U is merely to scale up the temperatures at which the various transitions occur. Figure 12 is a schematic diagram depicting the various regimes.

In retrospect, it is clear that the new renormalization-group formalism provides a *unified* approach to solving the Anderson Hamiltonian that performs rather well for all ranges of the parameter U and Γ. It gives the correct results in all the limiting cases when such results can be obtained by perturbation theory. For any given U and Γ, the method provides approximate numerical results for the whole range of temperatures less than the band edge D. It also makes clear the ranges of temperature where analytical (perturbative) calculations ought to be possible, and includes clear prescriptions for performing such calculations. The evidence in favor of the applicability of the principal approximation, namely the logarithmic discretization, is excellent, indication being that the results obtainable at Λ even as large as 3 are representative of the continuum limit ($\Lambda \to 1$) to within an error of about 10%.

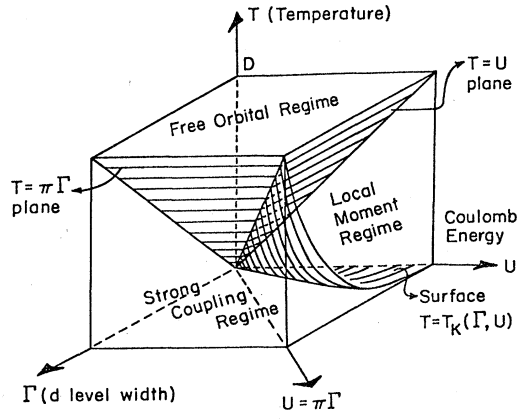

FIG. 12. Schematic sketch of the various regimes for the symmetric Anderson model. The separation between the various regimes, in contrast to the drawing, are actually quite fuzzy.

ACKNOWLEDGMENTS

One of us (H.R.K.) would like to thank the IBM Fellowship for financial support. One of us (J.W.W.) was supported in part by the NSF, Grant No. DMR 77-18329. One of us (K.G.W.) was supported in part by the NSF, Grant No. PHY 77-22336.

APPENDIX A: TRANSFORMATION INTO THE ENERGY REPRESENTATION

We first go from the discrete $\vec{k}$ in Eq. (2.1) to a continuum $\vec{k}$ in the standard way. If $a_{\vec{k}}$ denotes the continuum operator

$$\sum_{\vec{k}} \epsilon_{\vec{k}} c^\dagger_{\vec{k}} c_{\vec{k}} \to \int d^3k\, \epsilon_{\vec{k}} a^\dagger_{\vec{k}} a_{\vec{k}} \ ;$$

$$\sum_{\vec{k}} V_{\vec{k}d} c_{\vec{k}} \to \left(\frac{\Omega_0}{(2\pi)^3}\right)^{1/2} \int d^3k\, V_{\vec{k}d} a_{\vec{k}} \ , \qquad \text{(A1)}$$

where Ω_0 is the volume of the system.

Now we introduce a spherical harmonic expansion for $a_{\vec{k}}$

$$a_{\vec{k}} = \frac{1}{k} \sum_{lm} a_{klm} Y_{lm}(\hat{k}) \ ;$$

$$a_{klm} = k \int d\Omega_{\hat{k}} Y^*_{lm}(\hat{k}) a_{\vec{k}} \ , \qquad \text{(A2)}$$

which makes

$$\{a_{klm}, a^\dagger_{k'l'm'}\} = \delta(k-k')\delta_{ll'}\delta_{mm'} \ .$$

In terms of these operators and given that $\epsilon_{\vec{k}} = \epsilon_k$ and $V_{\vec{k}d} = V_{kd}$, we have

$$\int d^3k\, \epsilon_k a^\dagger_{\vec{k}} a_{\vec{k}} = \sum_{lm} \int dk\, \epsilon_k a^\dagger_{klm} a_{klm} \ , \qquad \text{(A3)}$$

$$\left(\frac{\Omega_0}{(2\pi)^3}\right)^{1/2} \int d^3k\, V_{kd} a_{\vec{k}} = \left(\frac{\Omega_0}{2\pi^2}\right)^{1/2} \int k\, dk\, a_{k00} \ . \qquad \text{(A4)}$$

Because of Eq. (A4), we need only keep the $l=0$, $m=0$ operators, and hereafter we drop the subscripts (00).

Next we introduce the energy representation by defining $a_\epsilon = (d\epsilon_k/dk)^{-1/2} a_k$ when $\epsilon = \epsilon_k$. This makes

$$\{a_\epsilon, a^\dagger_{\epsilon'}\} = \left(\frac{d\epsilon_K}{dk}\right)^{-1} \delta(k-k') = \delta(\epsilon-\epsilon') \ . \qquad \text{(A5)}$$

Introducing the energy cutoff from $-D$ to $+D$ about

the Fermi level,

$$\int dk\ \epsilon_k a_k^\dagger a_k = \int dk\ \epsilon_k \left(\frac{d\epsilon_k}{dk}\right) a_\epsilon^\dagger a_\epsilon = \int_{-D}^{D} d\epsilon\ \epsilon\ a_\epsilon^\dagger a_\epsilon\ ; \tag{A6}$$

$$\left(\frac{\Omega_0}{2\pi^2}\right)^{1/2} \int k\ dk\ V_{kd} a_k = \left(\frac{\Omega_0}{2\pi^2}\right)^{1/2} \int k\ dk\ V_{kd} \left(\frac{d\epsilon_k}{dk}\right)^{1/2} a_\epsilon = \left(\frac{\Omega_0}{2\pi^2}\right)^{1/2} \int_{-D}^{D} k_\epsilon\, d\epsilon \left(\frac{dk}{d\epsilon}\right)^{1/2} V_d(\epsilon) a_\epsilon\ . \tag{A7}$$

Using the result that $\rho(\epsilon) = (\Omega_0/2\pi^2) k^2 (dk/d\epsilon)$ we get

$$\left(\frac{\Omega_0}{2\pi^2}\right)^{1/2} \int k\ dk\ V_{kd} = \int_{-D}^{D} d\epsilon\, [\rho(\epsilon)]^{1/2} V_d(\epsilon) a_\epsilon\ . \tag{A8}$$

Equations (A6) and (A8) are the results stated in Eq. (2.3).

APPENDIX B: DETAILS ABOUT THE ITERATIVE DIAGONALIZATION

Let $|Q,S,S_z,r\rangle$ denote the states of H_N that have charge Q, spin S, z component of spin S_z. We will relabel the states defined in Eq. (2.23) as follows:

$$\begin{aligned} |Q,S,S_z,r;0\rangle &\equiv |Q,S,S_z,r\rangle\ , \\ |Q,S,S_z,r;\uparrow\rangle &\equiv f^\dagger_{(N+1)\uparrow} |Q,S,S_z,r\rangle\ , \\ |Q,S,S_z,r;\downarrow\rangle &\equiv f^\dagger_{(N+1)\downarrow} |Q,S,S_z,r\rangle\ , \\ |Q,S,S_z,r;\uparrow\downarrow\rangle &\equiv f^\dagger_{(N+1)\uparrow} f^\dagger_{(N+1)\downarrow} |Q,S,S_z,r\rangle\ . \end{aligned} \tag{B1}$$

Using theses states, we can form the following basis states of H_{N+1} that are also eigenstates of Q_{N+1}, $\vec{S}^2_{N+1}$, and $S_{(N+1)z}$

$$\begin{aligned} |Q,S,S_z,r,1\rangle_{N+1} &\equiv |Q+1,S,S_z,r;0\rangle_N\ , \\ |Q,S,S_z,r,2\rangle_{N+1} &\equiv \left(\frac{S+S_z}{2S}\right)^{1/2} |Q,S-\tfrac{1}{2},S_z-\tfrac{1}{2},r;\uparrow\rangle_N + \left(\frac{S+S_z}{2S}\right)^{1/2} |Q,S-\tfrac{1}{2},S_z+\tfrac{1}{2},r;\downarrow\rangle_N\ , \\ |Q,S,S_z,r3\rangle_{N+1} &\equiv -\left(\frac{S-S_z+1}{2S+2}\right)^{1/2} |Q,S,+\tfrac{1}{2},S_z-\tfrac{1}{2},r;\uparrow\rangle_N + \left(\frac{S+S_z+1}{2S+2}\right)^{1/2} |Q,S+\tfrac{1}{2},S_z+\tfrac{1}{2},,r;\downarrow\rangle_N\ , \\ |Q,S,S_z,r,4\rangle_{N+1} &\equiv |Q-1,S,S_z,r;\uparrow\downarrow\rangle_N\ . \end{aligned} \tag{B2}$$

Now we write the recursion relation (2.21) in the form

$$H_{N+1} = \Lambda^{1/2} H_N + \xi_N H_{NI}\ . \tag{B3}$$

The states (B2) are eigenstates of H_N (suppressing S_z)

$$\begin{aligned} H_N|Q,S,r,1\rangle &= E_N(Q+1,S,r)|Q,S,r,1\rangle\ , \\ H_N|Q,S,r,2\rangle &= E_N(Q,S-\tfrac{1}{2},r)|Q,S,r,2\rangle\ , \\ H_N|Q,S,r,3\rangle &= E_N(Q,S+\tfrac{1}{2},r)|Q,S,r,3\rangle\ , \\ H_N|Q,S,r,4\rangle &= E_N(Q-1,S,r)|Q,S,r,4\rangle\ . \end{aligned} \tag{B4}$$

To obtain the matrix elements of H_{NI} between the states (B2) we use the Wigner-Eckart theorem according to which

$$\langle Q',S',S_z',r'|f_\mu^\dagger|Q,S,S_z,r\rangle = \langle Q',S',r'\|f^\dagger\|Q,S,r\rangle \times \langle S,S_z;\tfrac{1}{2}\mu|S',S_z'\rangle\ , \tag{B5}$$

where $\langle\|f^\dagger\|\rangle$ are the invariant matrix elements and $\langle S,S_z;\frac{1}{2}\mu|S',S_z'\rangle$ are the Clebsh-Gordan coefficients. Using this theorem and various rules of angular momentum algebra, it is straightforward to demonstrate that (i) S_z plays no role in the diagonalization of H_{N+1}, (ii) the only nonvanishing matrix elements of H_{NI} are given by (dropping S_z now)

$$\begin{aligned} \langle Q,S,r',1|H_{NI}|Q,S,r,2\rangle &= \langle Q+1,S,r'\|f_N^\dagger\|Q,S-\tfrac{1}{2},r\rangle\ , \\ \langle Q,S,r',1|H_{NI}|Q,S,r,3\rangle &= \langle Q+1,S,r'\|f_N^\dagger\|Q,S+\tfrac{1}{2},r\rangle\ , \\ \langle Q,S,r',2|H_{NI}|Q,S,r,4\rangle &= \left(\frac{2S}{2S+1}\right)^{1/2} \langle Q,S-\tfrac{1}{2},r'\|f_N^\dagger\|Q-1,S,r\rangle\ , \\ \langle Q,S,r',3|H_{NI}|Q,S,r,4\rangle &= -\left(\frac{2S+2}{2S+1}\right)^{1/2} \langle Q,S+\tfrac{1}{2},r'\|f_N^\dagger\|Q-1,S,r\rangle\ . \end{aligned} \tag{B6}$$

In obtaining Eqs. (B6) we have made use of the following results which follows from Eqs. (B2):

$$\langle Q+1,S+\tfrac{1}{2},r,2\|f^{\dagger}_{N+1}\|Q,S,r,1\rangle=1\ ,$$

$$\langle Q+1,S-\tfrac{1}{2},r,3\|f^{\dagger}_{N+1}\|Q,S,r,1\rangle=1\ ,$$

$$\langle Q+1,S-\tfrac{1}{2},r,4\|f^{\dagger}_{N+1}\|Q,S,r,2\rangle=-\left(\frac{2S+1}{S}\right)^{1/2}\ , \tag{B7}$$

$$\langle Q+1,S+\tfrac{1}{2},r,4\|f^{\dagger}_{N+1}\|Q,S,r,3\rangle=\left(\frac{2S+1}{2S+2}\right)^{1/2}\ .$$

(The above are the only nonvanishing invariant matrix elements of $f^{\dagger}_{N+1}$.)

From Eqs. (B4)–(B6), it is clear that, starting with the knowledge of the energy levels $E_N(Q,S,r)$ and the matrix elements $\langle Q+1,S\pm\frac{1}{2},r'\|f^{\dagger}_{N}\|Q,S,r\rangle$, we can set up the matrix for H_{N+1}.

The actual iteration upon entering the stage $(N+1)$ would proceed as follows. We first start with the lowest allowed value of Q_{N+1}, and then increase it in steps of 1. For each Q, we start with the smallest permitted value of S_{N+1} (0 or $\frac{1}{2}$), and then increase it in steps of 1. Within a given (Q,S) subspace, we construct the matrix

$$H(ri;r'i')\equiv\langle Q,S,r,i|H_{N+1}|Q,S,r',i'\rangle\ . \tag{B8}$$

Diagonalization of this matrix gives a set of eigenstates

$$|Q,S,\omega\rangle=\sum_{i,r}U_{QS}(\omega;ri)|Q,S,r,i\rangle\ , \tag{B9}$$

where U will be an orthogonal matrix. The diagonalization means no more than the knowledge of $E_{N+1}(Q,S,\omega)$ and $U_{QS}(\omega;ri)$. After completing the diagonalization for one (QS), we proceed up, first increasing S in steps of 1, and then Q in steps of 1.

In order to go to the next iteration we need to calculate $\langle Q+1,S\pm\frac{1}{2},\omega'\|f^{\dagger}_{N+1}\|Q,S,\omega\rangle$. Using the results (B7) it is easy to verify that

$$\langle Q,S,\omega\|f^{\dagger}_{N+1}\|Q',S',\omega'\rangle=\sum_{r}U_{QS}(\omega;rk)\,U_{Q'S'}(\omega';r1)\pm\left(\frac{2S'+1}{2S+1}\right)^{1/2}U_{QS}(\omega;r4)\times U_{Q'S'}(\omega';rk')\ . \tag{B10}$$

where the + sign, $k=2$, and $k'=3$ are used if $S=S'+\frac{1}{2}$; the − sign, $k=3$, and $k'=2$ are used if $S=S'-\frac{1}{2}$.

APPENDIX C: CONTINUUM LIMIT FOR THE FREE-ORBITAL REGIME

Consider the quantities within the square brackets in Eqs. (5.5) and (5.6)

$$\chi_{1,\mathrm{FO}}(T,\bar{\beta},\Lambda)\equiv\left(\frac{4}{1+\Lambda^{-1}}\right)\times\sum_{l=1}^{(N+1)/2}\frac{\alpha_{0l}^2}{\eta_l^*}\frac{e^{-\bar{\beta}\eta_l^*}(1-e^{-\bar{\beta}\eta_l^*})}{(1+e^{-\bar{\beta}\eta_l^*})^3}\ , \tag{C1}$$

$$F_{1,\mathrm{FO}}(T,\bar{\beta},\Lambda)\equiv\left(\frac{4}{1+\Lambda^{-1}}\right)\times\sum_{l=1}^{(N+1)/2}\frac{\alpha_{0l}^2}{\eta_l^*}\frac{1-e^{-\bar{\beta}\eta_l^*}}{1+e^{-\bar{\beta}\eta_l^*}}\ , \tag{C2}$$

where, given the temperature T, N is determined by the condition that $\bar{\beta}\Lambda^{(N-1)/2}=\frac{1}{2}(1+\Lambda^{-1})D\beta$ ($\beta=1/k_BT$ as usual). We want to evaluate these sums in the limit as $\bar{\beta}\to0$ and $N\to\infty$ at a fixed temperature, and finally take the limit as $\Lambda\to1$.

For small $\bar{\beta}$, the dominant contributions to Eqs. (C1) and (C2) come from large l, where we can substitute $\alpha_{0l}=\alpha_0\Lambda^{(l-1)/2}$ and $\eta_l^*=\Lambda^{l-1}$ (cf. Table II). Hence

$$\chi_{1,\mathrm{FO}}\cong\frac{4\alpha_0^2}{1+\Lambda^{-1}}\times\sum_{l=1}^{(N+1)/2}\frac{e^{-\bar{\beta}\Lambda^{l-1}}(1-e^{-\bar{\beta}\Lambda^{l-1}})}{(1+e^{-\bar{\beta}\Lambda^{l-1}})^3}\ ;$$
$$F_{1,\mathrm{FO}}\cong\frac{4\alpha_0^2}{1+\Lambda^{-1}}\times\sum_{l=1}^{(N+1)/2}\frac{1-e^{-\bar{\beta}\Lambda^{l-1}}}{1+e^{-\bar{\beta}\Lambda^{l-1}}}\ . \tag{C3}$$

Let $m\equiv\frac{1}{2}(N-1)-(l-1)$. As N is odd, m runs from 0 to $\frac{1}{2}(N-1)$. Furthermore,

$$\bar{\beta}\Lambda^{l-1}=\bar{\beta}\Lambda^{(N-1)/2}\Lambda^{-m}=\tfrac{1}{2}(1+\Lambda^{-1})\beta D\Lambda^{-m}\equiv\beta\epsilon_m\ , \tag{C4}$$

say. Therefore, one gets

$$\chi_{1,\mathrm{FO}}\cong\frac{4\alpha_0^2}{1+\Lambda^{-1}}\sum_{m=0}^{(N-1)/2}\frac{e^{-\beta\epsilon_m}(1-e^{-\beta\epsilon_m})}{(1+e^{-\beta\epsilon_m})^3}\ .$$
$$F_{1,\mathrm{FO}}\cong\frac{4\alpha_0^2}{1+\Lambda^{-1}}\sum_{m=0}^{(N-1)/2}\frac{1-e^{-\beta\epsilon_m}}{1+e^{-\beta\epsilon_m}}\ . \tag{C5}$$

One may now safely take the $\bar{\beta}\to0$ or the $N\to\infty$

limit. From Eq. (C4), it is clear that for m large $\epsilon_m \to 0$, so that $(1-e^{-\beta\epsilon_m}) \to 0$ and both the sums above converge.

Next consider the $\Lambda \to 1$ limit. If Λ is close to 1, ϵ_m, which is equal to $\frac{1}{2}(1+\Lambda^{-1})D\Lambda^{-m}$, varies slowly with m. For small change Δm in m, one clearly has $\Delta\epsilon_m = -\epsilon_m(\ln\Lambda)\,\Delta m$. When Λ is close to 1, one can therefore write

$$\chi_{1,\mathrm{FO}}(T,0,\Lambda) \cong -\frac{1}{A_\Lambda}\sum_{m=0}^{\infty}\frac{\Delta\epsilon_m}{\epsilon_m}\frac{e^{-\beta\epsilon_m}(1-e^{-\beta\epsilon_m})}{(1+e^{-\beta\epsilon_m})^3}\ , \tag{C6}$$

$$F_{1,\mathrm{FO}}(T,0,\Lambda) \cong -\frac{1}{A_\Lambda}\sum_{m=0}^{\infty}\frac{\Delta\epsilon_m}{\epsilon_m}\frac{1-e^{-\beta\epsilon_m}}{1+e^{-\beta\epsilon_m}}\ , \tag{C6}$$

where we have defined [as in Eq. (5.42)]

$$A_\Lambda \equiv \frac{1+\Lambda^{-1}}{4\alpha_0^2}\ln\Lambda = \frac{1+\Lambda^{-1}}{1-\Lambda^{-1}}\frac{1}{2}\ln\Lambda$$

$$= 1+\tfrac{1}{12}(\ln\Lambda)^2 - \tfrac{1}{720}(\ln\Lambda)^4 + \cdots\ . \tag{C8}$$

As m goes from 0 to ∞, ϵ_m goes from $\frac{1}{2}(1+\Lambda^{-1})D$ to 0. In the limit $\Lambda \to 1$, $\Delta\epsilon_m \to 0$, and the sums in Eqs. (C6) and (C7) become integrals running from 0 to D. Also, $A_\Lambda \to 1$. Hence we get the results stated in Sec. V A, namely,

$$\lim_{\Lambda\to 1}\lim_{\beta\to\infty}\chi_{1,\mathrm{FO}}(T,\bar\beta,\Lambda) = \int_0^D \frac{d\epsilon}{\epsilon}\frac{e^{-\beta\epsilon}(1-e^{-\beta\epsilon})}{(1+e^{-\beta\epsilon})^3}\ , \tag{C9}$$

$$\lim_{\Lambda\to 1}\lim_{\beta\to\infty}F_{1,\mathrm{FO}}(T,\bar\beta,\Lambda) = \int_0^D \frac{d\epsilon}{\epsilon}\frac{1-e^{-\beta\epsilon}}{1+e^{-\beta\epsilon}}\ . \tag{C10}$$

APPENDIX D: CONTINUUM LIMIT FOR THE STRONG-COUPLING REGIME

All the results quoted in Eq. (5.31) can be proved analytically based on the following three observations. (i) When $\bar\beta$ is very small, the dominant contributions to all the expressions (5.25)–(5.29) come from large l, whence one can put (cf. Table II) $\hat\eta_l^* = \Lambda^{l-1/2}$, $\eta_l^* = \Lambda^{l-1}$, $\hat\alpha_{0l} = \alpha_0\Lambda^{(l-1/2)/2}$, and $\hat\alpha_{1l} = \alpha_1\Lambda^{3(l-1/2)/2}$. (ii) In the limit that $\bar\beta \to 0$, the lower limits on the index l in all the expressions can be replaced by $-\infty$. (iii) In the limit $\Lambda \to 1$, the summand in each of the expressions varies slowly with l, so that the sums can be converted into integrals, which can then be evaluated. This procedure will be illustrated using $\chi_{1,\mathrm{SC}}$. See Sec. IX of Ref. 6 for details.

Using the observations (i) and (ii) above we see that

$$\chi_{1,\mathrm{SC}}(\bar\beta,\Lambda) \cong \bar\beta^2\ln\Lambda \times \sum_{l=-\infty}^{\infty}\Lambda^{2(l-1/2)}\frac{e^{-\bar\beta\Lambda^{l-1/2}}(1-e^{-\bar\beta\Lambda^{l-1/2}})}{(1+e^{-\bar\beta\Lambda^{l-1/2}})^3}\ . \tag{D1}$$

It is clear that the extra terms that have been added by extending the lower limit on l to $-\infty$, are smaller by $O(\bar\beta)$. Let $u_l \equiv \bar\beta\Lambda^{l-1/2}$. Then

$$\chi_{1,\mathrm{SC}}(\bar\beta,\Lambda) \cong \ln\Lambda\sum_{l=-\infty}^{\infty} u_l^2\frac{e^{-u_l}(1-e^{-u_l})}{(1+e^{-u_l})^3}\ . \tag{D2}$$

If Λ is close to 1, u_l changes slowly with l. For a change Δl in l one has $\Delta u_l = u_l(\ln\Lambda)\,\Delta l$. As l goes from $-\infty$ to $+\infty$, u_l goes from 0 to ∞. One can show that the error in replacing the sum (D1) by an integral over u vanishes as $\exp(-\pi^2/\ln\Lambda)$ as $\Lambda \to 1$. (See Sec. IX, Ref. 6, for the theorem from which the result follows.) Therefore one gets, as stated,

$$\chi_{1,\mathrm{SC}}(0,1) = \int_0^\infty u\,du\,\frac{e^{-u}(1-e^{-u})}{(1+e^{-u})^3} = \frac{1}{2}\ . \tag{D3}$$

APPENDIX E: ANALYTICAL TREATMENT OF THE $\Gamma \gg U$ CASE

When $\Gamma \gg U$, the full H_N can be broken up as

$$H_N = H_{N0} + \tilde U\Lambda^{(N-1)/2}(c_{d\mu}^\dagger c_{d\mu} - 1)^2\ , \tag{E1}$$

where we have defined H_{N0} to include the $\tilde\Gamma^{1/2}$ part, namely,

$$H_{N0} \equiv \Lambda^{(N-1)/2}\left[\sum_{n=0}^{N-1}\Lambda^{-n/2}\xi_n(f_{n\mu}^\dagger f_{n+1\,\mu} + f_{n+1\,\mu}^\dagger f_{n\mu}) + \tilde\Gamma^{1/2}(f_{0\mu}^\dagger c_{d\mu} + c_{d\mu}^\dagger f_{0\mu})\right]\ . \tag{E2}$$

The objective of this splitting of H_N is to diagonalize the quadratic Hamiltonian H_{N0} exactly and then to treat the $\tilde U$ term as a perturbation.

One approach to diagonalizing H_{N0} is to first express it in terms of the electron and hole operators that diagonalize H_N^0. Spin indices are unimportant for the following discussion and will be suppressed. One can hence write [compare Eq. (5.2)],

$$H_{N0} = \sum_{l=1}^{(N+1)/2}\eta_l^*(g_l^\dagger g_l + h_l^\dagger h_l) + \tilde\Gamma^{1/2}\Lambda^{(N-1)/4}\sum_l \alpha_{0l}(c_d^\dagger g_l + c_d^\dagger h_l^\dagger + g_l^\dagger c_d + h_l c_d)\ . \tag{E3}$$

It is convenient, at this point, to go back to a notation that involves negative energy electron operators rather than positive energy hole operators. We will therefore define a new set of $(N+2)$ electron operators (a_l), $-\frac{1}{2}(N+1) \leq l \leq \frac{1}{2}(N+1)$, given by

$$a_l \equiv g_l (l>0), \quad a_l \equiv h_{-l}^{\dagger} (l<0),$$

and

$$a_0 \equiv c_d \ . \tag{E4}$$

In terms of these operators H_{N0} becomes, apart from an unimportant constant,

$$H_{N0} = \sum_{l=-J}^{J} \eta_l^* a_l^{\dagger} a_l + \tilde{\Gamma}^{1/2} \Lambda^{(N-1)/4} \sum_{l=-J}^{J} \alpha_{0l} (a_0^{\dagger} a_l + a_l^{\dagger} a_0) \ , \tag{E5}$$

where we have defined

$$J = \tfrac{1}{2}(N+1), \quad \eta_{-l}^* = -\eta_l^* (l>0),$$

$$\eta_0^* = 0 \ \text{ and } \ \alpha_{00} = 0 \ . \tag{E6}$$

It is straightforward to verify that a new set of operators $\hat{a}_j$, $-J \leq j \leq J$, defined as $\hat{a}_j = \sum_l U_{lj} a_l$ where U_{lj} are the elements of an *orthogonal* matrix, will diagonalize H_{N0} into a set of single-particle levels $\hat{\eta}_j(N)$ provided the coefficients U_{lj} satisfy the following equations:

$$(\hat{\eta}_j - \eta_l^*) U_{lj} = \tilde{\Gamma}^{1/2} \Lambda^{(N-1)/4} \alpha_{0l} U_{0j} \quad (l \neq 0) \ , \tag{E7}$$

$$\hat{\eta}_j U_{0j} = \tilde{\Gamma}^{1/2} \Lambda^{(N-1)/4} \sum_{l=-J}^{J} \alpha_{0l} U_{lj} \ . \tag{E8}$$

Solving Eq. (E7) for U_{lj}, substituting into the right-hand side of Eq. (E8) and making use of the definitions in Eq. (E6) leads to the following equation for the eigenvalues $\hat{\eta}_j(N)$:

$$\hat{\eta}_j = \tilde{\Gamma} \Lambda^{(N-1)/2} \sum_{l=1}^{J} \alpha_{0l}^2 \frac{2\hat{\eta}_j}{\hat{\eta}_j^2 - \eta_l^{*2}} \ . \tag{E9}$$

$\hat{\eta}_j = 0$ is clearly a solution of this equation, and will be associated with the index $j=0$; i.e., $\hat{\eta}_0 = 0$. Furthermore, since the above equation remains invariant when $\hat{\eta}_j \rightarrow -\hat{\eta}_j$, we can choose $\hat{\eta}_{-j} = -\hat{\eta}_j$ $(j>0)$ where $\hat{\eta}_j$ $(j>0)$ are all positive and are given by the positive roots of the equation

$$\frac{1}{2\tilde{\Gamma}\Lambda^{(N-1)/2}} = \sum_{l=1}^{J} \frac{\alpha_{0l}^2}{\hat{\eta}^2 - \eta_l^{*2}} \equiv Y(N, \hat{\eta}) \ . \tag{E10}$$

A graphical method of determining $\hat{\eta}_j$ is to plot the quantity $Y(N, \hat{\eta})$ as a function of $\hat{\eta}$ and find its points of intersection with the horizontal line $Y = 1/(2\tilde{\Gamma}\Lambda^{(N-1/2)})$, as shown in Fig. 13. The coefficients U_{0j} can be determined from the equation

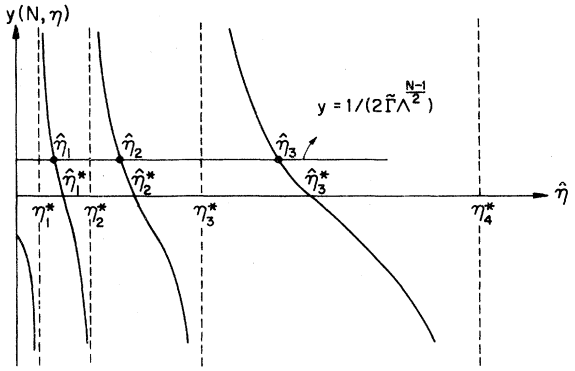

FIG. 13. Graphical method for determining the roots of Eq. (E10).

$$U_{0j} = \left[1 + \tilde{\Gamma} \Lambda^{(N-1)/2} \sum_{l=-J}^{J} \frac{\alpha_{0l}^2}{(\hat{\eta}_j - \eta_l^*)^2} \right]^{-1/2} \ . \tag{E11}$$

This equation follows from Eq. (E7) and the result $\sum_l U_{lj}^2 = 1$. The effect of the $\tilde{U}$ term in Eq. (E1), to $O(\tilde{U})$ can then be calculated by substituting $c_{d\mu} \equiv a_{0\mu} = \sum_j U_{0j} \hat{a}_j$ in Eq. (E1), i.e., by writing H_N as

$$H_N = \sum_{j=-J}^{J} \hat{\eta}_j(N) \hat{a}_{j\mu}^{\dagger} \hat{a}_{j\mu} + \tilde{U} \Lambda^{(N-1)/2} \times \left[\sum_{jj'} U_{0j} U_{0j'} \hat{a}_{j\mu}^{\dagger} \hat{a}_{j'\mu} - 1 \right]^2 \ . \tag{E12}$$

We want to calculate explicitly $\hat{\eta}_j$ and U_{0j} for the case when $\tilde{\Gamma} \ll 1$. For small $\hat{\eta}$ (i.e., $\hat{\eta} \ll \eta_j^* = \Lambda^{(N-1)/2}$), the N dependence of $Y(N, \hat{\eta})$ is negligible, so that the N dependence of the small eigenvalues (which are the ones of interest) is entirely due to the left-hand side of Eq. (E10).

Suppose that N is small enough that $\tilde{\Gamma}\Lambda^{(N-1)/2} \ll 1$. Then $\hat{\eta}_j$ is very close to η_j^*. Therefore $Y(N, \hat{\eta}_j) \cong \alpha_{0j}^2/(\hat{\eta}_j^2 - \eta_j^{*2})$, so that we have

$$\hat{\eta}_j^2 \cong \eta_j^{*2} + 2\tilde{\Gamma}\Lambda^{(N-1)/2} \alpha_{0j}^2$$

or

$$\hat{\eta}_j \cong \eta_j^* + \tilde{\Gamma}\Lambda^{(N-1)/2} \frac{\alpha_{0j}^2}{\eta_j^*} \ , \tag{E13}$$

which is the same result as obtained in Sec. V A for the free-orbital regime. Furthermore, in this case Eq. (E11) leads to the results

$$U_{00} \cong 1 - \tfrac{1}{2}\tilde{\Gamma}\Lambda^{(N-1)/2} \sum_{l \neq 0} \frac{\alpha_{0l}^2}{\eta_l^{*2}},$$

$$U_{0j} \cong \tilde{\Gamma}\Lambda^{(N-1)/2} \frac{\alpha_{0j}^2}{\eta_j^{*2}} \quad (j \neq 0) \ ; \tag{E14}$$

which shows that the dominant part of the second term in Eq. (E12) is given by $\tilde{U}\Lambda^{(N-1)/2}(\hat{a}^{\dagger}_{0\mu}\hat{a}_{0\mu}-1)^2$. This is again the same result as in Sec. V A, namely, that the effect of the $\tilde{U}$ term is to remove the degeneracy associated with the electron mode of zero energy.

However small $\tilde{\Gamma}$ may be, $\tilde{\Gamma}\Lambda^{(N-1)/2}$ increases as N increases so that $\hat{\eta}_j$ moves away from η^*_j. When $\tilde{\Gamma}\Lambda^{(N-1)/2}$ becomes much bigger than 1, $(\hat{\eta}_j)$ are close to the points of intersection of $Y(N,\hat{\eta})$ with the $\hat{\eta}$ axis, which points precisely determine the odd fixed-point energies $\hat{\eta}^*_j$ (see Fig. 13). Thus H_{N0} crosses over from $H^*_{\rm FO}$ for $\tilde{\Gamma}\Lambda^{(N-1)/2} \ll 1$ to $H^*_{\rm SC}$ for $\tilde{\Gamma}\Lambda^{(N-1)/2} \gg 1$, as asserted in Sec. V.

The equation for the fixed points $\hat{\eta}^*_j$ is clearly: $\sum_{l=1}^{\infty}\alpha_{0l}^2/(\hat{\eta}_j^{*2}-\eta_l^{*2})=0$. When $\tilde{\Gamma}\Lambda^{(N-1)/2}\gg 1$, for the small eigenvalues one can write $\hat{\eta}_j=\hat{\eta}^*_j+\delta_j$ where δ_j is small. Substituting this into Eq. (E10) and keeping terms only up to $O(\delta_j)$, one gets

$$\delta_j=-\frac{\Lambda^{-(N-1)/2}}{4\tilde{\Gamma}\hat{\eta}^*_j}\left[\sum_{l=1}^{\infty}\frac{\alpha_{0l}^2}{(\hat{\eta}_j^{*2}-\eta_l^{*2})^2}\right]^{-1} . \tag{E15}$$

Hence the leading deviations of the single-particle energies from their fixed-point values do indeed decay as $\Lambda^{-(N-1)/2}$ in the strong-coupling regime. One can compute the sum in Eq. (E15) numerically for any j. Comparing the resulting δ_j with the answer one expects from the discussion of Sec. V C, namely $\delta_j=2\omega_1\hat{\alpha}_{0j}\hat{\alpha}_{1j}\Lambda^{-(N-1)/2}$, allows one to determine ω_1.

However, there is a simpler, analytical way to obtain ω_1, which is to consider δ_j for $j\gg 1$ (but $j\ll\frac{1}{2}N$ still). Then $\hat{\eta}^*_j=\Lambda^{j-1/2}$. Furthermore, the dominant contribution to the sum in Eq. (E15) comes from $l\simeq j$, so that one may use $\eta^*_l=\Lambda^{l-1}$ and $\alpha_{0l}=\alpha_0\Lambda^{(l-1)/2}$. One may also let the sum over l run from $-\infty$ to $+\infty$. It is straighforward to verify that these approximations lead to

$$\delta_j\cong-\frac{\Lambda^{-(N-1)/2}}{4\tilde{\Gamma}\alpha_0^2}\frac{1}{\Lambda^{j-1/2}}\left[\sum_{l=-\infty}^{\infty}\frac{\Lambda^{l-1}}{(\Lambda^{2j-1}-\Lambda^{2l-2})^2}\right]^{-1}$$

$$=-\frac{\Lambda^{-(N-1)/2}}{4\tilde{\Gamma}\alpha_0^2}\Lambda^{2j-1}\left[\sum_{l'=-\infty}^{\infty}\frac{\Lambda^{l'-1/2}}{(1-\Lambda^{2l'-1})^2}\right]^{-1} , \tag{E16}$$

where the second result follows upon replacing the index l by $l'=l-j$.

For any given Λ, the sum over l' in Eq. (E16) can be evaluated exactly by means of Sommerfeld-Watson transformation.[15] One finds that

$$\sum_{l=-\infty}^{\infty}\frac{\Lambda^{l-1/2}}{(1-\Lambda^{2l-1})^2}=\frac{1}{4(\ln\Lambda)^2}\times\left[\pi^2+2\sum_{k=1}^{\infty}\frac{(-1)^k}{\cosh^2(\pi^2k/\ln\Lambda)}\right]$$

$$=\frac{\pi^2}{4(\ln\Lambda)^2}\quad(\Lambda\to 1) , \tag{E17}$$

since the terms other than π^2 in the above expression are of order $\exp(-2\pi^2k/\ln\Lambda)$ when Λ is close to 1, and are clearly negligible. Therefore one obtains, making use of Eq. (2.20),

$$\delta_j=-\frac{\Lambda^{-(N-1)/2}\Lambda^{2j-1}(\ln\Lambda)^2}{\tilde{\Gamma}\alpha_0^2\pi^2}$$

$$=-\Lambda^{(N-1)/2}\Lambda^{2j-1}[\tfrac{1}{2}(1+\Lambda^{-1})]^2\frac{D}{2\pi\Gamma}\frac{(\ln\Lambda)^2}{\alpha_0^2} . \tag{E18}$$

This is to be compared with the result

$$\delta_j=2\omega_1\hat{\alpha}_{0j}\hat{\alpha}_{1j}\Lambda^{-(N-1)/2}$$

$$=2\omega_1\alpha_0\alpha_1\Lambda^{2j-1}\Lambda^{-(N-1)/2}\quad(\text{for } j\gg 1) .$$

The j dependence of the two results is the same, so that one gets the result (5.38) for ω_1.

The result for ω_2 follows from Eq. (E11) for U_{0j}. Since $\tilde{\Gamma}\Lambda^{(N-1)/2}\gg 1$, the dominant contribution to U_{0j} will be given by

$$U_{0j}=\frac{\Lambda^{-(N-1)/4}}{\tilde{\Gamma}^{1/2}}\left[\sum_{l=1}^{\infty}\frac{\alpha_{0l}^2}{(\hat{\eta}^*_j-\eta^*_l)^2}+\sum_{l=1}^{\infty}\frac{\alpha_{0l}^2}{(\hat{\eta}^*_j+\eta^*_l)^2}\right]^{-1/2} . \tag{E19}$$

This implies that the N dependence of the expansion of $c_{d\mu}\equiv a_{0\mu}$ in terms of the operators $\hat{a}_{j\mu}$ that are equivalent, in the present context, to the electron operators that diagonalize $H_{N,\rm SC}$ is precisely of the form of Eq. (4.23). One may again verify the j dependence by working out U_{0j} for $j\gg 1$. In this case one can neglect the second sum in Eq. (E19), and make exactly the same approximations as before regarding the first sum, to get

$$U_{0j}\cong\frac{\Lambda^{-(N-1)/4}}{\alpha_0\tilde{\Gamma}^{1/2}}\left[\sum_{l=-\infty}^{\infty}\frac{\Lambda^{l-1}}{(\Lambda^{j-1/2}-\Lambda^{l-1})^2}\right]^{-1/2}$$

$$=\frac{\Lambda^{-(N-1)/4}}{\alpha_0\tilde{\Gamma}^{1/2}}\Lambda^{(j-1/2)/2}\times\left[\sum_{l'=-\infty}^{\infty}\frac{\Lambda^{l'-1/2}}{(1-\Lambda^{l'-1/2})^2}\right]^{-1/2} . \tag{E20}$$

The sum over l' can again be carried out using a Sommerfeld-Watson transformation[15]

$$\sum_{l}\frac{\Lambda^{1-1/2}}{(1-\Lambda^{l-1/2})^2}=\frac{1}{(\ln\Lambda)^2}\times\left[\pi^2+2\sum_{k=1}^{\infty}\frac{1}{\cosh^2(2\pi^2k/\ln\Lambda)}\right]$$

$$=\frac{\pi^2}{(\ln\Lambda)^2}\quad(\Lambda\to 1) ; \tag{E21}$$

so that one gets

$$U_{0j} \cong \frac{\ln\Lambda}{\alpha_0\pi\tilde{\Gamma}^{1/2}}\Lambda^{(j-1/2)/2}\Lambda^{-(N-1)/4}$$

$$= \frac{\ln\Lambda}{\alpha_0^2\pi\Gamma^{1/2}}\hat{\alpha}_{0j}\Lambda^{-(N-1)/4} \quad (j \gg 1) \ . \tag{E22}$$

It is now straightforward to verify that the substitution of Eq. (E22) into Eq. (E12) will lead to an irrelevant operator precisely of the form of the second irrelevant term in Eq. (5.22), with the coefficient ω_2 now being explicitly given by

$$\omega_2 = \tilde{U}\left(\frac{\ln\Lambda}{\alpha_0^2\pi\tilde{\Gamma}^{1/2}}\right)^4$$

$$= [\tfrac{1}{2}(1+\Lambda^{-1})]^3\frac{(\ln\Lambda)^4}{\alpha_0^8}\left(\frac{D}{2\pi\Gamma}\right)^2\frac{U}{2D} \ , \tag{E23}$$

where we have made use of the definitions (2.19) and (2.20) for $\tilde{U}$ and $\tilde{\Gamma}$. Equation (E23) is precisely the result (5.39) quoted earlier.

APPENDIX F: DETAILS ABOUT THE NUMERICAL CALCULATION OF $\chi_{\rm imp}$ AND $F_{\rm imp}$

The problem of calculating $\chi_{\rm imp}$ and $C_{\rm imp}$ is clearly that of calculating the traces [cf. Eqs. (2.30) and (2.31)]

$$Z \equiv \mathrm{Tr}(\exp -\bar{\beta}_M H_M) \ , \tag{F1}$$

$$X \equiv Z^{-1}\mathrm{Tr}(S_{Mz}^2 \exp -\bar{\beta}_M H_M) \ , \tag{F2}$$

and similar traces for H_M^0, which will be denoted Z_F and X_F.

In order to evaluate these traces in the limit $M \to \infty$, we split H_M and S_{Mz} so as to separate the degrees of freedom up to f_N from those beyond, as indicated in Sec. II E. Using a notation slightly different from that of Sec. II E, we write (with $\bar{\beta}_N \equiv \bar{\beta}$)

$$\bar{\beta}_M H_M = \bar{\beta}(H_N + H_B + H_I) \ , \tag{F3}$$

$$\vec{S}_M = \vec{S}_N + \vec{S}_B \ ; \tag{F4}$$

where we have defined

$$H_B \equiv \Lambda^{(N-1)/2}\left(\sum_{n=N+1}^{M-1}\Lambda^{-n/2}\xi_n(f_{n\mu}^\dagger f_{n+1\mu} + f_{n+1\mu}^\dagger f_{n\mu})\right) \ , \tag{F5}$$

$$H_I \equiv \Lambda^{-1/2}(f_{N\mu}^\dagger f_{(N+1)\mu} + f_{(N+1)\mu}^\dagger f_{N\mu}) \ , \tag{F6}$$

$$\vec{S}_B \equiv \tfrac{1}{2}\sum_{n=N+1}^{M} f_{n\mu}^\dagger \vec{\sigma}_{\mu\nu} f_{n\nu} \ . \tag{F7}$$

In this appendix we will prove what was stated in Sec. II E, namely that H_I can be treated as a perturbation; and the dominant contribution comes from terms ignoring (i.e., to zero order in) H_I, while the corrections to $O(H_I^2)$ are small, of order $(\bar{\beta}/\Lambda)$.

In order to carry out the perturbation theory, we make use of the standard result that

$$e^{-\bar{\beta}(H_0+H_I)} = e^{-\bar{\beta}H_0}T\exp\left(-\int_0^{\bar{\beta}} d\lambda\, H_I(\lambda)\right) \ , \tag{F8}$$

where T denotes ordering with respect to λ and

$$H_I(\lambda) \equiv e^{\lambda H_0}H_I e^{-\lambda H_0} \ . \tag{F9}$$

Let A be an operator that commutes with H_0 *and* H_I. Then it is straightforward to show that the following simplification is possible to $O(H_I^2)$:

$$\mathrm{Tr}(Ae^{-\bar{\beta}(H_0+H_I)})$$

$$= \mathrm{Tr}\left[Ae^{-\bar{\beta}H_0}\left(1 - \bar{\beta}H_I + \tfrac{1}{2}\bar{\beta}\int_0^{\bar{\beta}} d\lambda\, H_I(\lambda)H_I\right)\right] \ . \tag{F10}$$

We now use Eq. (F10) to evaluate Z and X, with $H_0 = H_N + H_B$, and $A = 1$ and S_{Mz}^2, respectively. It is straightforward to verify that the zero-order terms are

$$Z^{(0)} = (\mathrm{Tr}e^{-\bar{\beta}H_N})(\mathrm{Tr}e^{-\bar{\beta}H_B}) \equiv Z_N Z_B \ , \tag{F11}$$

$$\chi^{(0)} = \langle S_{Nz}^2\rangle_N + \langle S_{Bz}^2\rangle_B + 2\langle S_{Nz}\rangle_N\langle S_{Bz}\rangle_B$$

$$= \langle S_{Nz}^2\rangle_N + \langle S_{Bz}^2\rangle_B \equiv X_N + X_B \ , \tag{F12}$$

where the notation is that $\langle A\rangle_N$ stands for Z_N^{-1} $\times \mathrm{Tr}(Ae^{-\bar{\beta}H_N})$, and similarly for $\langle A\rangle_B$. Use has also been made in Eq. (F12) of the fact that $\langle S_{Nz}\rangle = \langle S_{Bz}\rangle = 0$.

Next consider the first-order terms in H_I. It is clear that H_N and H_B conserve their respective particle numbers, whereas f_N and f_{N+1} (or $f_N^\dagger$ and $f_{N+1}^\dagger$) change these particle numbers. As a result, the first-order terms vanish. For the same reason, the second-order contributions reduce to

$$\frac{Z^{(2)}}{Z^{(0)}} = \frac{\bar{\beta}}{2\Lambda}\int_0^{\bar{\beta}} d\lambda\,(\langle f_{N\mu}^\dagger(\lambda)f_{N\nu}\rangle_N\langle f_{(N+1)\mu}(\lambda)f_{(N+1)\nu}^\dagger\rangle_B + \langle f_{N\mu}(\lambda)f_{N\nu}^\dagger\rangle_N\langle f_{N+1\mu}^\dagger(\lambda)f_{N+1\nu}\rangle_B) \ , \tag{F13}$$

$$X^{(2)}=\frac{\bar{\beta}}{2\Lambda}\int_0^{\bar{\beta}}d\lambda\,(\langle S_{Nz}^2 f_{N\mu}^\dagger(\lambda)f_{N\nu}\rangle_N\langle f_{(N+1)\mu}(\lambda)f_{(N+1)\nu}^\dagger\rangle_B+\langle f_{N\mu}^\dagger(\lambda)f_{N\nu}\rangle_N\langle S_{Bz}^2 f_{(N+1)\mu}(\lambda)f_{(N+1)\nu}^\dagger\rangle_B$$
$$+2\langle S_{Nz}f_{N\mu}^\dagger(\lambda)f_{N\nu}\rangle_N\langle S_{Bz}f_{N+1\mu}(\lambda)f_{N+1\nu}^\dagger\rangle_B+\langle S_{Nz}^2 f_{N\mu}(\lambda)f_{N\nu}^\dagger\rangle_N\langle f_{N+1\mu}^\dagger(\lambda)f_{N+1\nu}\rangle_B$$
$$+\langle f_{N\mu}(\lambda)f_{N\nu}^\dagger\rangle_N\langle S_{Bz}^2 f_{N+1\mu}^\dagger(\lambda)f_{N+1\nu}\rangle_B$$
$$+2\langle S_{Nz}f_{N\mu}(\lambda)f_{N\nu}^\dagger\rangle_N\langle S_{Bz}f_{N+1\mu}^\dagger(\lambda)f_{N+1\nu}\rangle_B)-X^{(0)}\frac{Z^{(2)}}{Z^{(0)}}\ . \tag{F14}$$

We now proceed to evaluate the various traces defined above. The traces involving H_B can be done exactly, whereas the traces involving H_N will be expressed in terms of the energy levels of H_N and the matrix elements of f_N between its states.

1. *Evaluation of Traces Involving H_B*

Referring to Eq. (F5), we note that H_B is a quadratic Hamiltonian. It can hence be diagonalized exactly in terms of new operators a_j such that

$$H_B=\sum_j \epsilon_j a_{j\mu}^\dagger a_{j\mu}\ ; \tag{F15}$$

$$f_{N+1\mu}=\sum_j v_j a_{j\mu},\quad \vec{S}_B=\tfrac{1}{2}\sum_j a_{j\mu}^\dagger\,\vec{\sigma}_{\mu\nu}a_{j\nu}\ . \tag{F16}$$

Since H_B has $(M-N)$ operators $[f_{N+1},\ldots,f_M]$ and conserves particle-hole symmetry, we can choose j to take values $\pm1,\pm2,\ldots,\pm\frac{1}{2}(M-N)$ if $M-N$ is even; and values $0,\pm1,\pm2,\ldots,\pm\frac{1}{2}(M-N-1)$ if $(M-N)$ is odd, and obtain the results

$$\epsilon_0=0,\quad \epsilon_{-j}=-\epsilon_j,\quad v_{-j}=v_j\ . \tag{F17}$$

In what follows, we will let $\sum_j$ stand for the sum over j in both cases.

[In fact, by comparing H_B with the free-electron Hamiltonian discussed in Sec. III A, it is clear that except when $|j|$ is near $\frac{1}{2}(M-N)$ we can choose

$$(M-N)\text{ even: }\ \epsilon_j\cong\Lambda^{-(M-N)/2}\eta_j^*,\quad v_j\propto\Lambda^{-(M-N-2)/4}\alpha_{0j}\ ;$$
$$(M-N)\text{ odd: }\ \epsilon_j\cong\Lambda^{-(M-N)/2}\hat{\eta}_j^*,\quad v_j\propto\Lambda^{-(M-N-2)/4}\hat{\alpha}_{0j}\ .] \tag{F18}$$

Subsituting Eqs. (F15) and (F16) into the various traces involving H_B, and using standard fermion operator algebra, it is straightforward to verify that ($\mu,\nu=\pm\frac{1}{2}$ below)

$$Z_B=\prod_j(1+e^{-\bar{\beta}\epsilon_j})\ , \tag{F19}$$

$$X_B\equiv\langle S_{Bz}^2\rangle_B=\tfrac{1}{2}\sum_j\frac{e^{-\bar{\beta}\epsilon_j}}{(1+e^{-\bar{\beta}\epsilon_j})^2}\ , \tag{F20}$$

$$\langle f_{N+1\mu}(\lambda)f_{N+1\nu}^\dagger\rangle_B=\delta_{\mu\nu}\sum_j v_j^2 e^{-\lambda\epsilon_j}\frac{1}{1+e^{-\bar{\beta}\epsilon_j}}\ , \tag{F21}$$

$$\langle S_{Bz}f_{N+1\mu}(\lambda)f_{N+1\nu}^\dagger\rangle_B=\delta_{\mu\nu}\sum_j v_j^2 e^{-\lambda\epsilon_j}\frac{-\mu e^{-\bar{\beta}\epsilon_j}}{(1+e^{-\bar{\beta}\epsilon_j})^2}\ , \tag{F22}$$

$$\langle S_{Bz}^2 f_{N+1\mu}(\lambda)f_{N+1\nu}^\dagger\rangle_B=\langle S_{Bz}^2\rangle_B\langle f_{N+1\mu}(\lambda)f_{N+1\nu}^\dagger\rangle_B+\delta_{\mu\nu}\sum_j v_j^2 e^{-\lambda\epsilon_j}\frac{1}{4}\frac{e^{-\bar{\beta}\epsilon_j}(e^{-\bar{\beta}\epsilon_j}-1)}{(1+e^{-\bar{\beta}\epsilon_j})^3}\ , \tag{F23}$$

$$\langle f_{N+1\mu}^\dagger(\lambda)f_{N+1\nu}\rangle_B=\delta_{\mu\nu}\sum_j v_j^2 e^{\lambda\epsilon_j}\frac{e^{-\bar{\beta}\epsilon_j}}{1+e^{-\bar{\beta}\epsilon_j}}\ , \tag{F24}$$

$$\langle S_{Bz} f^{\dagger}_{N+1\mu}(\lambda) f_{N+1\nu}\rangle_B = \delta_{\mu\nu}\sum_j v_j^2 \frac{e^{\lambda\epsilon_j}\mu e^{-\bar\beta\epsilon_j}}{(1+e^{-\bar\beta\epsilon_j})^2} \quad , \tag{F25}$$

$$\langle S_{Bz}^2 f^{\dagger}_{N+1\mu}(\lambda) f_{N+1\nu}\rangle_B = \langle S_{Bz}^2\rangle_B \langle f^{\dagger}_{N+1\mu}(\lambda) f_{N+1\nu}\rangle_B + \delta_{\mu\nu}\sum_j v_j^2 e^{\lambda\epsilon_j}\frac{1}{4}\frac{e^{-\bar\beta\epsilon_j}(1-e^{-\bar\beta\epsilon_j})}{(1+e^{-\bar\beta\epsilon_j})^3} \quad . \tag{F26}$$

2. *Evaluation of Traces Involving H_N*

Let $|k,S,S_z\rangle$ denote the states of H_N, where k takes care of all indices other than the spin and its z component. As discussed in Sec. II D, the energies are independent of S_z and can be denoted E_{kS}. Then it is straightforward to verify that

$$Z_N = \sum_{kS} n_s e^{-\bar\beta E_{kS}} \quad , \tag{F27}$$

$$\langle S_{Nz}^2\rangle_N = Z_N^{-1}\sum_{kS}\tfrac{1}{12} n_S(n_s^2-1)e^{-\bar\beta E_{kS}} \equiv X_N \quad , \tag{F28}$$

where $n_S \equiv (2S+1)$ is the degeneracy of the state $|k,S\rangle$. Furthermore, we get (no sum over μ below)

$$\left\langle \begin{pmatrix} 1 \\ S_{Nz} \\ S_{Nz}^2 \end{pmatrix} f^{\dagger}_{N\mu}(\lambda) f_{N\mu}\right\rangle_N = Z_N^{-1}\sum_{\substack{kSS_z' \\ k'S'S_z'}} |\langle kSS_z| f^{\dagger}_{N\mu}|k'S'S_z'\rangle|^2 \begin{pmatrix} 1 \\ S_z \\ S_z^2 \end{pmatrix} e^{-\bar\beta E_{kS}} e^{\lambda(E_{kS}-E_{k'S'})} \quad , \tag{F29}$$

$$\left\langle \begin{pmatrix} 1 \\ S_{Nz} \\ S_{Nz}^2 \end{pmatrix} f_{N\mu}(\lambda) f^{\dagger}_{N\mu}\right\rangle_N = Z_N^{-1}\sum_{\substack{kSS_z' \\ k'S'S_z'}} |\langle kSS_z| f^{\dagger}_{N\mu}|k'S'S_z'\rangle|^2 \begin{pmatrix} 1 \\ S_z' \\ S_z'^2 \end{pmatrix} e^{-\bar\beta E_{k'S'}} e^{\lambda(E_{k'S'}-E_{kS})} \quad . \tag{F30}$$

Substituting the results (F21)–(F26) and (F29) and (F30), and the result (cf. Appendix B)

$$\langle kSS_z| f^{\dagger}_{N\mu}|k'S'S_z'\rangle = \langle kS\| f^{\dagger}_N\|k'S'\rangle \langle S'S_z';\tfrac{1}{2}\mu|SS_z\rangle \tag{F31}$$

into the expressions for $Z^{(2)}$ and $X^{(2)}$ we get

$$\frac{Z^{(2)}}{Z^{(0)}} = \frac{\bar\beta}{2\Lambda} Z_N^{-1}\sum_{kS,k'S'} |\langle kS\| f^{\dagger}_N\|k'S'\rangle|^2 \sum_j \frac{v_j^2}{1+e^{-\bar\beta\epsilon_j}} \frac{e^{-\bar\beta(E'+\epsilon_j)}-e^{-\bar\beta E}}{E-E'-\epsilon_j} \; 2\sum_{S_zS_z'\mu} |\langle S'S_z';\tfrac{1}{2}\mu|SS_z\rangle|^2 \quad , \tag{F32}$$

$$\begin{aligned} X^{(2)} = \frac{\bar\beta}{2\Lambda} Z_N^{-1}\sum_{kS,k'S'} |\langle kS\| f^{\dagger}_N\|k'S'\rangle|^2 \sum_j \frac{v_j^2}{1+e^{-\bar\beta\epsilon_j}} \frac{e^{-\bar\beta(E'+\epsilon_j)}-e^{-\bar\beta E}}{E-E'-\epsilon_j} \\ \times \sum_{S_zS_z'\mu} |\langle S'S_z';\tfrac{1}{2}\mu|SS_z\rangle|^2 \\ \times\left(S_z^2 + \frac{e^{-\bar\beta\epsilon_j}(e^{-\bar\beta\epsilon_j}-1)}{4(1+e^{-\bar\beta\epsilon_j})^2} - \frac{2S_z\mu e^{-\bar\beta\epsilon_j}}{(1+e^{-\bar\beta\epsilon_j})} \right. \\ \left. + S_z'^2 + \frac{1-e^{-\bar\beta\epsilon_j}}{4(1+e^{-\bar\beta\epsilon_j})^2} + \frac{2S_z'\mu}{(1+e^{-\bar\beta\epsilon_j})} \right) - X_N\frac{Z^{(2)}}{Z^{(0)}} \quad . \end{aligned} \tag{F33}$$

In the above expressions (as well as hereafter) $E \equiv E_{kS}$, and $E' \equiv E_{k'S'}$.

Using standard rules of angular momentum algebra one can demonstrate that

$$\sum_{S_z S_z' \mu} |\langle S' S_z', \tfrac{1}{2}\mu | S S_z\rangle|^2 \begin{bmatrix} 1 \\ \mu S_z \\ \mu S_z' \\ S_z^2 \\ S_z'^2 \end{bmatrix} = \begin{bmatrix} n_S \\ \frac{1}{24} n_S (n_S^2 - n_{S'}^2 + 3) \\ \frac{1}{24} n_S (n_S^2 - n_{S'}^2 - 3) \\ \frac{1}{12} n_S (n_S^2 - 1) \\ \frac{1}{12} n_S (2 n_S n_{S'} - n_S^2) \end{bmatrix} . \tag{F34}$$

The combinations on the right-hand side are not unique, and can be reexpressed in other forms using the basic result that $(n_{S'} - n_S)^2 = 1$.

Substituting Eq. (F34) into Eqs. (F32) and (F33), we get

$$\frac{Z^{(2)}}{Z^{(0)}} = \frac{\bar{\beta}}{\Lambda} Z_N^{-1} \sum_{kS,k'S'} n_S |\langle kS \| f_N^\dagger \| k'S' \rangle|^2 \sum_j \frac{v_j^2}{1 + e^{-\bar{\beta}\epsilon_j}} \frac{e^{-\bar{\beta}(E' + \epsilon_j)} - e^{-\bar{\beta}E}}{E - E' - \epsilon_j} , \tag{F35}$$

$$\begin{aligned} X^{(2)} = \frac{\bar{\beta}}{2\Lambda} Z_N^{-1} \sum_{kS,k'S'} n_S |\langle kS \| f_N^\dagger \| k'S' \rangle|^2 \\ \times \sum_j \frac{v_j^2}{1 + e^{-\bar{\beta}\epsilon_j}} \frac{e^{-\bar{\beta}(E' + \epsilon_j)} - e^{-\bar{\beta}E}}{E - E' - \epsilon_j} \left[\frac{1}{12}(2 n_S n_{S'} - 1) + \frac{1}{4} \frac{(1 - e^{-\bar{\beta}\epsilon_j})^2}{(1 + e^{-\bar{\beta}\epsilon_j})^2} \right. \\ \left. + \frac{1}{12}(n_S^2 - n_{S'}^2) \frac{1 - e^{-\bar{\beta}\epsilon_j}}{1 + e^{-\bar{\beta}\epsilon_j}} - \frac{1}{4} \right] - X_N \frac{Z^{(2)}}{Z^{(0)}} . \end{aligned} \tag{F36}$$

It is convenient to rewrite $X^{(2)}$ as

$$\begin{aligned} X^{(2)} = \frac{\bar{\beta}}{2\Lambda} Z_N^{-1} \sum_{kS,k'S'} nS |\langle kS \| f_N^\dagger \| k'S' \rangle \\ \times \sum_j \frac{v_j^2}{1 + e^{-\bar{\beta}\epsilon_j}} \frac{e^{-\bar{\beta}(E' + \epsilon_j)} - e^{-\bar{\beta}E}}{E' - E - \epsilon_j} \left[\frac{1}{12}(2 n_S n_{S'} - 4) - \frac{e^{-\bar{\beta}\epsilon_j}}{(1 + e^{-\bar{\beta}\epsilon_j})^2} \right. \\ \left. + \frac{1}{12}(n_S^2 - n_{S'}^2) \frac{1 - e^{-\bar{\beta}\epsilon_j}}{1 + e^{-\bar{\beta}\epsilon_j}} \right] + \left(\frac{1}{8} - X_N\right) \frac{Z^{(2)}}{Z^{(0)}} . \end{aligned} \tag{F37}$$

Finally, in order to further simplify the expressions for $Z^{(2)}$ and $X^{(2)}$ we add to Eqs. (F35) and (F37) the results obtained by letting $j \to -j$ and divide by 2. Since $\epsilon_{-j} = \epsilon_j$, $v_{-j} = v_j$, and since

$$\frac{e^{-\bar{\beta}(E' + \epsilon_j)} - e^{-\bar{\beta}E}}{(1 + e^{-\bar{\beta}\epsilon_j})(E - E' - \epsilon_j)} \pm \frac{e^{-\bar{\beta}(E' - \epsilon_j)} - e^{-\bar{\beta}E}}{(1 + e^{\bar{\beta}\epsilon_j})(E - E' + \epsilon_j)} = \frac{(e^{-\bar{\beta}E} + e^{-\bar{\beta}E'})}{(E - E')^2 - \epsilon_j^2} \begin{cases} (E - E') \dfrac{1 - e^{-\bar{\beta}(E - E')}}{1 + e^{-\bar{\beta}(E - E')}} - \epsilon_j \dfrac{1 - e^{-\bar{\beta}\epsilon_j}}{1 + e^{-\bar{\beta}\epsilon_j}} \\ -(E - E') \dfrac{1 - e^{-\bar{\beta}\epsilon_j}}{1 + e^{-\bar{\beta}\epsilon_j}} + \epsilon_j \dfrac{1 - e^{-\bar{\beta}(E - E')}}{1 + e^{-\bar{\beta}(E - E')}} \end{cases} , \tag{F38}$$

we see that the sums over j can be expressed entirely in terms of the following three functions (evaluated at $\delta E = E - E'$):

$$u_1(\delta E) \equiv \sum_j \frac{v_j^2}{\delta E^2 - \epsilon_j^2} \left[\delta E \frac{1 - e^{-\bar{\beta}\delta E}}{1 + e^{-\bar{\beta}\delta E}} - \epsilon_j \frac{1 - e^{-\bar{\beta}\epsilon_j}}{1 + e^{-\bar{\beta}\epsilon_j}} \right] , \tag{F39}$$

$$u_2(\delta E)\equiv\sum_j \frac{v_j^2}{\delta E^2-\epsilon_j^2}\left[\delta E\frac{1-e^{-\bar\beta\delta E}}{1+e^{-\bar\beta\delta E}}-\epsilon_j\frac{1-e^{-\bar\beta\epsilon_j}}{1+e^{-\bar\beta\epsilon_j}}\right]\frac{e^{-\bar\beta\epsilon_j}}{(1+e^{-\bar\beta\epsilon_j})^2}\ , \tag{F40}$$

$$u_3(\delta E)\equiv\sum_j \frac{v_j^2}{\delta E^2-\epsilon_j^2}\left[\delta E\frac{1-e^{-\bar\beta\epsilon_j}}{1+e^{-\bar\beta\epsilon_j}}-\epsilon_j\frac{1-e^{-\bar\beta\delta E}}{1+e^{-\bar\beta\delta E}}\right]\frac{1-e^{-\bar\beta\epsilon_j}}{1+e^{-\bar\beta\epsilon_j}}\ . \tag{F41}$$

In terms of these functions we finally have

$$\frac{Z^{(2)}}{Z^{(0)}}=\frac{\bar\beta}{\Lambda}Z_N^{-1}\sum_{ks,k'S'} n_S\tfrac{1}{2}(e^{-\bar\beta E}+e^{-\bar\beta E'})\,|\langle kS||f_N^\dagger||k'S'\rangle|^2 u_1(E-E')\ , \tag{F42}$$

$$\begin{aligned}X^{(2)}=\frac{\bar\beta}{2\Lambda}Z_N^{-1}\sum_{kS,k'S'} & n_S\tfrac{1}{2}(e^{-\bar\beta E}+e^{-\bar\beta E'})\,|\langle kS||f_N^\dagger||k'S'\rangle|^2\\ &\times(\tfrac{1}{6}(n_Sn_{S'}-2)u_1(E-E')-u_2(E-E')-\tfrac{1}{12}(n_S^2-n_{S'}^2)u_3(E-E'))+(\tfrac{1}{8}-X_N)\frac{Z^{(2)}}{Z^{(0)}}\ .\end{aligned} \tag{F43}$$

Next consider the calculation of Z_F and X_F for the free-electron Hamiltonian. An approximate calculation such as the above is now no longer necessary since H_M^0 is exactly diagonalizable (cf. Sec. III A) like H_B. If M is odd we get

$$Z_F=\prod_j(1+e^{-\bar\beta\Lambda^{-(M-N)/2}\eta_j^*})^2,\quad X_F=\tfrac{1}{2}\sum_j\frac{e^{-\bar\beta\Lambda^{-(M-N)/2}\eta_j^*}}{(1+e^{-\bar\beta\Lambda^{-(M-N)/2}\eta_j^*})^2}\ , \tag{F44}$$

where j takes values $\pm1,\ \pm2,\ \ldots,\ \pm\frac{1}{2}(M+1)$. If M is even, η_j^* in Eq. (F44) is replaced by $\hat\eta_j^*$, and j now runs through the value $0,\ \pm1,\ \pm2,\ \ldots,\ \pm\frac{1}{2}M$.

We can now put together all the pieces that we have calculated. For definiteness we assume that $(M-N)$ is even. Then

$$F(T_N)=-k_BT_N[\ln Z_N+\ln(Z_B/Z_F)+Z^{(2)}/Z^{(0)}]\ , \tag{F45}$$

$$\frac{k_BT_N\chi(T_N)}{(g\mu_B)^2}=X_N+(X_B-X_F)+X^{(2)}\ , \tag{F46}$$

where the combinations (Z_B/Z_F) and (X_B-X_F) depend on whether N is odd (whence M is odd) or even (whence M is even). By rearranging the expressions for Z_F and X_F, it is easily verified that:

(i) when N is odd

$$\frac{Z_B}{Z_F}\cong\prod_{l=1}^{(M-N)/2}\frac{(1+e^{-\bar\beta\epsilon_l})^4}{(1+e^{-\bar\beta\Lambda^{-l}})^4}\prod_{l'=1}^{(N+1)/2}(1+e^{-\bar\beta\Lambda^{l'-1}})^{-4}\ , \tag{F47}$$

$$X_B-X_F\cong\sum_{l=1}^{(M-N)/2}\left[\frac{e^{-\bar\beta\epsilon_l}}{(1+e^{-\bar\beta\epsilon_l})^2}-\frac{e^{-\bar\beta\Lambda^{-l}}}{(1+e^{-\bar\beta\Lambda^{-l}})^2}\right]-\sum_{l'=1}^{(N+1)/2}\frac{e^{-\bar\beta\Lambda^{l'-1}}}{(1+e^{-\bar\beta\Lambda^{l'-1}})^2}\ ; \tag{F48}$$

(ii) when N is even

$$\frac{Z_B}{Z_F} \cong \prod_{l=1}^{(M-N)/2} \frac{(1+e^{-\bar{\beta}\epsilon_l})^4}{(1+e^{-\bar{\beta}\Lambda^{-l+1/2}})^4} \left[\prod_{l'=1}^{N/2} (1+e^{-\bar{\beta}\Lambda^{l'-1/2}})^{-4} \right]^{\frac{1}{4}} , \tag{F49}$$

$$X_B - X_F \cong \sum_{l=1}^{(M-N)/2} \left[\frac{e^{-\bar{\beta}\epsilon_l}}{(1+e^{-\bar{\beta}\epsilon_l})^2} - \frac{e^{-\bar{\beta}\Lambda^{-l+1/2}}}{(1+e^{-\bar{\beta}\Lambda^{-l+1/2}})^2} \right] - \sum_{l'=1}^{N/2} \frac{e^{-\bar{\beta}\Lambda^{l'-1/2}}}{(1+e^{-\bar{\beta}\Lambda^{l'-1/2}})^2} - \frac{1}{8} . \tag{F50}$$

In writing down the above expressions for (Z_B/Z_F), we have taken out the ground-state-energy terms. We note that the quantities (Z_B/Z_F), $(X_B - X_F)$ and the sums, u_1, u_2, and u_3 defined in Eqs. (F39)–(F41) have well-defined limits as $M \to \infty$. They are even independent of N for large N, and need be numerically evaluated only once for all the iterations.

---

*Permanent address: Indian Institute of Science, Bangalore-560012, India.

[1]P. W. Anderson, Phys. Rev. 124, 41 (1961).
[2]H. R. Krishna-murthy, K. G. Wilson, and J. W. Wilkins, Phys. Rev. Lett. 35, 1101 (1975).
[3]H. R. Krishna-murthy, K. G. Wilson, and J. W. Wilkins, in *Valence Instabilities and Related Narrow-Band Phenomena,* edited by R. D. Parks (Plenum, New York, 1977), p. 177.
[4]*Magnetism,* edited by G. T. Rado and H. Suhl (Academic New York, 1973), Vol. V.
[5]D. J. Scalapino, Phys. Rev. Lett. 16, 937 (1966).
[6]K. G. Wilson, Rev. Mod. Phys. 47, 773 (1975). A brief discussion of the calculations can be found in *Nobel Symposia–Medicine and Natural Sciences* (Academic, New York, 1974), Vol. 24, p. 68.
[7]K. G. Wilson and Kogut, Phys. Rep. C, 12, 75 (1974).
[8]F. Wegner, Phys. Rev. B 5, 4529 (1972).
[9]These results can be obtained, for example, after some algebra starting from the results given in Ref. 5, above.
[10]J. R. Schrieffer and P. A. Wolff, Phys. Rev. 149, 491 (1966).
[11]F. D. M. Haldane, J. Phys. C 11, 5015 (1978).
[12]L. Oliveira and J. W. Wilkins (private communication).
[13]K. Yamada, Progr. Theor. Phys. 53, 970 (1975); 54, 316 (1975); K. Yosida and K. Yamada, Progr. Theor. Phys. 53, 1286 (1975).
[14]M. L. Mills, M. T. Beal-Monod, and P. Lederer, in Ref. 4, p. 89. This model is also called the Wolff model: P. A. Wolff, Phys. Rev. 124, 59 (1961).
[15]J. Mathews and R. L. Walker, *Mathematical Methods of Physics* (Benjamin, California, 1973), p. 73.